arXiv:2504.21487v1 [cs.CV] 30 Apr 2025

DGSolver: Diffusion Generalist Solver with Universal Posterior Sampling for Image Restoration

Hebaixu Wang
Wuhan University
wanghebaixu@gmail.com

Jing Zhang*
Wuhan University
jingzhang.cv@gmail.com

Haonan Guo
Wuhan University
haonan.guo@whu.edu.cn

Di Wang
Wuhan University
d_wang@whu.edu.cn

Jiayi Ma*
Wuhan University
jyma2010@gmail.com

Bo Du*
Wuhan University
dubo@whu.edu.cn

Abstract

Diffusion models have achieved remarkable progress in universal image restoration. While existing methods speed up inference by reducing sampling steps, substantial step intervals often introduce cumulative errors. Moreover, they struggle to balance the commonality of degradation representations and restoration quality. To address these challenges, we introduce **DGSolver**, a diffusion generalist solver with universal posterior sampling. We first derive the exact ordinary differential equations for generalist diffusion models and tailor high-order solvers with a queue-based accelerated sampling strategy to improve both accuracy and efficiency. We then integrate universal posterior sampling to better approximate manifold-constrained gradients, yielding a more accurate noise estimation and correcting errors in inverse inference. Extensive experiments show that DGSolver outperforms state-of-the-art methods in restoration accuracy, stability, and scalability, both qualitatively and quantitatively. Code and models will be available at https://github.com/MiliLab/DGSolver.

1 Introduction

Universal image restoration strives to achieve a versatile model capable of discerning and mitigating various types of degradations. Capitalizing on the superior attributes of the restored details with high fidelity, it has emerged as a promising approach for enabling applications such as autonomous driving [36], remote sensing [43], and other related fields [65].

Owing to the substantial advancements in deep learning, a surge of universal image restoration frameworks has emerged. Typically, the existing methods can be delineated into two categories based on the dependency of representations across varied degradation distributions [58, 66, 9], namely blend-representation-based methods and distinct-representation-based methods, as displayed in Fig. 1. The former approaches promote the commonality among degradation representations by projecting diverse degradation distributions into a shared representation space, where the commonality measures the degradation-agnostic extent of representations within the shared representation space [33]. However, the complexity of restoration escalates as the commonality of degradation representations intensifies [10, 27, 28]. DiffUIR [67] reaches a compromise by projecting the disparate distributions onto an impure Gaussian distribution, retaining partial degradation conditions. FoundIR [23] further implements a mixture-of-experts system to mitigate the diminished performance resulting from the pursuit of commonality. Consequently, the compensation systems that are incurred significantly reduce efficiency. The latter approaches utilize multi-encoder architectures or prompts from foundation

*Corresponding author.

Preprint. Under review.

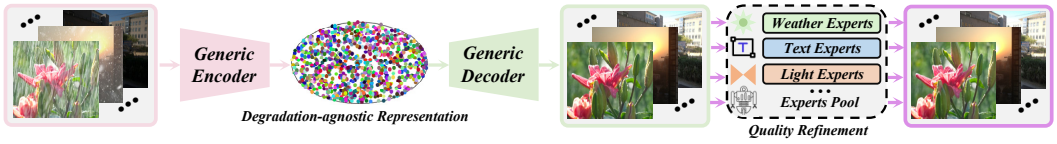

(a) Blend-representation-based for image restoration

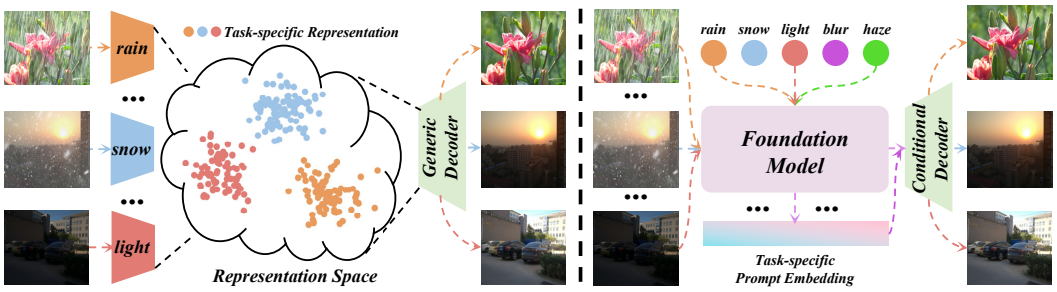

(b) Distinct-representation-based image restoration

Figure 1: Overview of the mainstream universal image restoration methods.

models to acquire distinct representations tailored for specific degradation distributions [26, 41, 13]. Afterwards, customized conditional guidance is incorporated into a shared decoder to reconstruct the distorted information [7, 11]. Nevertheless, their performance is constrained by the limited exploration of degradation correlations, as different tasks may potentially share complementary information that could augment the efficacy of individual tasks [25]. For instance, low light conditions and noise frequently coexist, while rain and raindrops are often interlinked.

In this paper, we aim to develop a precise and efficient method for universal image restoration. It is observed that the existing methods are plagued by two major drawbacks: One is the dilemma between the commonality of degradation representations and restoration quality, and the other is the lack of a versatile and effective compensatory mechanism for quality refinement. To this end, we propose **DGSolver**, a diffusion generalist solver with universal posterior sampling for image restoration, as presented in Fig. 2. It amalgamates the merits of ordinary differential equation (ODEs) solvers for high-precision inference and leverages diffusion posterior sampling as universal accuracy compensation for refinement under high commonality conditions. Specifically, we adopt the diffusion generalist models (DGMs) [67, 28] to unify diverse degradation types into a purely degradation-agnostic latent distribution. Subsequently, we tackle the alternative sampling from DGMs by solving the corresponding semi-linear ODEs to alleviate the discretization error accumulated in the multi-step inference process. Benefiting from the analytical structure, the solutions can be equivalently simplified to a linearly weighted integral of the neural networks with an accelerated sampling strategy. Furthermore, we seamlessly integrate the underlying mechanism of generalist modeling with Bayesian posterior sampling, thereby universally serving as manifold-constrained gradients for restoration guidance without incurring computational expenditures. Consequently, high-order ODEs numerical approximation and universal posterior sampling are combined to effectively improve the solution accuracy and stability in a training-free manner. Extensive experiments on natural and remote sensing scenes are conducted to verify the superior performance of our method, showcasing its remarkable restoration capability across different application scenes. Our key contributions are as follows:

1. We reformulate the generalist diffusion process using ODEs and derive its analytical solution form. Besides, high-order solvers equipped with an accelerated sampling strategy are customized to mitigate accumulated discretization errors and boost efficiency during inverse inference.
2. To further enhance the accuracy and stability of restoration, we introduce a universal posterior sampling strategy to offer manifold-constrained gradient guidance for noise estimation. It is seamlessly integrated into generalist diffusion solvers requiring no training.
3. Extensive experiments validate that our method outperforms the state-of-the-art methods across various restoration tasks, real-world scenarios, and diverse application domains, highlighting its exceptional accuracy, generalizability, and scalability.

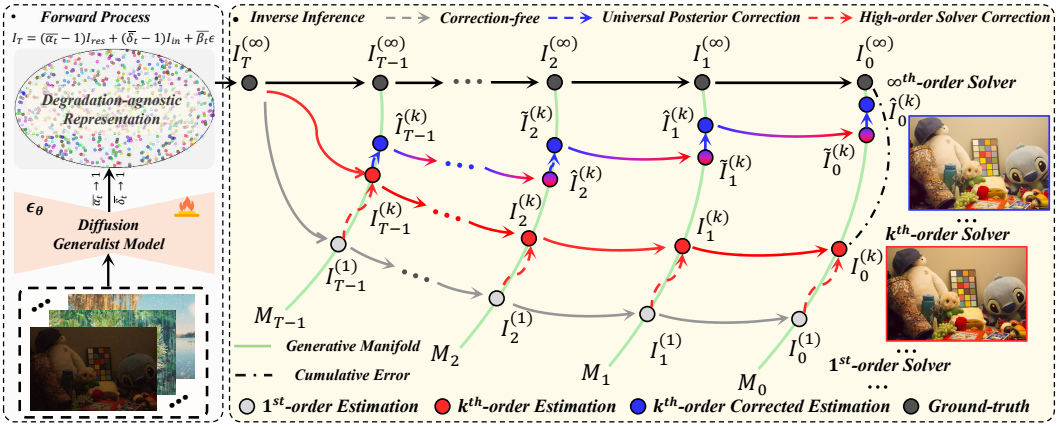

Figure 2: Illustration of the DGSolver. In the forward process, we utilize a diffusion generalist model to uniformly represent diverse degradation categories into degradation-agnostic distributions. In the inverse inference, we employ a kth-order solver to alleviate the discretization error accumulated in the multi-step sampling process. Simultaneously, universal posterior sampling is used to stabilize the solution and further minimize the discrepancies with the ideal one generated by a ∞^{th}-order solver.

2 Background

2.1 Diffusion-based Image Restoration Model

Grounded in solid mathematical foundations, diffusion models [14, 49, 50] have emerged as powerful frameworks for image restoration (see Appendix A). Initially, lots of works focus on structural improvements to facilitate the restoration of details [56, 39, 48] by simply treating degraded images as conditional inputs of the denoising network. Afterwards, InDI [10] and I^{2}SB [27] pioneer profound theoretical and practical improvements in the reverse process, opting for estimating the target image or its linear transformation term to replace the noise estimation. RDDM [28] extends beyond the single diffusion paradigm to independent double diffusion processes corresponding to residual and noise estimations, respectively. Consequently, the residual prioritizes certainty to restore the major structures while the noise emphasizes diversity to retrieve the dismissed details. Furthermore, DiffUIR [67] incorporates partially degraded information into the forward process and constructs a non-pure Gaussian distribution representation of different degradation types. Nevertheless, the commonality of degradation representations and the performance of restoration are mutually constrained, with no versatile and effective approach available to simultaneously enhance both.

2.2 Diffusion Posterior Sampling

To tackle the ill-posed attributes of linear inverse problem [19], diffusion posterior sampling has been developed as a novel approximation tool to reduce the solution uncertainty [11, 44]. Specifically, it leverages the Bayesian framework to accurately estimate the clear image I_0 from its degraded observation $I_{in} = \mathcal{A}I_0 + n$, where $\mathcal{A}$ is a measurement operator and n is usually the Gaussian noise. The stochastic differential equations (SDEs) of diffusion probabilistic models [50] with diffusion term $f(I_t, t)$ and drift term $g(t)$ can be formulated as:

$$dI_t = f(I_t, t)dt + g(t)d\omega_t, \tag{1}$$

where ω_t is the standard Wiener process. The reverse SDE of this process can be:

$$dI_t = [f(I_t, t) - g^2(t)\nabla_{I_t} \log q_t(I_t)]dt + g(t)d\overline{\omega}_t, \tag{2}$$

where $\nabla_{I_t} \log q_t(I_t)$ defines the predicted score functions. In the case of inverse problems, we want to generate the posterior distribution $q_t(I_t|I_{in}, \mathcal{A})$. Leveraging Bayesian rule, Eq. (2) becomes:

$$dI_t = [f(I_t, t) - g^2(t)(\nabla_{I_t} \log q_t(I_t) + \nabla_{I_t} \log q(I_{in}|I_t))]dt + g(t)d\overline{\omega}_t. \tag{3}$$

Nevertheless, $\nabla_{I_t} \log q(I_{in}|I_t))$ can be computationally intractability. Chung *et al.* [7] first approximate gradient of the log likelihood by assuming $p(I_{in}|I_t) \approx q(I_{in}|\hat{I}_0 := \mathbb{E}[I_0|I_t]) = \mathcal{N}(I_{in}; \mu =$

$\mathcal{A}\mathbb{E}[I_0|I_t], \Sigma = \sigma_{I_{in}}^2 \boldsymbol{I})$. Essentially, they substitute the unknown clean image I_0 with its conditional expectation $E[I_0|I_t]$ and known operator $\mathcal{A}$, making the term $p(I_{in}|I_t)$ tractable. Afterwards, PSLD [47] extends pixel-level posterior sampling into latent space, showing provable sample recovery in a low-dimensional subspace. Furthermore, BlindDPS [6] introduces multiple diffusion models to construct a parallel reverse procedure to jointly estimate the operator kernel and clear image. In summary, existing posterior sampling relies on known or estimated degradation operators. The former still suffers from ill-posedness in the practical scene due to the availability of measurement operators, while the latter only fits well in kernel-based degradation modeling with extensive computational overhead and cannot be generalized to more complex degradation scenarios.

3 Methodology

3.1 Diffusion Generalist Formulations

Assume that a clear image $I_0 \in \mathbb{R}^D$ is obtained by sampling from an unknown distribution $q_0(I_0)$. We define a forward process $\{I_t\}_{t\in[0,T]}$ starting with I_0, such that for any $t \in [0, T]$, the distribution of I_t is conditioned on I_0, I_{in}, and I_{res}, which satisfies:

$$q_{0t}(I_t|I_0, I_{res}, I_{in}) = \mathcal{N}(I_t; I_0 + \overline{\alpha}(t)I_{res} - \overline{\delta}(t)I_{in}, \overline{\beta}^2(t)\boldsymbol{I}), \tag{4}$$

where $\overline{\alpha}(t), \overline{\delta}(t), \overline{\beta}^2(t) \in \mathbb{R}^+$ are differentiable functions of t with bounded derivatives, and I_{res} is the residual items equal to $I_{in} - I_0$. when $t \to T, \overline{\alpha}(T) \to 1, \overline{\delta}(T) \to 1$, the endpoint $I_t = \overline{\beta}(t)\boldsymbol{I}$ is merely represented by a pure Gaussian distribution with a $\overline{\beta}(t)$-modulated variance. Therefore, we refer to the *linear noise schedule* [14] to generate parameter series and modify the value of $\overline{\alpha}(T), \overline{\delta}(T)$ to 1. Consequently, these variables are monotonic, and we denote them as $\overline{\alpha}_t, \overline{\delta}_t, \overline{\beta}_t$ for simplicity. We prove that the following stochastic differential equation (SDE) possesses an identical transition distribution $q_{0t}(I_t|I_0, I_{res}, I_{in})$ as in Eq. (4) for any $t \in [0, T]$ (proof in Appendix A.15):

$$dI_t = f(t)I_{res}dt + h(t)I_{in}dt + g(t)d\omega_t, \quad I_0 \sim q_0(I_0), \tag{5}$$

$$f(t) = \frac{\mathrm{d}\overline{\alpha}_t}{\mathrm{d}t}, \quad h(t) = -\frac{\mathrm{d}\overline{\delta}_t}{\mathrm{d}t}, \quad g^2(t) = \frac{\mathrm{d}\overline{\beta}_t^2}{\mathrm{d}t}. \tag{6}$$

To accelerate the sampling process, we consider the associated *probability flow ODE* with the same marginal distribution at each time t as that of the SDE, which can be formulated as:

$$\frac{dI_t}{dt} = f(t)I_{res} + h(t)I_{in} - \frac{1}{2}g^2(t)\nabla_{I_t}\log q_t(I_t), \quad I_t \sim q_T(I_T). \tag{7}$$

Apparently, the *r.h.s* of Eq. (7) comprises two indeterminate variables, *i.e.* residual components I_{res} and score functions $\nabla_{I_t}\log q_t(I_t)$, necessitating estimation via neural networks conditioned on the temporal variable t. Pursuant to the *Tweedie formula*, the score functions $\nabla_{I_t}\log q_t(I_t)$ can be equivalent to noise prediction, implying that $\epsilon = -\overline{\beta}_t\nabla_{I_t}\log q_t(I_t)$. Hence, the optimal sample can be obtained by solving the following ODE from T to 0:

$$\frac{dI_t}{dt} = f(t)I_{res}^{\theta}(I_t, I_{in}, t) + h(t)I_{in} + \frac{g^2(t)}{2\overline{\beta}_t}\epsilon_{\theta}(I_t, I_{in}, t), \quad I_t \sim q_T(I_T), \tag{8}$$

where $I_{res}^{\theta}(I_t, I_{in}, t)$ and $\epsilon_{\theta}(I_t, I_{in}, t)$ are the residual estimator and noise predictor, respectively. In Eq. (8), $h(t)I_{in}$ is a linear function of I_{in}, while the other two parts $I_{res}^{\theta}(I_t, I_{in}, t)$ and $\frac{g^2(t)}{2\overline{\beta}_t}$ typically exhibit nonlinear dependencies on I_t because of neural networks. *Previous works are ignorant of this semi-linear structure by decorating the entire Eq. (8) into a black-box ODE solver, which not only increases the complexity of the solution but also exacerbates the discretization errors of both linear and nonlinear terms.* Given an initial value I_s at time $s > 0$, the solution I_t at time $s < t < T$ can be precisely formulated as follows:

$$I_t = I_s + \int_s^t \frac{d\overline{\alpha}_\tau}{d\tau}I_{res}^{\theta}(I_\tau, I_{in}, \tau)d\tau - I_{in}\int_s^t \frac{d\overline{\delta}_\tau}{d\tau}d\tau + \int_s^t \frac{d\overline{\beta}_\tau}{d\tau}\epsilon_{\theta}(I_\tau, I_{in}, \tau)d\tau. \tag{9}$$

Such a taxonomy decouples the origin of discrete error, where the linear part can be accurately computed, but the integrals of the nonlinear parts are still complicated. As $\overline{\alpha}_t, \overline{\delta}_t, \overline{\beta}_t$ are

strictly monotonic function of t, there exist inverse functions $t_{\overline{\alpha}}(\cdot)$, $t_{\overline{\delta}}(\cdot)$, and $t_{\overline{\beta}}(\cdot)$ satisfying $t = t_\lambda(\lambda(t)), \lambda \in \{\overline{\alpha}, \overline{\delta}, \overline{\beta}\}$, respectively. We change the subscripts of I^θ_{res} and ϵ_θ from t to λ and denote $I^\theta_{res}(I_\tau, I_{in}, \tau) = \widehat{I}^\theta_{res}(\widehat{I}_{\overline{\alpha}}, I_{in}, \overline{\alpha})$, $\epsilon_\theta(I_\tau, I_{in}, \tau) = \widehat{\epsilon}_\theta(\widehat{I}_{\overline{\beta}}, I_{in}, \overline{\beta})$. For each λ, Eq. (9) can be reformulated as:

Proposition 1 *(Exact solution of ODEs for diffusion generalist models, proof in Appendix B). Given an initial value I_s at time $s > 0$, the solution I_t at time $s < t < T$ of that ODEs in Eq. (8) is*

$$I_t = I_s - (\overline{\delta}_t - \overline{\delta}_s)I_{in} + \int_{\overline{\alpha}_{t_s}}^{\overline{\alpha}_t} \widehat{I}^\theta_{res}(\widehat{I}_{\overline{\alpha}}, I_{in}, \overline{\alpha})d\overline{\alpha} + \int_{\overline{\beta}_{t_s}}^{\overline{\beta}_t} \widehat{\epsilon}_\theta(\widehat{I}_{\overline{\beta}}, I_{in}, \overline{\beta})d\overline{\beta}. \tag{10}$$

In consequence, Eq. (10) provides a new perspective for approximating the optimal solution, where estimating the solution at time t is equivalent to directly approximating the integral of $\widehat{I}^\theta_{res}(\widehat{I}_{\overline{\alpha}}, I_{in}, \overline{\alpha})$ from $\overline{\alpha}_s$ to $\overline{\alpha}_t$, and $\widehat{\epsilon}_\theta(\widehat{I}_{\overline{\beta}}, I_{in}, \overline{\beta})$ from $\overline{\beta}_s$ to $\overline{\beta}_t$. In light of such formulation, we are capable of customizing diffusion generalist solvers to improve the convergence and accuracy of solutions.

3.2 Diffusion Generalist Solvers

To enhance the precision in solving Eq. (8), we propose high-order solvers for the ODEs with a convergence order guarantee. Specifically, given an initial point I_T at time T and total $M+1$ time steps $\{t_i\}_{i=0}^M$ decreasing from $t_0 = T$ to $t_M = 0$. Let $\{I_{t_i}\}_{i=0}^M$ be the sequence iteratively computed at time steps $\{t_i\}_{i=0}^M$ using the presented solvers. To mitigate the cumulative effect of significant errors, we endeavor to minimize the inaccuracy for the solution I_{t_i} at each step. Starting with the previous solution $I_{t_{i-1}}$ at time t_{i-1}, the exact solution $I_{t_{i-1}\to t_i}$ at target time t_i is:

$$I_{t_{i-1}\to t_i} = I_{t_{i-1}} - (\overline{\delta}_{t_i} - \overline{\delta}_{t_{i-1}})I_{in} + \int_{\overline{\alpha}_{t_{i-1}}}^{\overline{\alpha}_{t_i}} \widehat{I}^\theta_{res}(\widehat{I}_{\overline{\alpha}}, I_{in}, \overline{\alpha})d\overline{\alpha} + \int_{\overline{\beta}_{t_{i-1}}}^{\overline{\beta}_{t_i}} \widehat{\epsilon}_\theta(\widehat{I}_{\overline{\beta}}, I_{in}, \overline{\beta})d\overline{\beta}. \tag{11}$$

We utilize the Taylor expansion to make k orders approximation to calculate the integral of both $\widehat{I}^\theta_{res}(\widehat{I}_{\overline{\alpha}}, I_{in}, \overline{\alpha})$ from $\overline{\alpha}_{t_{i-1}}$ to $\overline{\alpha}_{t_i}$ and $\widehat{\epsilon}_\theta(\widehat{I}_{\overline{\beta}}, I_{in}, \overline{\beta})$ from $\overline{\beta}_{t_{i-1}}$ to $\overline{\beta}_{t_i}$:

$$\widehat{I}^\theta_{res}(\widehat{I}_{\overline{\alpha}}, I_{in}, \overline{\alpha}) = \sum_{n=0}^{k-1} \frac{(\overline{\alpha} - \overline{\alpha}_{t_{i-1}})^n}{n!} \widehat{I}^\theta_{res}(\widehat{I}_{\overline{\alpha}_{t_{i-1}}}, I_{in}, \overline{\alpha}_{t_{i-1}}) + \mathcal{O}((\overline{\alpha} - \overline{\alpha}_{t_{i-1}})^k), \tag{12}$$

$$\widehat{\epsilon}_\theta(\widehat{I}_{\overline{\beta}}, I_{in}, \overline{\beta}) = \sum_{n=0}^{k-1} \frac{(\overline{\beta} - \overline{\beta}_{t_{i-1}})^n}{n!} \widehat{\epsilon}_\theta(\widehat{I}_{\overline{\beta}_{t_{i-1}}}, I_{in}, \overline{\beta}_{t_{i-1}}) + \mathcal{O}((\overline{\beta} - \overline{\beta}_{t_{i-1}})^k). \tag{13}$$

Substituting the above Taylor expansions into Eq. (11), yields:

$$\begin{aligned} I_{t_{i-1}\to t_i} = I_{t_{i-1}} - (\overline{\delta}_{t_i} - \overline{\delta}_{t_{i-1}})I_{in} + \sum_{n=0}^{k-1} \frac{(\overline{\alpha}_{t_i} - \overline{\alpha}_{t_{i-1}})^{n+1}}{(n+1)!} \widehat{I}^{\theta(n)}_{res}(\widehat{I}_{t_{i-1}}, I_{in}, t_{i-1}) \\ + \sum_{n=0}^{k-1} \frac{(\overline{\beta}_{t_i} - \overline{\beta}_{t_{i-1}})^{n+1}}{(n+1)!} \widehat{\epsilon}^{(n)}_\theta(\widehat{I}_{t_{i-1}}, I_{in}, t_{i-1}) + \mathcal{O}((\overline{\alpha} - \overline{\alpha}_{t_{i-1}})^{k+1}) + \mathcal{O}((\overline{\beta} - \overline{\beta}_{t_{i-1}})^{k+1}). \end{aligned} \tag{14}$$

By discarding the approximation errors terms $\mathcal{O}(\cdot)$, we can approximate the n-th order total derivatives $\widehat{I}^{\theta(n)}_{res}(\cdot)$ and $\widehat{\epsilon}^{(n)}_\theta(\cdot)$ for $n \leq k-1$ with finite difference [37]. In the case of $k = 1$, Eq. (14) becomes:

$$I_{t_i} = I_{t_{i-1}} - (\overline{\delta}_{t_i} - \overline{\delta}_{t_{i-1}})I_{in} + (\overline{\alpha}_{t_i} - \overline{\alpha}_{t_{i-1}})I^\theta_{res}(I_{t_{i-1}}, I_{in}, t_{i-1}) + (\overline{\beta}_{t_i} - \overline{\beta}_{t_{i-1}})\epsilon_\theta(I_{t_{i-1}}, I_{in}, t_{i-1}). \tag{15}$$

Notably, prior works [67, 23] are a special case of the first-order solver within our methods by omitting the discrete error. For $k = 2$, the calculation of the first derivative requires additional intermediate time points $t_u = rt_i + (1-r)t_{i-1}$ in the range of $[t_i, t_{i-1}]$ with controllable parameters r, and we have:

$$\begin{aligned} I_{t_i} = I_{t_{i-1}} - (\overline{\delta}_{t_i} - \overline{\delta}_{t_{i-1}})I_{in} + (\overline{\alpha}_{t_i} - \overline{\alpha}_{t_{i-1}})I^\theta_{res}(I_{t_{i-1}}, I_{in}, t_{i-1}) + (\overline{\beta}_{t_i} - \overline{\beta}_{t_{i-1}})\epsilon_\theta(I_{t_{i-1}}, I_{in}, t_{i-1}) + \frac{(\overline{\alpha}_{t_i} - \overline{\alpha}_{t_{i-1}})}{2r} \cdot \\ \big(I^\theta_{res}(I_{t_u}, I_{in}, t_u) - I^\theta_{res}(I_{t_{i-1}}, I_{in}, t_{i-1})\big) + \frac{(\overline{\beta}_{t_i} - \overline{\beta}_{t_{i-1}})}{2r} \cdot \big(\epsilon_\theta(I_{t_u}, I_{in}, t_u) - \epsilon_\theta(I_{t_{i-1}}, I_{in}, t_{i-1})\big). \end{aligned} \tag{16}$$

For $k \geq 2$, the technical derivation details and algorithms are deferred to Appendix B.

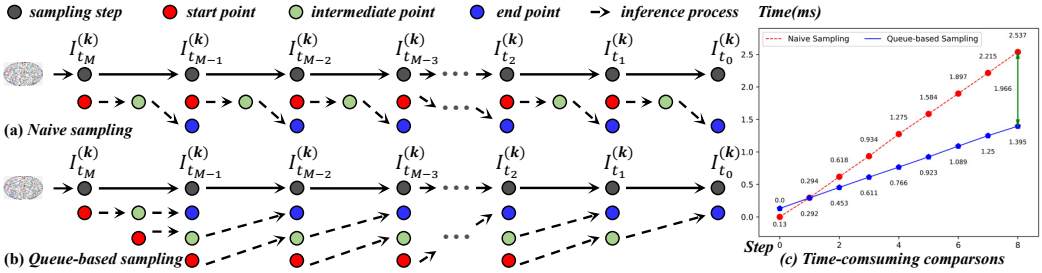

Figure 3: Different sampling strategies of diffusion generalist solvers ($k = 2$).

3.3 Universal Posterior Sampling

Under well-defined conditions, Eq. (4) adequately unifies diverse degradations into a degradation-agnostic representation, facilitating the perception of commonalities while exacerbating the restoration burden for discriminability reduction. Eq. (3) offers insights that $\nabla_{I_t} \log q(I_{in}|I_t)$ can be adapted to prevent samples from deviating from the generative manifolds when the measurements are deteriorated, as illustrated in Fig. 2. In contrast to linear inverse modeling, we endeavor to leverage the underlying mechanism of generalist modeling by universally formulating the degradation as $I_{in} = I_0 + I^{\theta}_{res} + n$. Such a model exhibits versatility across various degradation scenarios. In order to seek a tractable approximation for $q(I_{in}|I_t)$, we utilize surrogate functions to maximize the likelihood, yielding approximations of universal posterior sampling (UPS). Specifically, given the formulation $q(I_{in}|I_t) = \mathbb{E}_{I_0, I_{res} \sim q(I_0, I^{\theta}_{res}|I_t)}[q(I_{in}|I_0, I^{\theta}_{res})]$, we can make approximations by replacing the outer expectation of $q(I_{in}|I_0, I^{\theta}_{res})$ over the posterior distribution with inner expectations:

$$q(I_{in}|I_t) \simeq q(I_{in}|\widehat{I}_0 := \mathbb{E}[I_0|I_t, \widehat{I}^{\theta}_{res}], \widehat{I}^{\theta}_{res} := \mathbb{E}[I^{\theta}_{res}|I_t]). \tag{17}$$

As the clean images are continuously disrupted by Gaussian noise in the diffusion process, we can derive the closed-form upper bound of the Jensen gap for the general degradation modeling.

Theorem 1 *For the measurement model $I_{in} = I_0 + I_{res} + n$ in linear verse problem with $n \sim \mathcal{N}(0, \sigma^2 \boldsymbol{I})$, we have (proof in Appendix C):*

$$q(I_{in}|I_t) \simeq q(I_{in}|\widehat{I}_0, \widehat{I}_{res}), \tag{18}$$

the approximation error can be quantified with the Jensen gap, which is upper bounded by:

$$\mathcal{J}(\sigma, M) \leq \frac{d}{\sqrt{2\pi\sigma^2}} \exp\left(-\frac{1}{2\sigma^2}\right) M, \tag{19}$$

where $M := \int \|(I_0 + I_{res}) - (\widehat{I}_0 + \widehat{I}_{res})\| q(I_0, I_{res}|I_t) dI_0 dI_{res}$.

Note that M is finite for most of the distribution in practice, which can be considered as the generalized absolute distance between the observed reference and estimated data. $\mathcal{J}(\sigma, M)$ can approach 0 as $\sigma \to 0$ or ∞, suggesting that the approximation errors reduce with extreme measurement noise. Specifically, if the predictions of $\widehat{I}_0$ and $\widehat{I}_{res}$ are accurate, the upper bound $\mathcal{J}(\sigma, M)|_{\sigma \to 0, M \to 0}$ shrinks due to the low variance and distortion. Oppositely, if the predictions lack accuracy, the upper bound of the $\mathcal{J}(\sigma, M)|_{\sigma \to \infty, M \to M_{max}}$ shrinks as well for large variance and limited distortion. According to Theorem 1, universal posterior sampling can stabilize the multi-step inverse sampling process and provide the tractable gradient approximations of log-likelihood, as measurement distribution is given:

$$\nabla_{I_t} \log q(I_{in}|I_t) \simeq \nabla_{I_t} \log q(I_{in}|\widehat{I}_0, \widehat{I}^{\theta}_{res}) = -1/\sigma^2 \nabla_{I_t} \|I_{in} - (\widehat{I}_0 + \widehat{I}_{res})\|, \tag{20}$$

It serves as a compensatory mechanism to furnish reliable gradient guidance for optimization in the latent manifold, thereby mitigating the restoration burden and efficiency deterioration. Notably, our method is formed through the collaboration of diffusion generalist solvers and universal posterior sampling. Both components exclusively depend on I^{θ}_{res} and ϵ_{θ} predictors, which are intended for inverse inference. Once the neural networks are adequately optimized, restoration improvements can be achieved without re-training. For the different solvers in Eq. (14), we employ universal posterior sampling to modify the noise $\epsilon_{\theta}(\cdot)$ predicted by neural networks as follows (See Appendix D):

$$\widehat{\epsilon}_{\theta}(\widehat{I}_{t_i}, I_{in}, t_i) := \epsilon_{\theta}(\widehat{I}_{t_i}, I_{in}, t_i) + \overline{\beta}_{t_i}/\sigma^2 \nabla_{I_{t_i}} \|I_{in} - (\widehat{I}_0 + I^{\theta}_{res}(I_{t_i}, I_{in}, t_i))\|. \tag{21}$$

Table 1: Quantitative comparisons of five image restoration tasks. The FLOPS is calculated in the inference stage with 256×256 resolution. The best results of task-specific models and universal models are shown in **blue** and **red**, respectively.

Method	Year	Deraining		Enhancement		Desnowing		Dehazing		Deblurring		Average		Complexity	
		PSNR↑	SSIM↑	PSNR↑	SSIM↑	PSNR↑	SSIM↑	PSNR↑	SSIM↑	PSNR↑	SSIM↑	PSNR↑	SSIM↑	Params(M)	FLOPs(G)
Task-specific Method															
SwinIR [26]	2021	27.81	0.845	17.49	0.715	25.90	0.913	24.22	0.886	28.01	0.839	-	-	0.87	58.71
Restormer [61]	2022	**30.02**	**0.878**	23.07	0.774	**33.24**	**0.958**	**32.04**	**0.969**	**32.87**	**0.939**	-	-	26.12	140.99
MAXIM [52]	2022	29.36	0.875	**23.73**	**0.893**	29.93	0.954	28.50	0.931	32.86	0.939	-	-	22.14	158.16
IR-SDE [31]	2023	24.37	0.782	18.76	0.625	19.78	0.866	16.36	0.826	27.91	0.865	-	-	137.13	379.33
RDDM [28]	2024	25.61	0.919	19.94	0.727	26.79	0.891	27.87	0.941	27.87	0.848	-	-	15.47	65.87
Universal Method															
Restomer [61]	2022	28.54	0.847	21.75	0.742	28.53	0.919	26.54	0.924	26.44	0.799	27.61	0.869	26.09	140.99
AirNet [22]	2022	24.78	0.774	13.05	0.485	25.80	0.885	18.53	0.827	25.76	0.782	24.01	0.809	5.76	301.27
Prompt-IR [41]	2023	28.97	0.856	20.97	0.733	29.52	0.938	25.80	0.929	26.25	0.797	27.89	0.878	32.96	158.14
ProRes [34]	2023	22.42	0.752	20.31	0.741	24.53	0.859	24.81	0.888	26.08	0.792	24.08	0.814	370.26	97.17
IDR [64]	2023	28.40	0.844	20.95	0.706	27.77	0.911	24.48	0.914	26.33	0.799	26.96	0.863	6.19	32.16
AutoDIR [18]	2024	29.32	0.863	15.65	0.707	15.31	0.706	19.01	0.829	28.47	0.864	22.43	0.799	115.86	63.38
DA-CLIP [32]	2024	28.63	0.854	19.50	0.730	28.23	0.934	27.26	0.941	26.47	0.818	27.54	0.881	32.96	158.14
DiffUIR [67]	2024	30.67	0.887	21.21	0.769	30.70	0.943	30.29	0.944	29.00	0.877	29.93	0.907	7.73	32.93
Ours-T	-	28.10	0.841	19.48	0.719	26.47	0.896	22.03	0.875	25.82	0.784	25.95	0.849	0.45	5.74
Ours-S	-	28.99	0.852	20.36	0.749	26.98	0.905	25.73	0.906	25.89	0.785	26.93	0.861	1.07	8.01
Ours-B	-	29.50	0.874	20.85	0.747	31.04	0.948	28.12	0.937	27.74	0.850	29.16	0.898	3.65	23.97
Ours-L	-	**31.46**	**0.896**	**23.84**	**0.801**	**32.69**	**0.955**	**31.68**	**0.946**	**30.15**	**0.899**	**31.36**	**0.920**	7.73	32.93

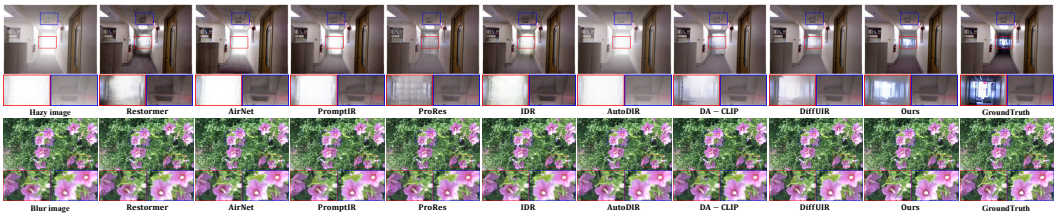

Figure 4: Visualization comparison with state-of-the-art methods on different restoration tasks.

Our computational overhead primarily originates from the total derivatives of $\widehat{I}_{res}^{\theta(n)}(\cdot), \widehat{\epsilon}_{\theta}^{(n)}(\cdot)$, and the approximation of $\nabla_{I_t} \log q(I_{in}|I_t)$. To accelerate the inverse inference, we introduce a queue-based sampling strategy to improve efficiency, as illustrated in Fig. 3. Specifically, we precompute the items of intermediate time points during the initial sampling, and subsequent sampling operations will use these items of intermediate time points as their starting points. Furthermore, each sampling iteration solely necessitates the calculation of updated intermediate time points to obtain the final results. Consequently, this approach improves efficiency by effectively reducing the consumption of computational resources. For more details, please refer to the Appendix D.

4 Experiment

4.1 Benchmarks and Implementations

Extensive experiments are conducted on five image restoration tasks, encompassing deraining [17, 42, 60, 62, 3, 24], low-light enhancement [55, 29, 35], desnowing [4, 30], dehazing [21, 8, 1, 2] and deblurring [38, 45]. Datasets details are as summarized in Appendix E.1, and we use PSNR [16] and SSIM [54] to evaluate the performance on RGB space. For fairness, five task-specific methods [26, 61, 52, 31, 28] are trained separately on task-related datasets and all universal methods [61, 41, 34, 64, 32, 67] except for [18] are re-implemented on the mixed datasets.

Our method is trained using 8 Nvidia A800 40GB GPUs with PyTorch [40] framework for 210h. Adam optimizer and L1 loss are employed for 500k iterations with a learning rate of 1e-4. We set the batch sizes as 20 and distribute it evenly to each task. We randomly crop 256×256 patch from the original image as network input for training and use 8 timesteps for full-resolution testing. We use U-Net [46] architecture and change the channel number of the hidden layers C to obtain different versions with varied parameter quantities: Ours-T(C = 32, 32, 32, 32), Ours-S(C = 32, 64, 64, 128), Ours-B(C = 64, 128, 128, 256), Ours-L(C = 64, 128, 256, 512).

4.2 Comparative Experiments

Quantitative results are presented in Tab. 1. In contrast to universal methods, we achieve substantial performance improvement across all tasks, indicating our highest accuracy. Compared with task-specific methods, we still achieve competitive results with the lowest number of parameters and

Table 2: Effects of universal posterior sampling and solver orders of our method.

Configurations			Deraining		Enhancement		Desnowing		Dehazing		Deblurring		Average	
	Order	UPS	PSNR↑	SSIM↑	PSNR↑	SSIM↑	PSNR↑	SSIM↑	PSNR↑	SSIM↑	PSNR↑	SSIM↑	PSNR↑	SSIM↑
(i)	$k = 1$	×	30.69	0.886	23.04	0.795	32.06	0.952	31.47	0.947	29.33	0.887	30.70	0.913
(ii)	$k = 1$	✓	31.10	0.892	23.07	0.798	32.32	0.954	31.54	0.947	29.80	0.895	31.01	0.918
(iii)	$k = 2$	×	31.31	0.894	23.08	0.798	32.51	0.955	31.62	0.948	30.07	0.897	31.20	0.919
(iv)	$k = 2$	✓	31.46	0.896	23.84	0.801	32.69	0.955	31.68	0.946	30.15	0.899	31.36	0.920
(v)	$k = 3$	×	31.33	0.894	23.13	0.799	32.52	0.955	31.71	0.948	30.09	0.898	31.23	0.919
(vi)	$k = 3$	✓	31.45	0.896	23.84	0.801	32.69	0.955	31.67	0.946	30.15	0.899	31.36	0.920

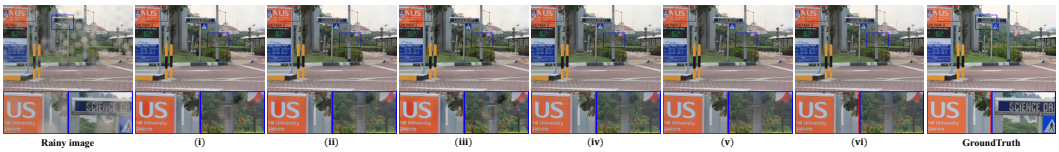

Figure 5: Visualization effects of varied solver and universal posterior sampling.

computational overhead. Evidently, the performance of our method gets better as the network capacity increases, fully validating its scalability. Visual comparisons are shown in Fig. 4, and for more results please refer to Appendix E.2. Our method outperforms others and is the most similar to ground-truth.

4.3 Ablation Study

To thoroughly harness the effectiveness of each component, we conduct ablation studies that include three categories: (i) Effects of varied solver orders and universal posterior sampling, (ii) influence of the value of $\overline{\delta}_T$, and (iii) impact of the sampling steps.

Effects of varied solver orders and universal posterior sampling. We present the qualitative comparisons and quantitative analysis in Fig. 5 and Tab. 2, respectively. Obviously, metric assessments improve as order increases and the performance of our method reaches saturation in configuration (iv). Besides, the activation of UPS can steadily enhance the solution accuracy and its effect weakens as solver order increases. Therefore, we select $k = 2$ with UPS enabled as our default settings to strike a balance between performance and efficiency.

Influence of the value of $\overline{\delta}_T$. $\overline{\delta}_T$ determines the commonality of degradation representation in a positively correlated manner. We show the restoration performance with various $\overline{\delta}_T$ settings in Tab. 3. Clearly, the optimal commonality ratio varies across different tasks, and the performance under low commonality is markedly inferior to that under high commonality. To fully verify that our method can handle complicated distribution conditions, we perform image restoration with $\overline{\delta}_T = 1$.

Impact of the sampling steps. The quality of the restored image and the efficiency of the inverse inference depend on sampling steps. Restoration performance with different sampling steps is provided in Tab 4. As a result, more steps do not necessarily yield better performance. Considering the balance between efficiency and performance, we select 8 as the optimal number of steps.

4.4 Compound Image Restoration

To verify that we can handle complex degradations, we perform our method multiple times in night dehazing, night deblurring, and multi-exposure restoration, as shown in Appendix E.3). Our method eliminates the former degradation before the latter one within its capability range. It incurs no additional information interference for well-restored data, ensuring high fidelity.

Table 3: Quantitative results of our method with different values of $\overline{\delta}_T$.

$\overline{\delta}_T$	Deraining		Enhancement		Desnowing		Dehazing		Deblurring		Average	
	PSNR↑	SSIM↑	PSNR↑	SSIM↑	PSNR↑	SSIM↑	PSNR↑	SSIM↑	PSNR↑	SSIM↑	PSNR↑	SSIM↑
0.1	29.44	0.875	21.03	0.751	32.24	0.955	29.11	0.942	29.31	0.883	29.99	0.908
0.25	29.44	0.877	21.75	0.765	32.25	0.956	29.57	0.945	29.36	0.884	30.10	0.910
0.5	30.83	0.887	22.56	0.786	32.12	0.953	31.58	0.944	30.13	0.897	30.91	0.915
0.75	31.37	0.896	22.46	0.786	32.32	0.955	31.52	0.948	30.26	0.899	31.15	0.919
0.9	31.40	0.896	23.75	0.807	32.34	0.954	32.05	0.946	30.13	0.897	31.26	0.919
1	31.46	0.896	23.84	0.801	32.69	0.955	31.68	0.946	30.15	0.899	31.36	0.920

Table 4: Restoration performance of different sampling steps.

Steps	Denoising		Enhancement		Deblur		Decloud		Super-resolve		Average	
	PSNR↑	SSIM↑	PSNR↑	SSIM↑	PSNR↑	SSIM↑	PSNR↑	SSIM↑	PSNR↑	SSIM↑	PSNR↑	SSIM↑
4	31.35	0.895	23.30	0.801	32.56	0.956	31.70	0.948	30.09	0.898	31.25	0.920
7	31.33	0.894	23.22	0.800	32.52	0.956	31.66	0.948	30.08	0.898	31.22	0.919
8	31.46	0.896	23.84	0.801	32.69	0.955	31.68	0.946	30.15	0.899	31.36	0.920
9	31.31	0.894	22.99	0.798	32.46	0.955	31.67	0.948	30.05	0.897	31.18	0.919
10	31.28	0.893	23.09	0.799	32.46	0.955	31.57	0.948	30.04	0.897	31.16	0.919

Table 5: Performance comparison of our method with other universal image restoration methods in remote sensing image restoration tasks. The best results are highlighted in **bold**.

Method	Year	Denoising		Enhancement		Deblur		Decloud		Super-resolve		Average	
		PSNR↑	SSIM↑	PSNR↑	SSIM↑	PSNR↑	SSIM↑	PSNR↑	SSIM↑	PSNR↑	SSIM↑	PSNR↑	SSIM↑
Restomer [61]	2022	29.21	0.773	32.61	0.976	28.14	0.781	20.13	0.520	28.58	0.809	28.97	0.810
AirNet [22]	2022	28.37	0.770	25.91	0.881	26.00	0.684	20.04	0.516	28.06	0.798	26.58	0.761
Prompt-IR [41]	2023	30.06	0.796	33.03	0.982	25.72	0.639	19.54	0.498	27.97	0.788	28.56	0.778
ProRes [34]	2023	28.30	0.769	30.73	0.932	25.63	0.654	20.28	0.508	27.95	0.793	27.57	0.764
IDR [64]	2023	27.56	0.695	30.32	0.967	25.32	0.625	18.98	0.476	27.81	0.784	27.07	0.740
DA-CLIP [32]	2024	29.98	0.780	33.69	0.986	27.80	0.747	19.06	0.463	27.11	0.762	29.01	0.793
DiffUIR [67]	2024	29.59	0.740	35.28	0.988	30.01	0.837	20.34	0.554	28.63	0.818	30.17	0.821
Ours-T	-	25.57	0.671	28.34	0.963	24.78	0.610	17.40	0.425	27.63	0.786	25.79	0.725
Ours-S	-	27.38	0.713	31.59	0.976	26.97	0.711	18.12	0.462	28.49	0.809	27.78	0.772
Ours-B	-	29.22	0.748	32.00	0.980	29.48	0.829	18.96	0.510	28.75	0.823	29.10	0.817
Ours-L	-	**31.83**	**0.802**	**35.52**	**0.988**	**31.84**	**0.875**	**21.35**	**0.597**	**29.47**	**0.839**	**31.52**	**0.854**

Figure 6: Visualization of real-world scenes generalization on Snow100K-Real [30].

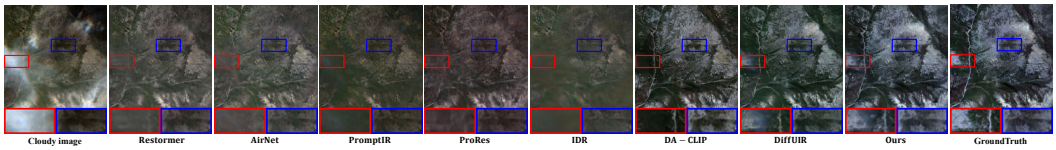

Figure 7: Visualization of cloud removal on Sen2_MTC [15].

4.5 Zero-shot generalization in real-world scenes

To evaluate the generalization ability, we conduct the zero-shot generalization on real-world scenes. Due to the absence of ground-truth, we merely supplement the qualitative results, as shown in Fig. 6. We achieve the best visual effects. More details and comparisons are placed in Appendix E.4.

4.6 Remote Sensing Image Restoration

Remote sensing imaging possesses different depth attributes and degradation types. To further validate the superiority of our method, we adapt all universal methods to remote sensing image restoration tasks, including denoising, illumination adjustment, deblurring, cloud removal, and super-resolution. Metric evaluations and visual comparisons are presented in Tab. 5 and Fig. 7, respectively. We achieve the best quantitative and qualitative results (See more details in Appendix E.5).

5 Conclusion

In this paper, we introduced DGSolver, a diffusion generalist solver with universal posterior sampling for image restoration. We derived exact ODE formulations for diffusion generalist models and developed customized high-order solvers with a queue-based sampling strategy to reduce cumulative discretization errors and enhance efficiency. Additionally, our universal posterior sampling improves the approximation of manifold-constrained gradients, leading to more accurate noise and residual estimation. Extensive experiments across natural and remote sensing datasets demonstrate that DGSolver consistently outperforms state-of-the-art methods in accuracy, stability, and scalability.

References

[1] Codruta O Ancuti, Cosmin Ancuti, Mateu Sbert, and Radu Timofte. Dense-haze: A benchmark for image dehazing with dense-haze and haze-free images. In *Proceedings of the International Conference on Image Processing*, pages 1014–1018. IEEE, 2019.

[2] Codruta O. Ancuti, Cosmin Ancuti, and Radu Timofte. NH-HAZE: an image dehazing benchmark with non-homogeneous hazy and haze-free images. In *Proceedings of the Conference on Computer Vision and Pattern Recognition Workshops*, 2020.

[3] Yunhao Ba, Howard Zhang, Ethan Yang, Akira Suzuki, Arnold Pfahnl, Chethan Chinder Chandrappa, Celso de Melo, Suya You, Stefano Soatto, Alex Wong, and Achuta Kadambi. Not just streaks: Towards ground truth for single image deraining. In *Proceedings of the European Conference on Computer Vision*, 2022.

[4] Wei-Ting Chen, Hao-Yu Fang, Cheng-Lin Hsieh, Cheng-Che Tsai, I Chen, Jian-Jiun Ding, Sy-Yen Kuo, et al. All snow removed: Single image desnowing algorithm using hierarchical dual-tree complex wavelet representation and contradict channel loss. In *Proceedings of the International Conference on Computer Vision*, pages 4196–4205, 2021.

[5] Gong Cheng, Junwei Han, and Xiaoqiang Lu. Remote sensing image scene classification: Benchmark and state of the art. *Proceedings of the IEEE*, 105(10):1865–1883, 2017.

[6] Hyungjin Chung, Jeongsol Kim, Sehui Kim, and Jong Chul Ye. Parallel diffusion models of operator and image for blind inverse problems. In *Proceedings of the Conference on Computer Vision and Pattern Recognition*, pages 6059–6069, 2023.

[7] Hyungjin Chung, Jeongsol Kim, Michael T McCann, Marc L Klasky, and Jong Chul Ye. Diffusion posterior sampling for general noisy inverse problems. In *Proceedings of the International Conference on Learning Representations*, 2023.

[8] Christophe De Vleeschouwer Cosmin Ancuti, Codruta O. Ancuti. D-hazy: A dataset to evaluate quantitatively dehazing algorithms. In *Proceedings of the International Conference on Image Processing*, ICIP'16, 2016.

[9] Yuning Cui, Wenqi Ren, Xiaochun Cao, and Alois Knoll. Revitalizing convolutional network for image restoration. *IEEE Transactions on Pattern Analysis and Machine Intelligence*, 2024.

[10] Mauricio Delbracio and Peyman Milanfar. Inversion by direct iteration: An alternative to denoising diffusion for image restoration. *Transactions on Machine Learning Research*.

[11] Zehao Dou and Yang Song. Diffusion posterior sampling for linear inverse problem solving: A filtering perspective. In *Proceedings of the International Conference on Learning Representations*, 2024.

[12] Xiang Gao, Meera Sitharam, and Adrian E Roitberg. Bounds on the jensen gap, and implications for mean-concentrated distributions. *arXiv preprint arXiv:1712.05267*, 2017.

[13] Hang Guo, Jinmin Li, Tao Dai, Zhihao Ouyang, Xudong Ren, and Shu-Tao Xia. Mambair: A simple baseline for image restoration with state-space model. In *Proceedings of the European Conference on Computer Vision*, pages 222–241. Springer, 2024.

[14] Jonathan Ho, Ajay Jain, and Pieter Abbeel. Denoising diffusion probabilistic models. *Advances in Neural Information Processing Systems*, 33:6840–6851, 2020.

[15] Gi-Luen Huang and Pei-Yuan Wu. Ctgan: Cloud transformer generative adversarial network. In *Proceedings of the International Conference on Image Processing*, pages 511–515. IEEE, 2022.

[16] Quan Huynh-Thu and Mohammed Ghanbari. Scope of validity of psnr in image/video quality assessment. *Electronics letters*, 44(13):800–801, 2008.

[17] Kui Jiang, Zhongyuan Wang, Peng Yi, Chen Chen, Baojin Huang, Yimin Luo, Jiayi Ma, and Junjun Jiang. Multi-scale progressive fusion network for single image deraining. In *Proceedings of the Conference on Computer Vision and Pattern Recognition*, June 2020.

[18] Yitong Jiang, Zhaoyang Zhang, Tianfan Xue, and Jinwei Gu. Autodir: Automatic all-in-one image restoration with latent diffusion. In *Proceedings of the European Conference on Computer Vision*, pages 340–359. Springer, 2024.

[19] Zahra Kadkhodaie and Eero Simoncelli. Stochastic solutions for linear inverse problems using the prior implicit in a denoiser. *Advances in Neural Information Processing Systems*, 34:13242–13254, 2021.

[20] Diederik Kingma, Tim Salimans, Ben Poole, and Jonathan Ho. Variational diffusion models. *Advances in Neural Information Processing Systems*, 34:21696–21707, 2021.

[21] Boyi Li, Wenqi Ren, Dengpan Fu, Dacheng Tao, Dan Feng, Wenjun Zeng, and Zhangyang Wang. Benchmarking single-image dehazing and beyond. *IEEE Transactions on Image Processing*, 28(1):492–505, 2018.

[22] Boyun Li, Xiao Liu, Peng Hu, Zhongqin Wu, Jiancheng Lv, and Xi Peng. All-in-one image restoration for unknown corruption. In *Proceedings of the Conference on Computer Vision and Pattern Recognition*, pages 17452–17462, 2022.

[23] Hao Li, Xiang Chen, Jiangxin Dong, Jinhui Tang, and Jinshan Pan. Foundir: Unleashing million-scale training data to advance foundation models for image restoration. *arXiv preprint arXiv:2412.01427*, 2024.

[24] Wei Li, Qiming Zhang, Jing Zhang, Zhen Huang, Xinmei Tian, and Dacheng Tao. Toward real-world single image deraining: A new benchmark and beyond. *arXiv preprint arXiv:2206.05514*, 2022.

[25] Xin Li, Yulin Ren, Xin Jin, Cuiling Lan, Xingrui Wang, Wenjun Zeng, Xinchao Wang, and Zhibo Chen. Diffusion models for image restoration and enhancement–a comprehensive survey. *arXiv preprint arXiv:2308.09388*, 2023.

[26] Jingyun Liang, Jiezhang Cao, Guolei Sun, Kai Zhang, Luc Van Gool, and Radu Timofte. Swinir: Image restoration using swin transformer. In *Proceedings of the International Conference on Computer Vision*, pages 1833–1844, 2021.

[27] Guan-Horng Liu, Arash Vahdat, De-An Huang, Evangelos A Theodorou, Weili Nie, and Anima Anandkumar. I2sb: image-to-image schrodinger bridge. In *Proceedings of the International Conference on Machine Learning*, pages 22042–22062, 2023.

[28] Jiawei Liu, Qiang Wang, Huijie Fan, Yinong Wang, Yandong Tang, and Liangqiong Qu. Residual denoising diffusion models. In *Proceedings of the Conference on Computer Vision and Pattern Recognition*, pages 2773–2783, 2024.

[29] Jiaying Liu, Xu Dejia, Wenhan Yang, Minhao Fan, and Haofeng Huang. Benchmarking low-light image enhancement and beyond. *International Journal of Computer Vision*, 129:1153–1184, 2021.

[30] Yun-Fu Liu, Da-Wei Jaw, Shih-Chia Huang, and Jenq-Neng Hwang. Desnownet: Context-aware deep network for snow removal. *IEEE Transactions on Image Processing*, 27(6):3064–3073, 2018.

[31] Ziwei Luo, Fredrik K Gustafsson, Zheng Zhao, Jens Sjölund, and Thomas B Schön. Image restoration with mean-reverting stochastic differential equations. *International Conference on Machine Learning*, 2023.

[32] Ziwei Luo, Fredrik K Gustafsson, Zheng Zhao, Jens Sjölund, and Thomas B Schön. Controlling vision-language models for multi-task image restoration. In *Proceedings of the International Conference on Learning Representations*, 2024.

[33] Ziwei Luo, Fredrik K Gustafsson, Zheng Zhao, Jens Sjölund, and Thomas B Schön. Taming diffusion models for image restoration: a review. *arXiv preprint arXiv:2409.10353*, 2024.

[34] Jiaqi Ma, Tianheng Cheng, Guoli Wang, Qian Zhang, Xinggang Wang, and Lefei Zhang. Prores: Exploring degradation-aware visual prompt for universal image restoration. *CoRR*, 2023.

[35] Kede Ma, Kai Zeng, and Zhou Wang. Perceptual quality assessment for multi-exposure image fusion. *IEEE Transactions on Image Processing*, 24(11):3345–3356, 2015.

[36] Aboli Marathe, Pushkar Jain, Rahee Walambe, and Ketan Kotecha. Restorex-ai: A contrastive approach towards guiding image restoration via explainable ai systems. In *Proceedings of the Conference on Computer Vision and Pattern Recognition*, pages 3030–3039, 2022.

[37] Louis Melville Milne-Thomson. *The calculus of finite differences*. American Mathematical Soc., 2000.

[38] Seungjun Nah, Tae Hyun Kim, and Kyoung Mu Lee. Deep multi-scale convolutional neural network for dynamic scene deblurring. In *Proceedings of the Conference on Computer Vision and Pattern Recognition*, pages 3883–3891, 2017.

[39] Ozan Özdenizci and Robert Legenstein. Restoring vision in adverse weather conditions with patch-based denoising diffusion models. *IEEE Transactions on Pattern Analysis and Machine Intelligence*, 45(8):10346–10357, 2023.

[40] Adam Paszke, Sam Gross, Francisco Massa, Adam Lerer, James Bradbury, Gregory Chanan, Trevor Killeen, Zeming Lin, Natalia Gimelshein, Luca Antiga, et al. Pytorch: An imperative style, high-performance deep learning library. *Advances in neural information processing systems*, 32, 2019.

[41] Vaishnav Potlapalli, Syed Waqas Zamir, Salman H Khan, and Fahad Shahbaz Khan. Promptir: Prompting for all-in-one image restoration. *Advances in Neural Information Processing Systems*, 36:71275–71293, 2023.

[42] Rui Qian, Robby T Tan, Wenhan Yang, Jiajun Su, and Jiaying Liu. Attentive generative adversarial network for raindrop removal from a single image. In *Proceedings of the Conference on Computer Vision and Pattern Recognition*, pages 2482–2491, 2018.

[43] Behnood Rasti, Yi Chang, Emanuele Dalsasso, Loic Denis, and Pedram Ghamisi. Image restoration for remote sensing: Overview and toolbox. *IEEE Geoscience and Remote Sensing Magazine*, 10(2):201–230, 2021.

[44] Marien Renaud, Jiaming Liu, Valentin de Bortoli, Andrés Almansa, and Ulugbek Kamilov. Plug-and-play posterior sampling under mismatched measurement and prior models. In *Proceedings of the International Conference on Learning Representations*, 2024.

[45] Jaesung Rim, Haeyun Lee, Jucheol Won, and Sunghyun Cho. Real-world blur dataset for learning and benchmarking deblurring algorithms. In *Proceedings of the European Conference on Computer Vision*, 2020.

[46] Olaf Ronneberger, Philipp Fischer, and Thomas Brox. U-net: Convolutional networks for biomedical image segmentation. In *Proceedings of the Medical Image Computing and Computer-assisted Intervention*, pages 234–241. Springer, 2015.

[47] Litu Rout, Negin Raoof, Giannis Daras, Constantine Caramanis, Alex Dimakis, and Sanjay Shakkottai. Solving linear inverse problems provably via posterior sampling with latent diffusion models. *Advances in Neural Information Processing Systems*, 36:49960–49990, 2023.

[48] Chitwan Saharia, Jonathan Ho, William Chan, Tim Salimans, David J Fleet, and Mohammad Norouzi. Image super-resolution via iterative refinement. *IEEE Transactions on Pattern Analysis and Machine Intelligence*, 45(4):4713–4726, 2022.

[49] Jiaming Song, Chenlin Meng, and Stefano Ermon. Denoising diffusion implicit models. In *Proceedings of the International Conference on Learning Representations*.

[50] Yang Song, Jascha Sohl-Dickstein, Diederik P Kingma, Abhishek Kumar, Stefano Ermon, and Ben Poole. Score-based generative modeling through stochastic differential equations. In *Proceedings of the International Conference on Learning Representations*.

[51] James William Thomas. *Numerical partial differential equations: finite difference methods*, volume 22. Springer Science & Business Media, 2013.

[52] Zhengzhong Tu, Hossein Talebi, Han Zhang, Feng Yang, Peyman Milanfar, Alan Bovik, and Yinxiao Li. Maxim: Multi-axis mlp for image processing. In *Proceedings of the Conference on Computer Vision and Pattern Recognition*, pages 5769–5780, 2022.

[53] Shuhang Wang, Jin Zheng, Hai-Miao Hu, and Bo Li. Naturalness preserved enhancement algorithm for non-uniform illumination images. *IEEE Transactions on Image Processing*, 22(9):3538–3548, 2013.

[54] Zhou Wang, Alan C Bovik, Hamid R Sheikh, and Eero P Simoncelli. Image quality assessment: from error visibility to structural similarity. *IEEE Transactions on Image Processing*, 13(4):600–612, 2004.

[55] Chen Wei, Wenjing Wang, Wenhan Yang, and Jiaying Liu. Deep retinex decomposition for low-light enhancement. *arXiv preprint arXiv:1808.04560*, 2018.

[56] Jay Whang, Mauricio Delbracio, Hossein Talebi, Chitwan Saharia, Alexandros G Dimakis, and Peyman Milanfar. Deblurring via stochastic refinement. In *Proceedings of the Conference on Computer Vision and Pattern Recognition*, pages 16293–16303, 2022.

[57] Gui-Song Xia, Jingwen Hu, Fan Hu, Baoguang Shi, Xiang Bai, Yanfei Zhong, Liangpei Zhang, and Xiaoqiang Lu. Aid: A benchmark data set for performance evaluation of aerial scene classification. *IEEE Transactions on Geoscience and Remote Sensing*, 55(7):3965–3981, 2017.

[58] Hao Yang, Liyuan Pan, Yan Yang, and Wei Liang. Language-driven all-in-one adverse weather removal. In *Proceedings of the Conference on Computer Vision and Pattern Recognition*, pages 24902–24912, 2024.

[59] Kunping Yang, Gui-Song Xia, Zicheng Liu, Bo Du, Wen Yang, Marcello Pelillo, and Liangpei Zhang. Semantic change detection with asymmetric siamese networks. *arXiv preprint arXiv:2010.05687*, 2020.

[60] Wenhan Yang, Robby T Tan, Jiashi Feng, Jiaying Liu, Zongming Guo, and Shuicheng Yan. Deep joint rain detection and removal from a single image. In *Proceedings of the Conference on Computer Vision and Pattern Recognition*, pages 1357–1366, 2017.

[61] Syed Waqas Zamir, Aditya Arora, Salman Khan, Munawar Hayat, Fahad Shahbaz Khan, and Ming-Hsuan Yang. Restormer: Efficient transformer for high-resolution image restoration. In *Proceedings of the Conference on Computer Vision and Pattern Recognition*, pages 5728–5739, 2022.

[62] He Zhang and Vishal M Patel. Density-aware single image de-raining using a multi-stream dense network. In *Proceedings of the Conference on Computer Vision and Pattern Recognition*, pages 695–704, 2018.

[63] Jing Zhang, Yang Cao, Shuai Fang, Yu Kang, and Chang Wen Chen. Fast haze removal for nighttime image using maximum reflectance prior. In *Proceedings of the Conference on Computer Vision and Pattern Recognition*, pages 7418–7426, 2017.

[64] Jinghao Zhang, Jie Huang, Mingde Yao, Zizheng Yang, Hu Yu, Man Zhou, and Feng Zhao. Ingredient-oriented multi-degradation learning for image restoration. In *Proceedings of the Conference on Computer Vision and Pattern Recognition*, pages 5825–5835, 2023.

[65] Zhilu Zhang, Shuohao Zhang, Renlong Wu, Wangmeng Zuo, Radu Timofte, Xiaoxia Xing, Hyunhee Park, Sejun Song, Changho Kim, Xiangyu Kong, et al. Ntire 2024 challenge on bracketing image restoration and enhancement: Datasets methods and results. In *Proceedings of the Conference on Computer Vision and Pattern Recognition*, pages 6153–6166, 2024.

[66] Haiyu Zhao, Lei Tian, Xinyan Xiao, Peng Hu, Yuanbiao Gou, and Xi Peng. Avernet: All-in-one video restoration for time-varying unknown degradations. *Advances in Neural Information Processing Systems*, 37:127296–127316, 2025.

[67] Dian Zheng, Xiao-Ming Wu, Shuzhou Yang, Jian Zhang, Jian-Fang Hu, and Wei-Shi Zheng. Selective hourglass mapping for universal image restoration based on diffusion model. In *Proceedings of the Conference on Computer Vision and Pattern Recognition*, pages 25445–25455, 2024.

[68] Weixun Zhou, Shawn Newsam, Congmin Li, and Zhenfeng Shao. Patternnet: A benchmark dataset for performance evaluation of remote sensing image retrieval. *ISPRS Journal of Photogrammetry and Remote Sensing*, 145:197–209, 2018.

A Mathematical Theory of Diffusion Models

Diffusion models that are most pertinent to our methods are theoretically discussed as follows, including diffusion probabilistic models (DPMs), diffusion residual models (DRMs), and diffusion generalist models (DGMs). For each category, we analyze their discrete formulations of perturbed generation process [14] and deterministic implicit sampling [49], and continuous formulations of score-based stochastic differential equations (SDEs).

A.1 Forward Process of Diffusion Probabilistic Models

Diffusion probabilistic models consist of a non-parametric noise addition forward process and a denoising reverse process. In the forward process, it gradually disrupts the original image content by adding the Gaussian noise. The sampling distribution in a markovian manner between the adjacent time step, *i.e.* I_t and I_{t-1}, can be defined as $q(I_t|I_{t-1}) = \mathcal{N}(\alpha_t I_{t-1}, \beta_t \boldsymbol{I})$, which is equivalent to:

$$I_t = \alpha_t I_{t-1} + \beta_t \epsilon, \tag{22}$$

where α_t and $\beta_t = \sqrt{1-\alpha_t^2}$ are predefined coefficients over time t to modulate the image content and noise intensity, respectively. ϵ is a random variable following the normal Gaussian distribution $\mathcal{N}(0, \boldsymbol{I})$.

A.2 Perturbed Generation Process of Diffusion Probabilistic Models

By the property of the markovian chain, Eq. (22) can be converted to the below formula that DPMs can diffuse from the clean image I_0 to any intermediate variable I_t at time step t in just one step:

$$I_t = \overline{\alpha}_t I_0 + \overline{\beta}_t \epsilon, \tag{23}$$

where $\overline{\alpha}_t = \prod_{i=0}^{t} \alpha_i$ and $\overline{\beta}_t = \sqrt{1-\overline{\alpha}_t^2}$ are denoted for simplicity. Based on Bayesian formula, we have:

$$q(I_t|I_{t-1}) = \mathcal{N}(\alpha_t I_{t-1}, \beta_t \boldsymbol{I}),\ q(I_{t-1}|I_0) = \mathcal{N}(\overline{\alpha}_{t-1} I_0, \overline{\beta}_{t-1} \boldsymbol{I}),\ q(I_t|I_0) = \mathcal{N}(\overline{\alpha}_t I_0, \overline{\beta}_t \boldsymbol{I}). \tag{24}$$

$$\begin{aligned} q(I_{t-1}|I_t, I_0) &= \frac{q(I_t|I_{t-1})q(I_{t-1}|I_0)}{q(I_t|I_0)} = \exp\{\log q(I_t|I_{t-1}) + \log q(I_{t-1}|I_0) - \log q(I_t|I_0)\} \\ &\propto \exp\left\{ -\frac{(I_t - \alpha_t I_{t-1})^2}{2\beta_t^2} - \frac{(I_{t-1} - \overline{\alpha}_{t-1} I_0)^2}{2\overline{\beta}_{t-1}^2} + \frac{(I_t - \overline{\alpha}_t I_0)^2}{2\overline{\beta}_t^2} \right\} \\ &\propto \exp\left\{ -\frac{1}{2}\left(\frac{\alpha_t^2}{\beta_t^2} + \frac{1}{\overline{\beta}_{t-1}^2}\right) I_{t-1}^2 - 2I_{t-1}\left(\frac{\alpha_t I_t}{\beta_t^2} + \frac{\overline{\alpha}_{t-1} I_0}{\overline{\beta}_{t-1}^2}\right) + C(I_t, I_0) \right\}. \end{aligned} \tag{25}$$

Apparently, Eq. (25) can be supposed as a general Gaussian distribution $\mathcal{N}(\mu_{t-1}, \Sigma_{t-1}\boldsymbol{I})$:

$$\Sigma_{t-1}^2(I_{t-1}|I_t, I_0) = \left(\frac{\alpha_t^2}{\beta_t^2} + \frac{1}{\overline{\beta}_{t-1}^2}\right)^{-1} = \frac{\beta_t^2 \overline{\beta}_{t-1}^2}{\overline{\beta}_t^2}, \tag{26}$$

$$\mu_{t-1}(I_{t-1}|I_t, I_0) = \left(\frac{\alpha_t I_t}{\beta_t^2} + \frac{\overline{\alpha}_{t-1} I_0}{\overline{\beta}_{t-1}^2}\right)\frac{\beta_t^2 \overline{\beta}_{t-1}^2}{\overline{\beta}_t^2} = \frac{\alpha_t \overline{\beta}_{t-1}^2}{\overline{\beta}_t^2} I_t + \frac{\overline{\alpha}_{t-1} \beta_t^2}{\overline{\beta}_t^2} I_0. \tag{27}$$

Consequently, the inverse process is regarded as sampling from the following Gaussian distribution step by step:

$$q(I_{t-1}|I_t, I_0) = \mathcal{N}\left(\frac{\alpha_t \overline{\beta}_{t-1}^2}{\overline{\beta}_t^2} I_t + \frac{\overline{\alpha}_{t-1} \beta_t^2}{\overline{\beta}_t^2} I_0, \frac{\beta_t^2 \overline{\beta}_{t-1}^2}{\overline{\beta}_t^2} \boldsymbol{I}\right), \tag{28}$$

$$I_{t-1} = \frac{\alpha_t \overline{\beta}_{t-1}^2}{\overline{\beta}_t^2} I_t + \frac{\overline{\alpha}_{t-1} \beta_t^2}{\overline{\beta}_t^2} I_0 + \frac{\beta_t^2 \overline{\beta}_{t-1}^2}{\overline{\beta}_t^2} \epsilon. \tag{29}$$

A.3 Deterministic Implicit Sampling of Diffusion Probabilistic Models

Discarding the markovian modeling $q(I_t|I_{t-1})$ in the forward process and assuming that the sampling distribution still follows the Gaussian distribution in the reverse process, we can obtain:

$$q(I_t|I_0) = \mathcal{N}(I_t; \overline{\alpha}_t I_0, \overline{\beta}_t^2 \boldsymbol{I}) \rightarrow I_t = \overline{\alpha}_t I_0 + \overline{\beta}_t \epsilon_1, \tag{30}$$

$$q(I_{t-1}|I_0) = \mathcal{N}(I_{t-1}; \overline{\alpha}_{t-1} I_0, \overline{\beta}_{t-1}^2 \boldsymbol{I}) \rightarrow I_{t-1} = \overline{\alpha}_{t-1} I_0 + \overline{\beta}_{t-1} \epsilon_2, \tag{31}$$

$$q(I_{t-1}|I_0, I_t) = \mathcal{N}(I_{t-1}; \kappa_t I_t + \lambda_t I_0, \sigma_t^2 \boldsymbol{I}) \rightarrow I_{t-1} = \kappa_t I_t + \lambda_t I_0 + \sigma_t \epsilon_3. \tag{32}$$

Substituting Eq. (30) into Eq. (32) and comparing the coefficients with Eq. (31), we have:

$$I_{t-1} = (\kappa_t \overline{\alpha}_t + \lambda_t) I_0 + \kappa_t \overline{\beta}_t \epsilon_1 + \sigma_t \epsilon_3 = (\kappa_t \overline{\alpha}_t + \lambda_t) I_0 + \sqrt{\kappa_t^2 \overline{\beta}_t^2 + \sigma_t^2} \epsilon, \tag{33}$$

$$\overline{\alpha}_{t-1} = \kappa_t \overline{\alpha}_t + \lambda_t, \quad \overline{\beta}_{t-1}^2 = \kappa_t^2 \overline{\beta}_t^2 + \sigma_t^2, \tag{34}$$

these parameters can be calculated as:

$$\kappa_t = \frac{\sqrt{\overline{\beta}_{t-1}^2 - \sigma_t^2}}{\overline{\beta}_t}, \quad \lambda_t = \overline{\alpha}_{t-1} - \frac{\overline{\alpha}_t \sqrt{\overline{\beta}_{t-1}^2 - \sigma_t^2}}{\overline{\beta}_t}. \tag{35}$$

Consequently, a common reverse process in the non-markovian manner is:

$$q(I_{t-1}|I_0, I_t) = \mathcal{N}(\frac{\sqrt{\overline{\beta}_{t-1}^2 - \sigma_t^2}}{\overline{\beta}_t} I_t + (\overline{\alpha}_{t-1} - \frac{\overline{\alpha}_t \sqrt{\overline{\beta}_{t-1}^2 - \sigma_t^2}}{\overline{\beta}_t}) I_0, \sigma_t^2 \boldsymbol{I}). \tag{36}$$

If we set the variance σ_t equal to $\frac{\beta_t^2 \overline{\beta}_{t-1}^2}{\overline{\beta}_t^2}$, Eq. (36) holds the identical distributions with Eq. (28). Typically, we can derive another representative sampling distribution by setting variance σ_t equal to 0:

$$q(I_{t-1}|I_0, I_t)|_{\sigma_t=0} = \mathcal{N}(\frac{\overline{\beta}_{t-1}}{\overline{\beta}_t} I_t + (\overline{\alpha}_{t-1} - \frac{\overline{\alpha}_t \overline{\beta}_{t-1}}{\overline{\beta}_t}) I_0, \sigma_t^2 \boldsymbol{I}), \tag{37}$$

in this way, the inverse process is deterministic for ignoring the random noise:

$$I_{t-1} = \frac{\overline{\beta}_{t-1}}{\overline{\beta}_t} I_t + (\overline{\alpha}_{t-1} - \frac{\overline{\alpha}_t \overline{\beta}_{t-1}}{\overline{\beta}_t}) I_0. \tag{38}$$

A.4 Training Objective of Diffusion Probabilistic Models

The training objective for the noise estimators ϵ_θ in DPMs is calculated as follows:

$$\mathcal{L} = \mathbb{E}_{I_0, \epsilon} \left[\|\epsilon - \epsilon_\theta(\overline{\alpha}_t I_0 + \overline{\beta}_t \epsilon)\|^2 \right]. \tag{39}$$

A.5 Stochastic Differential Equations of Diffusion Probabilistic Models

The formulation of SDEs of DPMs' forward process can be reformulated from a continuous perspective with diffusion term $f_t(I_t)$ and drift term g_t as follows:

$$dI_t = f_t(I_t) dt + g_t d\omega_t, \tag{40}$$

where ω_t is the standard Wiener process. Its formulation of inverse SDEs can be proved as follows [20]:

$$dI_t = [f_t(I_t) - g_t^2 \nabla_{I_t} \log p_{I_t}(I_t)] dt + g_t d\overline{\omega}_t. \tag{41}$$

Similarly, we modify the formulas in Eq. (30)-(32) and consider the linear solution $f_t(I_t) = f_t I_t$:

$$q(I_{t+\Delta t}|I_0) = \mathcal{N}(I_{t+\Delta t}; \overline{\alpha}_{t+\Delta t} I_0, \overline{\beta}_{t+\Delta t}^2 \boldsymbol{I}) \rightarrow I_{t+\Delta t} = \overline{\alpha}_{t+\Delta t} I_0 + \overline{\beta}_{t+\Delta t} \epsilon_1, \tag{42}$$

$$q(I_t|I_0) = \mathcal{N}(I_t; \overline{\alpha}_t I_0, \overline{\beta}_t^2 \boldsymbol{I}) \rightarrow I_t = \overline{\alpha}_t I_0 + \overline{\beta}_t \epsilon_2, \tag{43}$$

$$q(I_{t+\Delta t}|I_t) = \mathcal{N}(I_{t+\Delta t}; (1 + f_t \Delta t) I_t, g_t^2 \Delta t \boldsymbol{I}) \rightarrow I_{t+\Delta t} = (1 + f_t \Delta t) I_t + g_t \sqrt{\Delta t} \epsilon_3. \tag{44}$$

We can obtain:

$$\overline{\alpha}_{t+\Delta t} = (1 + f_t \Delta t) \overline{\alpha}_t, \tag{45}$$

$$\overline{\beta}_{t+\Delta t}^2 = (1 + f_t \Delta t)^2 \overline{\beta}_t^2 + g_t^2 \Delta t, \tag{46}$$

By setting $\Delta t \rightarrow 0$, we can derive:

$$f_t = \frac{1}{\overline{\alpha}_t} \frac{d\overline{\alpha}_t}{dt} = \frac{d}{dt} (\ln \overline{\alpha}_t), \quad g_t^2 = \overline{\alpha}_t^2 \frac{d}{dt} \left(\frac{\overline{\beta}_t^2}{\overline{\alpha}_t^2} \right) = 2 \overline{\alpha}_t \overline{\beta}_t \frac{d}{dt} \left(\frac{\overline{\beta}_t}{\overline{\alpha}_t} \right). \tag{47}$$

A.6 Forward Process of Diffusion Residual models

Diffusion residual models additionally incorporate a residual term I_{res} to assist the forward process. The forward process between adjacent steps is defined as:

$$q(I_t|I_{t-1}, I_{res}) = \mathcal{N}(I_t; I_{t-1} + \alpha_t I_{res}, \beta_t^2 \boldsymbol{I}), \tag{48}$$

$$I_t = I_{t-1} + \alpha_t I_{res} + \beta_t \epsilon, \tag{49}$$

where $I_{res} = I_{in} - I_0$. By the properties of Markov Chain and reparameterization, we have:

$$q(I_t|I_0, I_{res}) = \mathcal{N}(I_t; I_0 + \overline{\alpha}_t I_{res}, \overline{\beta}_t^2 \boldsymbol{I}), \tag{50}$$

$$\begin{aligned} I_t &= I_{t-1} + \alpha_t I_{res} + \beta_t \epsilon_t = \big[I_{t-2} + \alpha_{t-1} I_{res} + \beta_{t-1}\epsilon_{t-1}\big] + \alpha_t I_{res} + \beta_t \epsilon_t \\ &= I_{t-2} + \big[\alpha_{t-1} + \alpha_t\big] I_{res} + \sqrt{\big[\beta_{t-1}^2 + \beta_t^2\big]}\epsilon \\ &= \cdots \\ &= I_0 + \overline{\alpha}_t I_{res} + \overline{\beta}_t \epsilon, \end{aligned} \tag{51}$$

where $\overline{\alpha}_t = \sum_{i=1}^t \alpha_i$ and $\overline{\beta}_t = \sqrt{\sum_{i=1}^t \beta_i^2}$.

A.7 Perturbed Generation Process of Diffusion Residual Models

Evidently, if $\overline{\alpha}_t \to 1$, the forward process makes the representations of I_0 be the degraded version with additive noise $I_t = I_{in} + \overline{\beta}_t \epsilon$. Similarly, we can obtain:

$$q(I_t|I_{t-1}, I_{res}) = \mathcal{N}(I_t; I_{t-1} + \alpha_t I_{res}, \beta_t^2 \boldsymbol{I}), \tag{52}$$

$$q(I_{t-1}|I_0, I_{res}) = \mathcal{N}(I_{t-1}; I_0 + \overline{\alpha}_{t-1} I_{res}, \overline{\beta}_{t-1}^2 \boldsymbol{I}), \tag{53}$$

$$q(I_t|I_0, I_{res}) = \mathcal{N}(I_t; I_0 + \overline{\alpha}_t I_{res}, \overline{\beta}_t^2 \boldsymbol{I}). \tag{54}$$

Suppose the form of $q(I_{t-1}|I_t, I_0, I_{res})$ belongs to Gaussian distribution family as all the distributions are Gaussian, we can denote:

$$q(I_{t-1}|I_t, I_0, I_{res}) = \mathcal{N}(I_{t-1}|\mu_{t-1}(I_t, I_0, I_{res}), \Sigma_{t-1}(I_t, I_0, I_{res})). \tag{55}$$

To derive the expressions of variables $\mu_{t-1}(I_t, I_0, I_{res})$ and $\Sigma_{t-1}(I_t, I_0, I_{res})$, we take the logarithm directly and ignore the constant term:

$$q(I_{t-1}|I_t, I_0, I_{res}) = \frac{q(I_t|I_{t-1}, I_0, I_{res}) q(I_{t-1}|I_0, I_{res})}{q(I_t|I_0, I_{res})}, \tag{56}$$

$$\begin{aligned} q(I_{t-1}|I_t, I_0, I_{res}) &= \exp\Big\{ \log q(I_t|I_{t-1}, I_0, I_{res}) + \log q(I_{t-1}|I_0, I_{res}) - \log q(I_t|I_0, I_{res}) \Big\} \\ &\propto \exp\Big\{ -\frac{\big(I_t - (I_{t-1} + \alpha_t I_{res})\big)^2}{2\beta_t^2} - \frac{\big(I_{t-1} - (I_0 + \overline{\alpha}_{t-1} I_{res})\big)^2}{2\overline{\beta}_{t-1}^2} + \frac{\big(I_t - (I_0 + \overline{\alpha}_t I_{res})\big)^2}{2\overline{\beta}_t^2} \Big\} \\ &\propto \exp\Big\{ -\frac{1}{2}\Big((\frac{1}{\beta_t^2} + \frac{1}{\overline{\beta}_{t-1}^2}) I_{t-1}^2 - 2 I_{t-1} \big(\frac{I_t - \alpha_t I_{res}}{\beta_t^2} + \frac{I_0 + \overline{\alpha}_{t-1} I_{res}}{\overline{\beta}_{t-1}^2} \big) + C(I_t, I_0, I_{res}) \Big) \Big\}. \end{aligned} \tag{57}$$

Comparing the coefficients, we can derive the variables as below:

$$\Sigma_{t-1}^2(I_t, I_0, I_{res}) = \frac{\beta_t^2 \overline{\beta}_{t-1}^2}{\beta_t^2 + \overline{\beta}_{t-1}^2} = \frac{\beta_t^2 \overline{\beta}_{t-1}^2}{\overline{\beta}_t^2}, \tag{58}$$

$$\mu_{t-1}(I_t, I_0, I_{res}) = \big(\frac{I_t - \alpha_t I_{res}}{\beta_t^2} + \frac{I_0 + \overline{\alpha}_{t-1} I_{res}}{\overline{\beta}_{t-1}^2} \big) \frac{\beta_t^2 \overline{\beta}_{t-1}^2}{\overline{\beta}_t^2} = I_t - \alpha_t I_{res} - \frac{\beta_t^2}{\overline{\beta}_t} \epsilon. \tag{59}$$

A.8 Deterministic Implicit Sampling of Diffusion Residual Models

For generality, we discard the assumptions that the forward process follows a Markov Chain and denote:

$$q(I_{t-1}|I_0, I_{res}) = \mathcal{N}(I_{t-1}; I_0 + \overline{\alpha}_{t-1} I_{res}, \overline{\beta}_{t-1}^2 \boldsymbol{I}), \tag{60}$$

$$q(I_t|I_0, I_{res}) = \mathcal{N}(I_t; I_0 + \overline{\alpha}_t I_{res}, \overline{\beta}_t^2 \boldsymbol{I}), \tag{61}$$

then the conditional distribution $q(I_{t-1}|I_0, I_t)$ can be defined as:

$$q(I_{t-1}|I_0, I_t, I_{res}) = \mathcal{N}(I_{t-1}; \lambda_t I_0 + \kappa_t I_t + \eta_t I_{res}, \sigma_t^2 \boldsymbol{I}). \tag{62}$$

we can reformulate the probability formulas into algebraic expressions:

$$I_{t-1} = I_0 + \overline{\alpha}_{t-1} I_{res} + \overline{\beta}_{t-1} \epsilon, \tag{63}$$

$$I_t = I_0 + \overline{\alpha}_t I_{res} + \overline{\beta}_t \epsilon, \tag{64}$$

$$
\begin{aligned}
I_{t-1} &= \lambda_t I_0 + \kappa_t I_t + \eta_t I_{res} + \sigma_t \dot{\epsilon} \\
&= \lambda_t I_0 + \kappa_t (I_0 + \overline{\alpha}_t I_{res} + \overline{\beta}_t \epsilon) + \eta_t I_{res} + \sigma_t \dot{\epsilon} \\
&= (\lambda_t + \kappa_t) I_0 + (\kappa_t \overline{\alpha}_t + \eta_t) I_{res} + (\kappa_t^2 \overline{\beta}_t^2 + \sigma_t^2)^{\frac{1}{2}} \epsilon.
\end{aligned} \tag{65}
$$

By comparing the coefficients of Eq.(65) and Eq.(63), we can get the following quadratic equation:

$$
\begin{cases}
\lambda_t + \kappa_t = 1, \\
\kappa_t \overline{\alpha}_t + \eta_t = \overline{\alpha}_{t-1}, \\
\kappa_t^2 \overline{\beta}_t^2 + \sigma_t^2 = \overline{\beta}_{t-1}^2.
\end{cases} \tag{66}
$$

To complete the derivation, we treat σ_t^2 as a predefined parameters:

$$
\kappa_t = \sqrt{\frac{\overline{\beta}_{t-1}^2 - \sigma_t^2}{\overline{\beta}_t^2}}, \quad \eta_t = \overline{\alpha}_{t-1} - \overline{\alpha}_t \sqrt{\frac{\overline{\beta}_{t-1}^2 - \sigma_t^2}{\overline{\beta}_t^2}}, \quad \lambda_t = 1 - \sqrt{\frac{\overline{\beta}_{t-1}^2 - \sigma_t^2}{\overline{\beta}_t^2}}. \tag{67}
$$

Consequently, the inverse process can be formally simplified as:

$$
\mu_{t-1} = I_t - \alpha_t I_{res} - (\overline{\beta}_t - \sqrt{\overline{\beta}_{t-1}^2 - \sigma_t^2})\epsilon. \tag{68}
$$

Obviously, the mean of $q(I_{t-1}|I_0, I_t, I_{res})$ is manipulated by the variance intensity σ_t. If we make σ_t^2 equals that of Eq. (58), then the value of μ_{t-1} in Eq.(68) equals that of Eq. (59). Besides, if we make σ_t^2 equals to 0, then the deterministic inverse process can be denoted as:

$$
I_{t-1} = I_t - \alpha_t I_{res} - (\overline{\beta}_t - \overline{\beta}_{t-1})\epsilon. \tag{69}
$$

A.9 Training Objective of Diffusion Residual Models

The training objective of DRMs is calculated as follows:

$$
\mathcal{L} = \mathbb{E}\left[\left\| I_t - \alpha_t I_{res} - \frac{\beta_t^2}{\overline{\beta}}\epsilon - (I_t - \alpha_t I_{res}^{\theta} - \frac{\beta_t^2}{\overline{\beta}}\epsilon_\theta) \right\|\right]. \tag{70}
$$

Leveraging Eq. 51, then Eq. 70 can be simplified into two equivalent formulas:

$$
\mathcal{L} = \mathbb{E}\big[\lambda_{res} \big\| I_{res} - I_{res}^{\theta}(I_t, I_{in}, t) \big\|\big], \tag{71}
$$

$$
\mathcal{L} = \mathbb{E}\big[\lambda_{\epsilon} \big\| \epsilon - \epsilon_\theta(I_t, I_{in}, t) \big\|\big], \tag{72}
$$

where the weights, *i.e.*, $\lambda_{res}, \lambda_\epsilon \in \{0, 1\}$, are the balance coefficients.

A.10 Stochastic Differential Equations of Diffusion Residual Models

Like the derivation from Eq. (42) to Eq. (46), we have:

$$
q(I_t|I_0, I_{res}, I_{in}) = \mathcal{N}(I_t; I_0 + \overline{\alpha}_t I_{res}, \overline{\beta}_t^2 \boldsymbol{I}), \tag{73}
$$

$$
q(I_{t+\Delta t}|I_0, I_{res}, I_{in}) = \mathcal{N}(I_{t+\Delta t}; I_0 + \overline{\alpha}_{t+\Delta t} I_{res}, \overline{\beta}_{t+\Delta t}^2 \boldsymbol{I}), \tag{74}
$$

$$
q(I_{t+\Delta t}|I_t, I_{res}, I_{in}) = \mathcal{N}(I_{t+\Delta t}; (1 + f(t)\Delta t) I_t + h(t)\Delta t I_{res}, g^2(t)\Delta t \boldsymbol{I}), \tag{75}
$$

the marginal distribution $\int q(I_{t+\Delta t}|I_t) q(I_t|I_0) dI_t$ can be computed as:

$$
I_{t+\Delta t} = (1 + f(t)\Delta t)(I_0 + \overline{\alpha}_t I_{res} + \overline{\beta}_t \epsilon_1) + h(t)\Delta t I_{res} + g(t)\sqrt{\Delta t}\epsilon_2. \tag{76}
$$

Comparing the undetermined coefficients in Eq. 74 with Eq. 76:

$$
1 + f(t)\Delta t = 1, \tag{77}
$$

$$
h(t)\Delta t + (1 + f(t)\Delta t)\overline{\alpha}_t = \overline{\alpha}_{t+\Delta t}, \tag{78}
$$

$$
(1 + f(t)\Delta t)^2 \overline{\beta}_t^2 + g^2(t)\Delta t = \overline{\beta}_{t+\Delta t}^2, \tag{79}
$$

then the above four functions can be solved as follows:

$$
f(t) = 0, \quad h(t) = \frac{\overline{\alpha}_{t+\Delta t} - \overline{\alpha}_t}{\Delta t}, \quad g^2(t) = \frac{\overline{\beta}_{t+\Delta t}^2 - \overline{\beta}_t^2}{\Delta t}. \tag{80}
$$

Let $\Delta t \to 0$, then:

$$
f(t) = 0, \quad h(t) = \frac{d\overline{\alpha}_t}{dt}, \quad g^2(t) = \frac{d\overline{\beta}_t^2}{dt} = 2\overline{\beta}_t \frac{d\overline{\beta}_t}{dt}. \tag{81}
$$

A.11 Forward Process of Diffusion Generalist Model

Based on the formulation of DGMs, diffusion generalist models additionally incorporate the degraded image manipulated by δ_t in the forward process:

$$q(I_t|I_{t-1}, I_{res}, I_{in}) = \mathcal{N}(I_t; I_{t-1} + \alpha_t I_{res} - \delta_t I_{in}, \beta_t^2 \boldsymbol{I}), \tag{82}$$

$$I_t = I_{t-1} + \alpha_t I_{res} + \beta_t \epsilon_t - \delta_t I_{in}, \tag{83}$$

Leveraging the property of Markov Chain and reparameterization, we have:

$$\begin{aligned} I_t &= I_{t-1} + \alpha_t I_{res} + \beta_t \epsilon_t - \delta_t I_{in} \\ &= \big[I_{t-2} + \alpha_{t-1} I_{res} + \beta_{t-1}\epsilon_{t-1} - \delta_{t-1} I_{in}\big] + \alpha_t I_{res} + \beta_t \epsilon_t - \delta_t I_{in} \\ &= I_{t-2} + \big[\alpha_{t-1} + \alpha_t\big] I_{res} + \sqrt{\big[\beta_{t-1}^2 + \beta_t^2\big]}\epsilon + \big[\delta_{t-1} + \delta_t\big] I_{in} \\ &= \cdots \\ &= I_0 + \overline{\alpha}_t I_{res} + \overline{\beta}_t \epsilon - \overline{\delta}_t I_{in} \\ &= (\overline{\alpha}_t - 1) I_{res} + \overline{\beta}_t \epsilon + (1 - \overline{\delta}_t) I_{in}, \end{aligned} \tag{84}$$

where $\overline{\alpha}_t = \sum_{i=1}^t \alpha_i, \overline{\beta}_t = \sqrt{\sum_{i=1}^t \beta_i^2}$ and $\overline{\delta}_t = \sum_{i=1}^t \delta_i$. If $\overline{\alpha}_t \to 1$, clean images are diffused as:

$$I_t = (1 - \overline{\delta}_t) I_{in} + \overline{\beta}_t \epsilon. \tag{85}$$

Thus, we obtain an expression for degraded image representation, in which $\overline{\delta}_t$ plays a role in controlling the commonality. If $\overline{\delta}_t \to 0$, Eq. (85) degrades to the pattern of diffusion residual models; whereas if $\overline{\delta}_t \to 1$, all representations are unified into a pure Gaussian distribution.

A.12 Perturbed Generation Process of Diffusion Generalist Models

By repeating the aforementioned derivation process, akin to Eq. (52)-Eq. (57), we have:

$$q(I_t|I_{t-1}, I_{res}, I_{in}) = \mathcal{N}(I_t; I_{t-1} + \alpha_t I_{res} - \delta_t I_{in}, \beta_t^2 \boldsymbol{I}), \tag{86}$$

$$q(I_{t-1}|I_0, I_{res}, I_{in}) = \mathcal{N}(I_{t-1}; I_0 + \overline{\alpha}_{t-1} I_{res} - \overline{\delta}_{t-1} I_{in}, \overline{\beta}_{t-1}^2 \boldsymbol{I}), \tag{87}$$

$$q(I_t|I_0, I_{res}, I_{in}) = \mathcal{N}(I_t; I_0 + \overline{\alpha}_t I_{res} - \overline{\delta}_t I_{in}, \overline{\beta}_t^2 \boldsymbol{I}). \tag{88}$$

$$\begin{aligned} q(I_{t-1}|I_t, I_{res}, I_{in}) &= \exp\Big\{ \log q(I_t|I_{t-1}, I_{res}, I_{in}) + \log q(I_{t-1}|I_{res}, I_{in}) - \log q(I_t|I_{res}, I_{in}) \Big\} \\ &\propto \exp\Big\{ -\frac{\big(I_t - (I_{t-1} + \alpha_t I_{res} - \delta_t I_{in})\big)^2}{2\beta_t^2} - \frac{\big(I_{t-1} - (\overline{\alpha}_{t-1} - 1) I_{res} - (1 - \overline{\delta}_{t-1}) I_{in}\big)^2}{2\overline{\beta}_{t-1}^2} \\ &\qquad + \frac{\big(I_t - (\overline{\alpha}_t - 1) I_{res} - (1 - \overline{\delta}_t) I_{in}\big)^2}{2\overline{\beta}_t^2} \Big\} \\ &\propto \exp\Big\{ -\frac{1}{2}\Big((\frac{1}{\beta_t^2} + \frac{1}{\overline{\beta}_{t-1}^2}) I_{t-1}^2 - 2 I_{t-1} \big(\frac{I_t - \alpha_t I_{res} + \delta_t I_{in}}{\beta_t^2} + \frac{(\overline{\alpha}_{t-1} - 1) I_{res} + (1 - \overline{\delta}_{t-1}) I_{in}}{\overline{\beta}_{t-1}^2} \big) + C(I_t, I_0, I_{res}) \Big) \Big\}. \end{aligned} \tag{89}$$

Comparing the coefficients of each term, we can obtain:

$$\Sigma_{t-1}^2(I_t, I_{in}, I_{res}) = \frac{\beta_t^2 \overline{\beta}_{t-1}^2}{\beta_t^2 + \overline{\beta}_{t-1}^2} = \frac{\beta_t^2 \overline{\beta}_{t-1}^2}{\overline{\beta}_t^2}, \tag{90}$$

$$\begin{aligned} \mu_{t-1}(I_t, I_{in}, I_{res}) &= \big(\frac{I_t - \alpha_t I_{res} + \delta I_{in}}{\beta_t^2} + \frac{I_0 + \overline{\alpha}_{t-1} I_{res} - \overline{\delta}_{t-1} I_{in}}{\overline{\beta}_{t-1}^2} \big) \frac{\beta_t^2 \overline{\beta}_{t-1}^2}{\overline{\beta}_t^2} \\ &= \frac{1}{\overline{\beta}_t^2} \big(\overline{\beta}_{t-1}^2 I_t - \alpha_t \overline{\beta}_{t-1}^2 I_{res} + \delta_t \overline{\beta}_{t-1}^2 I_{in} + \beta_t^2 I_0 + \overline{\alpha}_{t-1} \beta_t^2 I_{res} - \overline{\delta}_{t-1} \beta_t^2 I_{in} \big) \\ &= \frac{\overline{\beta}_{t-1}^2}{\overline{\beta}_t^2} I_t + \frac{\overline{\alpha}_{t-1} \beta_t^2 - \alpha_t \overline{\beta}_{t-1}^2}{\overline{\beta}_t^2} I_{res} + \frac{\delta_t \overline{\beta}_{t-1}^2 - \overline{\delta}_{t-1} \beta_t^2}{\overline{\beta}_t^2} I_{in} + \frac{\beta_t^2}{\overline{\beta}_t^2} (I_t - \overline{\alpha}_t I_{res} - \overline{\beta}_t \epsilon + \overline{\delta}_t I_{in}) \\ &= I_t - \alpha_t I_{res} + \delta_t I_{in} - \frac{\beta_t^2}{\overline{\beta}_t} \epsilon, \end{aligned} \tag{91}$$

the inverse process can be considered as sampling from the following distribution:

$$q(I_{t-1}|I_t, I_0, I_{res}, I_{in}) \sim \mathcal{N}(I_{t-1}|I_t - \alpha_t I_{res} + \delta_t I_{in} - \frac{\beta_t^2}{\overline{\beta}_t} \epsilon; \frac{\beta_t \overline{\beta}_{t-1}}{\overline{\beta}_t} \boldsymbol{I}). \tag{92}$$

A.13 Deterministic Implicit Sampling of Diffusion Generalist Models

A common forward process can be determined as follows:

$$q(I_{t-1}|I_0, I_{res}, I_{in}) = \mathcal{N}(I_{t-1}; I_0 + \overline{\alpha}_{t-1} I_{res} - \overline{\delta}_{t-1} I_{in}, \overline{\beta}_{t-1}^2 \boldsymbol{I}), \tag{93}$$

$$q(I_t|I_0, I_{res}, I_{in}) = \mathcal{N}(I_t; I_0 + \overline{\alpha}_t I_{res} - \overline{\delta}_t I_{in}, \overline{\beta}_t^2 \boldsymbol{I}). \tag{94}$$

For simplicity, we still define the formula of the conditional distribution $q(I_{t-1}|I_0, I_t)$ as:

$$q(I_{t-1}|I_t, I_0, I_{res}, I_{in}) = \mathcal{N}(I_{t-1}; \kappa_t I_t + \eta_t I_{res} + \gamma_t I_0 + \zeta_t I_{in}, \sigma_t^2 \boldsymbol{I}), \tag{95}$$

then we can reformulate the probability formulas into algebraic expressions:

$$I_{t-1} = I_0 + \overline{\alpha}_{t-1} I_{res} - \overline{\delta}_{t-1} I_{in} + \overline{\beta}_{t-1} \epsilon_1, \tag{96}$$

$$I_t = I_0 + \overline{\alpha}_t I_{res} - \overline{\delta}_t I_{in} + \overline{\beta}_t \epsilon_2, \tag{97}$$

$$\begin{aligned} I_{t-1} &= \kappa_t I_t + \eta_t I_{res} + \gamma_t I_0 + \zeta_t I_{in} + \sigma_t \epsilon_3 \\ &= \kappa_t \left(I_0 + \overline{\alpha}_t I_{res} - \overline{\delta}_t I_{in} + \overline{\beta}_t \epsilon_2 \right) + \eta_t I_{res} + \gamma_t I_0 + \zeta_t I_{in} + \sigma_t \epsilon_3 \\ &= (\kappa_t + \gamma_t) I_0 + (\kappa_t \overline{\alpha}_t + \eta_t) I_{res} - (\kappa_t \overline{\delta}_t - \zeta_t) I_{in} + (\kappa_t^2 \overline{\beta}_t^2 + \sigma_t^2)^{\frac{1}{2}} \epsilon. \end{aligned} \tag{98}$$

By comparing the coefficients of Eq. (96) and Eq.(98), we have:

$$\kappa_t + \gamma_t = 1, \tag{99}$$

$$\kappa_t \overline{\alpha}_t + \eta_t = \overline{\alpha}_{t-1}, \tag{100}$$

$$\kappa_t \overline{\delta}_t - \zeta_t = \overline{\delta}_{t-1}, \tag{101}$$

$$\kappa_t^2 \overline{\beta}_t^2 + \sigma_t^2 = \overline{\beta}_{t-1}^2. \tag{102}$$

To complete the derivation, we treat σ_t^2 as a known variable:

$$\kappa_t = \sqrt{\frac{\overline{\beta}_{t-1}^2 - \sigma_t^2}{\overline{\beta}_t^2}}, \eta_t = \overline{\alpha}_{t-1} - \overline{\alpha}_t \sqrt{\frac{\overline{\beta}_{t-1}^2 - \sigma_t^2}{\overline{\beta}_t^2}}, \tag{103}$$

$$\gamma_t = 1 - \sqrt{\frac{\overline{\beta}_{t-1}^2 - \sigma_t^2}{\overline{\beta}_t^2}}, \zeta_t = \overline{\delta}_t \sqrt{\frac{\overline{\beta}_{t-1}^2 - \sigma_t^2}{\overline{\beta}_t^2}} - \overline{\delta}_{t-1}, \tag{104}$$

The inverse process in Eq.(98) can be reformulated as:

$$\begin{aligned} I_{t-1} = &\left(\sqrt{\frac{\overline{\beta}_{t-1}^2 - \sigma_t^2}{\overline{\beta}_t^2}} \right) I_t + \left(\overline{\alpha}_{t-1} - \overline{\alpha}_t \sqrt{\frac{\overline{\beta}_{t-1}^2 - \sigma_t^2}{\overline{\beta}_t^2}} \right) I_{res} \\ &+ \left(1 - \sqrt{\frac{\overline{\beta}_{t-1}^2 - \sigma_t^2}{\overline{\beta}_t^2}} \right) I_0 + \left(\overline{\delta}_t \sqrt{\frac{\overline{\beta}_{t-1}^2 - \sigma_t^2}{\overline{\beta}_t^2}} - \overline{\delta}_{t-1} \right) I_{in} + \sigma_t \epsilon. \end{aligned} \tag{105}$$

Furthermore, Eq. (105) can be simplified and decomposed into mean $\mu_{t-1}(I_t, I_0, I_{res})$ and variance $\Sigma_{t-1}^2(I_t, I_0, I_{res})$, which can be denoted as:

$$\mu_{t-1}(I_t, I_0, I_{res}) = I_t - (\overline{\alpha}_t - \overline{\alpha}_{t-1}) I_{res} + (\overline{\delta}_t - \overline{\delta}_{t-1}) I_{in} - \left(\overline{\beta}_t - \sqrt{\overline{\beta}_{t-1}^2 - \sigma_t^2} \right) \epsilon. \tag{106}$$

Similarly, we set the variance to zero for deterministic inverse inference:

$$I_{t-1} = I_t - (\overline{\alpha}_t - \overline{\alpha}_{t-1}) I_{res} + (\overline{\delta}_t - \overline{\delta}_{t-1}) I_{in} - (\overline{\beta}_t - \overline{\beta}_{t-1}) \epsilon. \tag{107}$$

A.14 Training Objective of Diffusion Generalist Models

The training objective of DGMs is calculated as follows:

$$\begin{aligned} \mathcal{L} &= \mathbb{E}\left[\left\| I_t - \alpha_t I_{res} + \delta_t I_{in} - \frac{\beta_t^2}{\overline{\beta}} \epsilon - (I_t - \alpha_t I_{res}^{\theta} + \delta_t I_{in} - \frac{\beta_t^2}{\overline{\beta}} \epsilon_\theta) \right\|_1 \right] \\ &= \mathbb{E}\left[\left\| \alpha_t (I_{res}^{\theta} - I_{res}) + \frac{\beta_t^2}{\overline{\beta}} (\epsilon_\theta - \epsilon) \right\|_1 \right]. \end{aligned} \tag{108}$$

Leveraging the Eq. 84, then Eq. 108 can be simplified into the following formula:

$$\begin{aligned}\mathcal{L} &= \mathbb{E}\big[\big\|\alpha_t(I_{res} - I^{\theta}_{res}(I_t, I_{in}, t)) + \frac{(1-\overline{\alpha}_t)\beta_t^2}{\overline{\beta}_t^2}(I_{res} - I^{\theta}_{res}(I_t, I_{in}, t))\big\|_1\big] \\ &= \mathbb{E}\big[\big\|\lambda_{res}(I_{res} - I^{\theta}_{res}(I_t, I_{in}, t))\big\|_1\big],\end{aligned} \tag{109}$$

where the coefficient λ_{res} is a constant. The detailed training algorithm is summarized in Alg. 1.

Algorithm 1: Training of diffusion generalist model.

Input: I_{in}, I_0 ,$I^{\theta}_{res} = I_{in} - I_0$, $\{\overline{\alpha}_{t_i}\}_{i=0}^{M}$, $\{\overline{\beta}_{t_i}\}_{i=0}^{M}$, $\{\overline{\delta}_{t_i}\}_{i=0}^{M}$, $\{t_i\}_{i=0}^{M}$.

repeat
- $I_0 \sim q(I_0)$
- $i \sim Uniform(1, ..., T)$
- $\epsilon \sim \mathcal{N}(0, \boldsymbol{I})$
- $I_t = I_0 + \overline{\alpha}_{t_i} I_{res} + \overline{\beta}_{t_i}\epsilon - \overline{\delta}_{t_i} I_{in}$
- Take the gradient descent step on
- $\nabla_\theta \|I_{res} - I^{\theta}_{res}(I_{t_i}, I_{in}, t_i)\|_1$

until;

Output: I_{t_0}.

A.15 Stochastic Differential Equations of Diffusion Generalist Models

The forward process is not only constrained by time-related variables I_t but also limited by I_{res} and I_{in}. Therefore, the stochastic differential equations and the inverse equations can be denoted as:

$$dI_t = f(I_t, t)dt + h(I_{res}, t)dt + l(I_{in}, t)dt + g(t)d\omega_t, \quad I_0 \sim q_0(I_0), \tag{110}$$

$$\frac{dI_t}{dt} = [f(I_t, t) + h(I_{res}, t) + l(I_{in}, t) - g^2(t)\nabla \log q_t(I_t)] + g(t)d\overline{\omega}_t, \quad I_t \sim q_T(I_t), \tag{111}$$

where $f(I_t, t) = f(t)I_t, h(I_{res}, t) = h(t)I_{res}$, and $l(I_{in}, t) = l(t)I_{in}$. According to the definitions of Eq. (84), we can derive:

$$q(I_t|I_0, I_{res}, I_{in}) = \mathcal{N}(I_t; I_0 + \overline{\alpha}_t I_{res} - \overline{\delta}_t I_{in}, \overline{\beta}_t^2 \boldsymbol{I}), \tag{112}$$

$$q(I_{t+\Delta t}|I_0, I_{res}, I_{in}) = \mathcal{N}(I_{t+\Delta t}; I_0 + \overline{\alpha}_{t+\Delta t} I_{res} - \overline{\delta}_{t+\Delta t} I_{in}, \overline{\beta}_{t+\Delta t}^2 \boldsymbol{I}), \tag{113}$$

we assume that the general form of the one-step forward process is:

$$q(I_{t+\Delta t}|I_t, I_{res}, I_{in}) = \mathcal{N}((1 + f(t)\Delta t)I_t + h(t)\Delta t I_{res} + l(t)\Delta t I_{in}, g^2(t)\Delta t \boldsymbol{I}), \tag{114}$$

similarly, we compute its marginal distribution $\int q(I_{t+\Delta t}|I_t)q(I_t|I_0)dI_t$:

$$I_{t+\Delta t} = (1 + f(t)\Delta t)(I_0 + \overline{\alpha}_t I_{res} - \overline{\delta}_t I_{in} + \overline{\beta}_t \epsilon_1) + h(t)\Delta t I_{res} + l(t)\Delta t I_{in} + g(t)\sqrt{\Delta t}\epsilon_2, \tag{115}$$

comparing the undetermined coefficients in Eq. 113 with Eq. 115, we have:

$$1 + f(t)\Delta t = 1, \tag{116}$$

$$h(t)\Delta t + (1 + f(t)\Delta t)\overline{\alpha}_t = \overline{\alpha}_{t+\Delta t}, \tag{117}$$

$$l(t)\Delta t - (1 + f(t)\Delta t)\overline{\delta}_t = -\overline{\delta}_{t+\Delta t}, \tag{118}$$

$$(1 + f(t)\Delta t)^2\overline{\beta}_t^2 + g^2(t)\Delta t = \overline{\beta}_{t+\Delta t}^2, \tag{119}$$

then the above four functions can be solved as follows:

$$f(t) = 0, h(t) = \frac{\overline{\alpha}_{t+\Delta t} - \overline{\alpha}_t}{\Delta t}, l(t) = \frac{\overline{\delta}_t - \overline{\delta}_{t+\Delta t}}{\Delta t}, g^2(t) = \frac{\overline{\beta}_{t+\Delta t}^2 - \overline{\beta}_t^2}{\Delta t}, \tag{120}$$

let $\Delta t \to 0$, then we get:

$$f(t) = 0, h(t) = \frac{d\overline{\alpha}_t}{dt}, l(t) = -\frac{d\overline{\delta}_t}{dt}, g^2(t) = \frac{d\overline{\beta}_t^2}{dt}. \tag{121}$$

B Customized Solver for Diffusion Generalist Model

B.1 Reverse ODEs Formulation of Diffusion Generalist Model

For generality, we follow the notations in Section 3. The inherent parameters are time continuous satisfying $\overline{\alpha}(t) = \overline{\alpha}_t, \overline{\delta}(t) = \overline{\delta}_t, \overline{\beta}(t) = \overline{\beta}_t$. The inverse ordinary differential equations can be concretely formulated as [50]:

$$\frac{dI_t}{dt} = \frac{d\overline{\alpha}_t}{dt} I_{res} - \frac{d\overline{\delta}_t}{dt} I_{in} - \frac{1}{2}\frac{d\overline{\beta}_t^2}{dt}\nabla \log q_t(I_t). \tag{122}$$

Given an initial value I_s at time $s > 0$, the solution I_t at each time $s < t < T$ can be computed as:

$$I_t = I_s + \int_s^t \frac{d\overline{\alpha}_\tau}{d\tau} I_{res} d\tau - \int_s^t \frac{d\overline{\delta}_\tau}{d\tau} I_{in} d\tau - \int_s^t \frac{1}{2} \frac{d\overline{\beta}_\tau^2}{d\tau} \nabla \log q_\tau(I_\tau) d\tau. \tag{123}$$

According to ***Tweedie's Formula*** in Lemma 1: Given a Gaussian variable $z \sim \mathcal{N}(z; \mu_z, \Sigma_z^2)$, the estimated parameters μ_z can be computed as follows:

$$\mu_z = z + \Sigma_z^2 \nabla \log P(z). \tag{124}$$

For forward process in Eq.(94), there exists:

$$I_0 + \overline{\alpha}_t I_{res} - \overline{\delta}_t I_{in} = I_t + \overline{\beta}_t^2 \nabla \log P(I_t) = I_t - \overline{\beta}_t \epsilon, \tag{125}$$

$$\nabla \log q_t(I_t) = -\frac{\epsilon}{\overline{\beta}_t}. \tag{126}$$

Hence, substituting the relationships between score functions and noise into Eq.(123), we have:

$$I_t = I_s + \int_s^t \frac{d\overline{\alpha}_\tau}{d\tau} I_{res} d\tau - \int_s^t \frac{d\overline{\delta}_\tau}{d\tau} I_{in} d\tau + \int_s^t \frac{d\overline{\beta}_\tau}{d\tau} \epsilon d\tau, \tag{127}$$

Furthermore, we have:

$$I_t = I_s + \int_s^t \frac{d\overline{\alpha}_\tau}{d\tau} I_{res}^\theta(I_t, I_{in}, \tau) d\tau - I_{in} \int_s^t \frac{d\overline{\delta}_\tau}{d\tau} d\tau + \int_s^t \frac{d\overline{\beta}_\tau}{d\tau} \epsilon_\theta(I_t, I_{in}, \tau) d\tau, \tag{128}$$

where $I_{res} = I_{res}^\theta(I_t, I_{in}, t)$ and $\epsilon_\theta(I_t, I_{in}, t)$ are time-relevant, I_{in} is input degraded image and can be considered as constant. Since the above inherent parameters are time continuous and monotonic for linear noise schedule, there must exist inverse functions satisfying $t = t_{\overline{\alpha}}(\overline{\alpha}(t)) = t_{\overline{\beta}}(\overline{\beta}(t)) = t_{\overline{\delta}}(\overline{\delta}(t))$. We denote $\widehat{I}_{\overline{\alpha}} := I_{t_{\overline{\alpha}}(\overline{\alpha})}$,$I_{res}^\theta(I_\tau, I_{in}, \tau) := \widehat{I}_{res}^\theta(\widehat{I}_{\overline{\alpha}}, I_{in}, \overline{\alpha})$ and $\widehat{I}_{\overline{\beta}} := I_{t_{\overline{\beta}}(\overline{\beta})}$,$\epsilon_\theta(I_\tau, I_{in}, \tau) := \widehat{\epsilon}_\theta(\widehat{I}_{\overline{\beta}}, I_{in}, \overline{\beta})$, and then we have:

$$I_t = I_s - (\overline{\delta}_t - \overline{\delta_s}) I_{in} + \int_{\overline{\alpha}_s}^{\overline{\alpha}_t} I_{res}^\theta(\widehat{I}_{\overline{\alpha}}, I_{in}, \overline{\alpha}) d\overline{\alpha} + \int_{\overline{\beta}_s}^{\overline{\beta}_t} \epsilon_\theta(\widehat{I}_{\overline{\beta}}, I_{in}, \overline{\beta}) d\overline{\beta}. \tag{129}$$

With the simplicity of the continuous formula of Eq. (129), we can propose high-order solvers that correspond to the ODEs. Specifically, given an initial point I_T at time T and total $M+1$ time steps $\{t_i\}_{i=0}^M$ decreasing from $t_0 = T$ to $t_M = 0$. Let $\{I_{t_i}\}_{i=0}^M$ be the sequence iteratively computed at time steps $\{t_i\}_{i=0}^M$ using the presented solvers. Starting with the previous solution $I_{t_{i-1}}$ at time t_{i-1}, the exact solution $I_{t_{i-1} \to t_i}$ at target time t_i is:

$$I_{t_{i-1} \to t_i} = I_{t_{i-1}} - (\overline{\delta}_{t_i} - \overline{\delta}_{t_{i-1}}) I_{in} + \int_{\overline{\alpha}_{t_{i-1}}}^{\overline{\alpha}_{t_i}} \widehat{I}_{res}^\theta(\widehat{I}_{\overline{\alpha}}, I_{in}, \overline{\alpha}) d\overline{\alpha} + \int_{\overline{\beta}_{t_{i-1}}}^{\overline{\beta}_{t_i}} \widehat{\epsilon}_\theta(\widehat{I}_{\overline{\beta}}, I_{in}, \overline{\beta}) d\overline{\beta}. \tag{130}$$

We need to approximate the integral of both $\widehat{I}_{res}^\theta(\widehat{I}_{\overline{\alpha}}, I_{in}, \overline{\alpha})$ from $\overline{\alpha}_{t_{i-1}}$ to $\overline{\alpha}_{t_i}$ and $\widehat{\epsilon}_\theta(\widehat{I}_{\overline{\beta}}, I_{in}, \overline{\beta})$ from $\overline{\beta}_{t_{i-1}}$ to $\overline{\beta}_{t_i}$. We utilize the Taylor expansion to make k orders approximation:

$$\widehat{I}_{res}^\theta(\widehat{I}_{\overline{\alpha}}, I_{in}, \overline{\alpha}) = \sum_{n=0}^{k-1} \frac{(\overline{\alpha} - \overline{\alpha}_{t_{i-1}})^n}{n!} \widehat{I}_{res}^\theta(\widehat{I}_{\overline{\alpha}_{t_{i-1}}}, I_{in}, \overline{\alpha}_{t_{i-1}}) + \mathcal{O}((\overline{\alpha} - \overline{\alpha}_{t_{i-1}})^k), \tag{131}$$

$$\widehat{\epsilon}_\theta(\widehat{I}_{\overline{\beta}}, I_{in}, \overline{\beta}) = \sum_{n=0}^{k-1} \frac{(\overline{\beta} - \overline{\beta}_{t_{i-1}})^n}{n!} \widehat{\epsilon}_\theta(\widehat{I}_{\overline{\beta}_{t_{i-1}}}, I_{in}, \overline{\beta}_{t_{i-1}}) + \mathcal{O}((\overline{\beta} - \overline{\beta}_{t_{i-1}})^k), \tag{132}$$

substituting the above Taylor expansion into Eq. (130), we can obtain:

$$\begin{aligned} I_{t_{i-1} \to t_i} = I_{t_{i-1}} - (\overline{\delta}_{t_i} - \overline{\delta}_{t_{i-1}}) I_{in} + \sum_{n=0}^{k-1} \widehat{I}_{res}^\theta(\widehat{I}_{\overline{\alpha}_{t_{i-1}}}, I_{in}, \overline{\alpha}_{t_{i-1}}) \int_{\overline{\alpha}_{t_{i-1}}}^{\overline{\alpha}_{t_i}} \frac{(\overline{\alpha} - \overline{\alpha}_{t_{i-1}})^n}{n!} d\overline{\alpha} \\ + \sum_{n=0}^{k-1} \widehat{\epsilon}_\theta(\widehat{I}_{\overline{\beta}_{t_{i-1}}}, I_{in}, \overline{\beta}_{t_{i-1}}) \int_{\overline{\beta}_{t_{i-1}}}^{\overline{\beta}_{t_i}} \frac{(\overline{\beta} - \overline{\beta}_{t_{i-1}})^n}{n!} d\overline{\beta} + \mathcal{O}((\overline{\alpha} - \overline{\alpha}_{t_{i-1}})^{k+1}) + \mathcal{O}((\overline{\beta} - \overline{\beta}_{t_{i-1}})^{k+1}). \end{aligned} \tag{133}$$

since the integral is linear, its analytical expression can be easily written as:

$$\begin{aligned} I_{t_{i-1} \to t_i} = I_{t_{i-1}} - (\overline{\delta}_{t_i} - \overline{\delta}_{t_{i-1}}) I_{in} + \sum_{n=0}^{k-1} \frac{(\overline{\alpha}_{t_i} - \overline{\alpha}_{t_{i-1}})^{n+1}}{(n+1)!} \widehat{I}_{res}^{\theta(n)}(\widehat{I}_{t_{i-1}}, I_{in}, t_{i-1}) \\ + \sum_{n=0}^{k-1} \frac{(\overline{\beta}_{t_i} - \overline{\beta}_{t_{i-1}})^{n+1}}{(n+1)!} \widehat{\epsilon}_\theta^{(n)}(\widehat{I}_{t_{i-1}}, I_{in}, t_{i-1}) + \mathcal{O}((\overline{\alpha} - \overline{\alpha}_{t_{i-1}})^{k+1}) + \mathcal{O}((\overline{\beta} - \overline{\beta}_{t_{i-1}})^{k+1}). \end{aligned} \tag{134}$$

Therefore, to approximate $I_{t_{i-1}} \rightarrow I_{t_i}$, we only need to approximate the n-th order total derivatives $I_{res}^{\theta(n)}(\widehat{I}_{t_{i-1}}, I_{in}, t_{i-1})$ and $\epsilon_\theta^{(n)}(\widehat{I}_{t_{i-1}}, I_{in}, t_{i-1})$ for $n \leq k-1$. In the case of $k=1$, Eq. (134) becomes:

$$I_{t_i} = I_{t_{i-1}} - (\overline{\delta}_{t_i} - \overline{\delta}_{t_{i-1}})I_{in} + (\overline{\alpha}_{t_i} - \overline{\alpha}_{t_{i-1}})I_{res}^{\theta}(I_{t_{i-1}}, I_{in}, t_{i-1}) + (\overline{\beta}_{t_i} - \overline{\beta}_{t_{i-1}})\epsilon_\theta(I_{t_{i-1}}, I_{in}, t_{i-1}). \tag{135}$$

By dropping the high-order error term $\mathcal{O}(\cdots)$, we can obtain the first-order approximation for $I_{t_{i-1}} \rightarrow I_{t_i}$. As $k=1$, we call this Diffusion Generalist Solver-1, and the detailed algorithm is as follows.

First-order Diffusion Generalist Solver Given an initial value I_T and $M+1$ time steps $\{t_i\}_{i=0}^M$ decreasing from $t_0 = T$ to $t_M = 0$. Starting with $\widehat{I}_{t_0} = I_T$, the sequence $\{\widehat{I}_{t_i}\}_{i=0}^M$ is computed iteratively as follows:

$$I_{t_i} = I_{t_{i-1}} - (\overline{\delta}_{t_i} - \overline{\delta}_{t_{i-1}})I_{in} + (\overline{\alpha}_{t_i} - \overline{\alpha}_{t_{i-1}})I_{res}^{\theta}(I_{t_{i-1}}, I_{in}, t_{i-1}) + (\overline{\beta}_{t_i} - \overline{\beta}_{t_{i-1}})\epsilon_\theta(I_{t_{i-1}}, I_{in}, t_{i-1}). \tag{136}$$

Apparently, it is consistent with Eq. 107, which is a special case of first-order solver within our methods by omitting the discrete error. The overall algorithm for first-order diffusion generalist solver is presented in Alg. 2.

Algorithm 2: First-order Diffusion Generalist Solver.

Input: I_{in}, I_{res}^{θ}, ϵ_θ, $\{\overline{\alpha}_{t_i}\}$, $\{\overline{\beta}_{t_i}\}$, $\{\overline{\delta}_{t_i}\}$, $\{t_i\}_{i=0}^M$.

$I_{t_0} = I_T \sim \mathcal{N}(0, \overline{\beta}_{t_0}\boldsymbol{I})$

for $i = 1$ to M **do**

  $\widehat{I}_{res} = I_{res}^{\theta}(I_{t_{i-1}}, I_{in}, t_{i-1})$

  $\widehat{\epsilon} = (I_{t_{i-1}} - (\overline{\alpha}_{t_{i-1}} - 1)\widehat{I}_{res} - (1 - \overline{\delta}_{t_{i-1}})I_{in})/\overline{\beta}_{t_{i-1}}$

  $\widehat{I}_0 = I_{t_{i-1}} - \overline{\alpha}_{t_{i-1}}\widehat{I}_{res} - \overline{\beta}_{t_{i-1}}\widehat{\epsilon} + \overline{\delta}_{t_{i-1}}I_{in}$

  $I_{t_i} = I_{t_{i-1}} - (\overline{\delta}_{t_i} - \overline{\delta}_{t_{i-1}})I_{in} + (\overline{\alpha}_{t_i} - \overline{\alpha}_{t_{i-1}})\widehat{I}_{res} + (\overline{\beta}_{t_i} - \overline{\beta}_{t_{i-1}})\widehat{\epsilon}$

Output: I_{t_M}.

For $k=2$, we need an auxiliary time variable $t_u = rt_i + (1-r)t_{i-1}$, where r is the controllable variable measuring the intermediate points in the range of $[t_i, t_{i-1}]$. Then Eq. (133) becomes:

$$\begin{aligned} I_{t_{i-1}\rightarrow t_i} = {} & I_{t_{i-1}} - (\overline{\delta}_{t_i} - \overline{\delta}_{t_{i-1}})I_{in} + (\overline{\alpha}_{t_i} - \overline{\alpha}_{t_{i-1}})I_{res}^{\theta}(\widehat{I}_{t_{i-1}}, I_{in}, t_{i-1}) + (\overline{\beta}_{t_i} - \overline{\beta}_{t_{i-1}})\epsilon_\theta(\widehat{I}_{t_{i-1}}, I_{in}, t_{i-1}) \\ & + \frac{1}{2}(\overline{\alpha}_{t_i} - \overline{\alpha}_{t_{i-1}})^2 I_{res}^{\theta(1)}(\widehat{I}_{t_{i-1}}, I_{in}, t_{i-1}) + \frac{1}{2}(\overline{\beta}_{t_i} - \overline{\beta}_{t_{i-1}})^2 \epsilon_\theta^{(1)}(\widehat{I}_{t_{i-1}}, I_{in}, t_{i-1}), \end{aligned} \tag{137}$$

leveraging the finite-difference methods [51], we can approximate the derivative part:

$$I_{res}^{\theta(1)}(\widehat{I}_{t_{i-1}}, I_{in}, t_{i-1}) \approx \frac{I_{res}^{\theta}(\widehat{I}_{\overline{\alpha}_u}, I_{in}, \overline{\alpha}_u) - I_{res}^{\theta}(\widehat{I}_{\overline{\alpha}_{i-1}}, I_{in}, \overline{\alpha}_{i-1})}{\overline{\alpha}_{t_u} - \overline{\alpha}_{t_{i-1}}} = \frac{1}{r}\frac{I_{res}^{\theta}(\widehat{I}_{t_u}, I_{in}, t_u) - I_{res}^{\theta}(\widehat{I}_{t_{i-1}}, I_{in}, t_{i-1})}{\overline{\alpha}_{t_i} - \overline{\alpha}_{t_{i-1}}}, \tag{138}$$

$$\epsilon_\theta^{(1)}(\widehat{I}_{t_{i-1}}, I_{in}, t_{i-1}) \approx \frac{\epsilon_\theta(\widehat{I}_{\overline{\beta}_u}, I_{in}, \overline{\beta}_u) - \epsilon_\theta(\widehat{I}_{\overline{\beta}_{i-1}}, I_{in}, \overline{\beta}_{i-1})}{\overline{\beta}_{t_u} - \overline{\beta}_{t_{i-1}}} = \frac{1}{r}\frac{\epsilon_\theta(\widehat{I}_{t_u}, I_{in}, t_u) - \epsilon_\theta(\widehat{I}_{t_{i-1}}, I_{in}, t_{i-1})}{\overline{\beta}_{t_i} - \overline{\beta}_{t_{i-1}}}. \tag{139}$$

Therefore, the simplified result of Eq. (137) is:

$$\begin{aligned} I_{t_i} = {} & I_{t_{i-1}} - (\overline{\delta}_{t_i} - \overline{\delta}_{t_{i-1}})I_{in} + (\overline{\alpha}_{t_i} - \overline{\alpha}_{t_{i-1}})I_{res}^{\theta}(\widehat{I}_{t_{i-1}}, I_{in}, t_{i-1}) + (\overline{\beta}_{t_i} - \overline{\beta}_{t_{i-1}})\epsilon_\theta(\widehat{I}_{t_{i-1}}, I_{in}, t_{i-1}) \\ & + \frac{1}{2r}(\overline{\alpha}_{t_i} - \overline{\alpha}_{t_{i-1}})(I_{res}^{\theta}(\widehat{I}_{t_u}, I_{in}, t_u) - I_{res}^{\theta}(\widehat{I}_{t_{i-1}}, I_{in}, t_{i-1})) \\ & + \frac{1}{2r}(\overline{\beta}_{t_i} - \overline{\beta}_{t_{i-1}})(\epsilon_\theta(\widehat{I}_{t_u}, I_{in}, t_u) - \epsilon_\theta(\widehat{I}_{t_{i-1}}, I_{in}, t_{i-1})). \end{aligned} \tag{140}$$

Second-order Diffusion Generalist Solver Given an initial value I_T and $M+1$ time steps $\{t_i\}_{i=0}^M$ decreasing from $t_0 = T$ to $t_M = 0$, starting with $\widehat{I}_{t=0} = I_T$, the sequence $\{\widehat{I}_{t_i}\}_{i=0}^M$ is computed iteratively as follows:

$$\begin{aligned} I_{t_i} = {} & I_{t_{i-1}} - (\overline{\delta}_{t_i} - \overline{\delta}_{t_{i-1}})I_{in} + (\overline{\alpha}_{t_i} - \overline{\alpha}_{t_{i-1}})I_{res}^{\theta}(\widehat{I}_{t_{i-1}}, I_{in}, t_{i-1}) + (\overline{\beta}_{t_i} - \overline{\beta}_{t_{i-1}})\epsilon_\theta(\widehat{I}_{t_{i-1}}, I_{in}, t_{i-1}) \\ & + \frac{1}{2r}(\overline{\alpha}_{t_i} - \overline{\alpha}_{t_{i-1}})(I_{res}^{\theta}(\widehat{I}_{t_u}, I_{in}, t_u) - I_{res}^{\theta}(\widehat{I}_{t_{i-1}}, I_{in}, t_{i-1})) \\ & + \frac{1}{2r}(\overline{\beta}_{t_i} - \overline{\beta}_{t_{i-1}})(\epsilon_\theta(\widehat{I}_{t_u}, I_{in}, t_u) - \epsilon_\theta(\widehat{I}_{t_{i-1}}, I_{in}, t_{i-1})). \end{aligned} \tag{141}$$

The overall algorithm for second-order diffusion generalist solver is presented in Alg. 3.

Algorithm 3: Second-order Diffusion Generalist Solver.

Input: I_{in}, I^{θ}_{res}, ϵ_θ, $\{\overline{\alpha}_{t_i}\}$, $\{\overline{\beta}_{t_i}\}$, $\{\overline{\delta}_{t_i}\}$, $\{t_i\}_{i=0}^{M}$, r.

$I_{t_0} \leftarrow I_T \sim \mathcal{N}(0, \overline{\beta}_{t_0}\boldsymbol{I})$

for $i = 1$ to M **do**

$t_u = rt_i + (1-r)t_{i-1}$

$\widehat{I}^{t_{i-1}}_{res} = I^{\theta}_{res}(I_{t_{i-1}}, I_{in}, t_{i-1})$

$\widehat{\epsilon}_{t_{i-1}} = (I_{t_{i-1}} - (\overline{\alpha}_{t_{i-1}} - 1)\widehat{I}^{t_i}_{res} - (1-\overline{\delta}_{t_{i-1}})I_{in})/\overline{\beta}_{t_{i-1}}$

$\widehat{I}^{t_{i-1}}_{0} = I_{t_{i-1}} - \overline{\alpha}_{t_{i-1}}\widehat{I}^{t_{i-1}}_{res} - \overline{\beta}_{t_{i-1}}\widehat{\epsilon}_{t_{i-1}} + \overline{\delta}_{t_{i-1}}I_{in}$

$I_{t_u} = I_{t_{i-1}} - (\overline{\delta}_{t_u} - \overline{\delta}_{t_{i-1}})I_{in} + (\overline{\alpha}_{t_u} - \overline{\alpha}_{t_{i-1}})\widehat{I}^{t_{i-1}}_{res} + (\overline{\beta}_{t_u} - \overline{\beta}_{t_{i-1}})\widehat{\epsilon}_{t_{i-1}}$

$\widehat{I}^{t_u}_{res} = I^{\theta}_{res}(I_{t_u}, I_{in}, t_u)$

$\widehat{\epsilon}_{t_u} = (I_{t_u} - (\overline{\alpha}_{t_u} - 1)\widehat{I}^{t_u}_{res} - (1-\overline{\delta}_{t_u})I_{in})/\overline{\beta}_{t_u}$

$\widehat{I}^{t_u}_{0} = I_{t_u} - \overline{\alpha}_{t_u}\widehat{I}^{t_u}_{res} - \overline{\beta}_{t_u}\widehat{\epsilon}_{t_u} + \overline{\delta}_{t_u}I_{in}$

$I_{t_i} = I_{t_{i-1}} - (\overline{\delta}_{t_i} - \overline{\delta}_{t_{i-1}})I_{in} + (\overline{\alpha}_{t_i} - \overline{\alpha}_{t_{i-1}})\widehat{I}^{t_{i-1}}_{res} + (\overline{\beta}_{t_i} - \overline{\beta}_{t_{i-1}})\widehat{\epsilon}_{t_{i-1}} + \frac{1}{2r}(\overline{\alpha}_{t_i} - \overline{\alpha}_{t_{i-1}})(\widehat{I}^{t_u}_{res} - \widehat{I}^{t_{i-1}}_{res}) + \frac{1}{2r}(\overline{\beta}_{t_i} - \overline{\beta}_{t_{i-1}})(\widehat{\epsilon}_{t_u} - \widehat{\epsilon}_{t_{i-1}})$

Output: I_{t_0}.

For $k = 3$, Eq. (133) becomes:

$$\begin{aligned} I_{t_{i-1}\to t_i} = I_{t_{i-1}} &- (\overline{\delta}_{t_i} - \overline{\delta}_{t_{i-1}})I_{in} + (\overline{\alpha}_{t_i} - \overline{\alpha}_{t_{i-1}})I^{\theta}_{res}(\widehat{I}_{t_{i-1}}, I_{in}, t_{i-1}) + (\overline{\beta}_{t_i} - \overline{\beta}_{t_{i-1}})\epsilon_\theta(\widehat{I}_{t_{i-1}}, I_{in}, t_{i-1}) \\ &+ \frac{1}{2}(\overline{\alpha}_{t_i} - \overline{\alpha}_{t_{i-1}})^2 I^{\theta(1)}_{res}(\widehat{I}_{t_{i-1}}, I_{in}, t_{i-1}) + \frac{1}{2}(\overline{\beta}_{t_i} - \overline{\beta}_{t_{i-1}})^2 \epsilon^{(1)}_{\theta}(\widehat{I}_{t_{i-1}}, I_{in}, t_{i-1}) \\ &+ \frac{1}{6}(\overline{\alpha}_{t_i} - \overline{\alpha}_{t_{i-1}})^3 I^{\theta(2)}_{res}(\widehat{I}_{t_{i-1}}, I_{in}, t_{i-1}) + \frac{1}{6}(\overline{\beta}_{t_i} - \overline{\beta}_{t_{i-1}})^3 \epsilon^{(2)}_{\theta}(\widehat{I}_{t_{i-1}}, I_{in}, t_{i-1}), \end{aligned} \tag{142}$$

we need two additional points to obtain the second-order derivative. Suppose the Taylor expansion of function $f(x)$ at $x + h_1$ and $x + h_2$ can be:

$$f(x + h_1) = f(x) + h_1 f'(x) + \frac{h_1^2}{2} f''(x) + \mathcal{O}(h_1^3), \tag{143}$$

$$f(x + h_2) = f(x) + h_2 f'(x) + \frac{h_2^2}{2} f''(x) + \mathcal{O}(h_2^3), \tag{144}$$

Then, we can derive the formulations by eliminating $f'(x)$:

$$f''(x) = \frac{2}{h_1 h_2 (h_2 - h_1)}\big[h_1 f(x + h_2) - h_2 f(x + h_1) + (h_2 - h_1)f(x)\big]. \tag{145}$$

Similarly, two time variables $t_u = r_1 t_i + (1 - r_1)t_{i-1}$ and $t_s = r_2 t_i + (1 - r_2)t_{i-1}$, satisfying $i > s > u > i - 1$. Therefore, we can compute that:

$$I^{\theta(2)}_{res}(\widehat{I}_{t_{i-1}}, I_{in}, t_{i-1}) = \frac{2(\overline{\alpha}_{t_i} - \overline{\alpha}_{t_{i-1}})^{-2}}{r_1 r_2 (r_2 - r_1)}\big[r_1 I^{t_s}_{res} - r_2 I^{t_u}_{res} + (r_2 - r_1)I^{\theta}_{res}(\widehat{I}_{t_{i-1}}, I_{in}, t_{i-1})\big], \tag{146}$$

$$\epsilon_{\theta(2)}(\widehat{I}_{t_{i-1}}, I_{in}, t_{i-1}) = \frac{2(\overline{\alpha}_{t_i} - \overline{\alpha}_{t_{i-1}})^{-2}}{r_1 r_2 (r_2 - r_1)}\big[r_1 \epsilon_{t_s} - r_2 \epsilon_{t_u} + (r_2 - r_1)\epsilon_\theta(\widehat{I}_{t_{i-1}}, I_{in}, t_{i-1})\big]. \tag{147}$$

where $I^{t_s}_{res} = I^{\theta}_{res}(\widehat{I}_{t_s}, I_{in}, t_s), I^{t_u}_{res} = I^{\theta}_{res}(\widehat{I}_{t_u}, I_{in}, t_u)$ and $\epsilon_{t_s} = \epsilon_\theta(\widehat{I}_{t_s}, I_{in}, t_s), \epsilon_{t_u} = \epsilon_\theta(\widehat{I}_{t_u}, I_{in}, t_u)$. Consequently, we can derive the formula as follows:

$$\begin{aligned} I_{t_i} = &I_{t_{i-1}} - (\overline{\delta}_{t_i} - \overline{\delta}_{t_{i-1}})I_{in} + (\overline{\alpha}_{t_i} - \overline{\alpha}_{t_{i-1}})I^{\theta}_{res}(\widehat{I}_{t_{i-1}}, I_{in}, t_{i-1}) + (\overline{\beta}_{t_i} - \overline{\beta}_{t_{i-1}})\epsilon_\theta(\widehat{I}_{t_{i-1}}, I_{in}, t_{i-1}) \\ &+ \frac{1}{2r_1}(\overline{\alpha}_{t_i} - \overline{\alpha}_{t_{i-1}})(I^{\theta}_{res}(\widehat{I}_{t_u}, I_{in}, t_u) - I^{\theta}_{res}(\widehat{I}_{t_{i-1}}, I_{in}, t_{i-1})) \\ &+ \frac{1}{2r_1}(\overline{\beta}_{t_i} - \overline{\beta}_{t_{i-1}})(\epsilon_\theta(\widehat{I}_{t_u}, I_{in}, t_u) - \epsilon_\theta(\widehat{I}_{t_{i-1}}, I_{in}, t_{i-1})) \\ &+ \frac{(\overline{\alpha}_{t_i} - \overline{\alpha}_{t_{i-1}})}{3r_1 r_2 (r_2 - r_1)}\big[r_1 I^{\theta}_{res}(\widehat{I}_{t_s}, I_{in}, t_s) - r_2 I^{\theta}_{res}(\widehat{I}_{t_u}, I_{in}, t_u) + (r_2 - r_1)I^{\theta}_{res}(\widehat{I}_{t_{i-1}}, I_{in}, t_{i-1})\big] \\ &+ \frac{(\overline{\alpha}_{t_i} - \overline{\alpha}_{t_{i-1}})}{3r_1 r_2 (r_2 - r_1)}\big[r_1 \epsilon_\theta(\widehat{I}_{t_s}, I_{in}, t_s) - r_2 \epsilon_\theta(\widehat{I}_{t_u}, I_{in}, t_u) + (r_2 - r_1)\epsilon_\theta(\widehat{I}_{t_{i-1}}, I_{in}, t_{i-1})\big]. \end{aligned} \tag{148}$$

The overall algorithm for second-order diffusion generalist solver is presented in Alg. 4.

Algorithm 4: Third-order Diffusion Generalist Solver.

Input: I_{in}, I^{θ}_{res}, ϵ_θ, $\{\overline{\alpha}_{t_i}\}$, $\{\overline{\beta}_{t_i}\}$, $\{\overline{\delta}_{t_i}\}$, $\{t_i\}_{i=0}^{M}$, r_1, r_2.

$I_{t_0} \leftarrow I_T \sim \mathcal{N}(0, \overline{\beta}_{t_0}\boldsymbol{I})$

for $i = 1$ to M **do**

$t_u = r_1 t_i + (1-r_1)t_{i-1}$, $t_s = r_2 t_i + (1-r_2)t_{i-1}$

$\widehat{I}^{t_{i-1}}_{res} = I^{\theta}_{res}(I_{t_{i-1}}, I_{in}, t_{i-1})$, $\widehat{\epsilon}_{t_{i-1}} = (I_{t_{i-1}} - (\overline{\alpha}_{t_{i-1}} - 1)\widehat{I}^{t_{i-1}}_{res} - (1-\overline{\delta}_{t_{i-1}})I_{in})/\overline{\beta}_{t_{i-1}}$,
$\widehat{I}^{t_{i-1}}_{0} = I_{t_{i-1}} - \overline{\alpha}_{t_{i-1}}\widehat{I}^{t_{i-1}}_{res} - \overline{\beta}_{t_{i-1}}\widehat{\epsilon}_{t_{i-1}} + \overline{\delta}_{t_{i-1}}I_{in}$

$I_{t_u} = I_{t_{i-1}} - (\overline{\delta}_{t_u} - \overline{\delta}_{t_{i-1}})I_{in} + (\overline{\alpha}_{t_u} - \overline{\alpha}_{t_{i-1}})\widehat{I}^{t_{i-1}}_{res} + (\overline{\beta}_{t_u} - \overline{\beta}_{t_{i-1}})\widehat{\epsilon}_{t_{i-1}}$

$\widehat{I}^{t_u}_{res} = I^{\theta}_{res}(I_{t_u}, I_{in}, t_u)$, $\widehat{\epsilon}_{t_u} = (I_{t_u} - (\overline{\alpha}_{t_u} - 1)\widehat{I}^{t_u}_{res} - (1-\overline{\delta}_{t_u})I_{in})/\overline{\beta}_{t_u}$,
$\widehat{I}^{t_u}_{0} = I_{t_u} - \overline{\alpha}_{t_u}\widehat{I}^{t_u}_{res} - \overline{\beta}_{t_u}\widehat{\epsilon}_{t_u} + \overline{\delta}_{t_u}I_{in}$

$I_{t_s} = I_{t_{i-1}} - (\overline{\delta}_{t_s} - \overline{\delta}_{t_{i-1}})I_{in} + (\overline{\alpha}_{t_s} - \overline{\alpha}_{t_{i-1}})\widehat{I}^{t_{i-1}}_{res} + (\overline{\beta}_{t_s} - \overline{\beta}_{t_{i-1}})\widehat{\epsilon}_{t_{i-1}} + \frac{r_2}{2r_1}(\overline{\alpha}_{t_s} - \overline{\alpha}_{t_{i-1}})(\widehat{I}^{t_u}_{res} - \widehat{I}^{t_{i-1}}_{res}) + \frac{r_2}{2r_1}(\overline{\beta}_{t_s} - \overline{\beta}_{t_{i-1}})(\widehat{\epsilon}_{t_u} - \widehat{\epsilon}_{t_{i-1}})$

$\widehat{I}^{t_s}_{res} = I^{\theta}_{res}(I_{t_s}, I_{in}, t_s)$, $\widehat{\epsilon}_{t_s} = (I_{t_s} - (\overline{\alpha}_{t_s} - 1)\widehat{I}^{t_s}_{res} - (1-\overline{\delta}_{t_s})I_{in})/\overline{\beta}_{t_s}$,
$\widehat{I}^{t_s}_{0} = I_{t_s} - \overline{\alpha}_{t_s}\widehat{I}^{t_s}_{res} - \overline{\beta}_{t_s}\widehat{\epsilon}_{t_s} + \overline{\delta}_{t_s}I_{in}$

$D^{res}_1 = \widehat{I}^{t_u}_{res} - \widehat{I}^{t_{i-1}}_{res}$, $D^{\epsilon}_1 = \widehat{\epsilon}_{t_u} - \widehat{\epsilon}_{t_{i-1}}$

$D^{res}_2 = \frac{2}{r_1 r_2(r_2 - r_1)}(r_1\widehat{I}^{t_s}_{res} - r_2\widehat{I}^{t_u}_{res} + (r_2 - r_1)\widehat{I}^{t_{i-1}}_{res})$

$D^{\epsilon}_2 = \frac{2}{r_1 r_2(r_2 - r_1)}(r_1\widehat{\epsilon}_{t_s} - r_2\widehat{\epsilon}_{t_u} + (r_2 - r_1)\widehat{\epsilon}_{t_{i-1}})$

$I_{t_i} = I_{t_{i-1}} - (\overline{\delta}_{t_i} - \overline{\delta}_{t_{i-1}})I_{in} + (\overline{\alpha}_{t_i} - \overline{\alpha}_{t_{i-1}})\widehat{I}^{t_{i-1}}_{res} + (\overline{\beta}_{t_i} - \overline{\beta}_{t_{i-1}})\widehat{\epsilon}_{t_{i-1}} + \frac{1}{2r_1}(\overline{\alpha}_{t_i} - \overline{\alpha}_{t_{i-1}})D^{res}_1 + \frac{1}{2r_1}(\overline{\beta}_{t_i} - \overline{\beta}_{t_{i-1}})D^{\epsilon}_1 + \frac{1}{6}(\overline{\alpha}_{t_i} - \overline{\alpha}_{t_{i-1}})D^{res}_2 + \frac{1}{6}(\overline{\beta}_{t_i} - \overline{\beta}_{t_{i-1}})D^{\epsilon}_2$

Output: I_{t_M}.

B.2 Cumulative Error Bound of Diffusion Generalist Solvers

For k-order diffusion generalist solvers, we make the following assumptions:

Assumption 1. The total derivatives $I^{\theta(n)}_{res}(I_{\overline{\alpha}_t}, I_{in}, \overline{\alpha}) = \frac{d^{(n)}\widehat{I}^{\theta}_{res}(\widehat{I}_{\overline{\alpha}_t}, I_{in}, \overline{\alpha})}{d\overline{\alpha}^{(n)}}$ and $\epsilon^{(n)}_{\theta}(I_{\overline{\beta}_t}, I_{in}, \overline{\beta}) = \frac{d^{(n)}\widehat{\epsilon}(\widehat{I}_{\overline{\beta}_t}, I_{in}, \overline{\beta})}{d\overline{\beta}^{(n)}}$ exist and are continuous for $0 \le n \le k+1$.

Assumption 2. The function $I^{\theta}_{res}(I_{\overline{\alpha}_t}, I_{in}, \overline{\alpha})$ and $\epsilon_\theta(I_{\overline{\beta}_t}, I_{in}, \overline{\beta})$ are Lipschitz with respect to I_t.

Assumption 3. The step sizes for $\overline{\alpha}$ and $\overline{\beta}$ are limited by $\max(\overline{\alpha}_{t_i} - \overline{\alpha}_{t_{i-1}}) = \mathcal{O}(1/M_{\overline{\alpha}})$ and $\max(\overline{\beta}_{t_i} - \overline{\beta}_{t_{i-1}}) = \mathcal{O}(1/M_{\overline{\beta}})$, respectively. Besides, $1/M_{\overline{\alpha}} < 1/M$ and $1/M_{\overline{\beta}} < 1/M$.

Proof of $k = 1$. Taking $n = 0$, $t = t_i$, $s = t_{i-1}$ in Eq. (134), we obtain:

$$\begin{aligned} I_{t_i} = I_{t_{i-1}} - (\overline{\delta}_{t_i} - \overline{\delta}_{t_{i-1}})I_{in} + (\overline{\alpha}_{t_i} - \overline{\alpha}_{t_{i-1}})I^{\theta}_{res}(I_{t_{i-1}}, I_{in}, t_{i-1}) + \mathcal{O}\big((\overline{\alpha}_t - \overline{\alpha}_{t_s})^2\big) \\ + (\overline{\beta}_{t_i} - \overline{\beta}_{t_{i-1}})\epsilon_\theta(I_{t_{i-1}}, I_{in}, t_{i-1}) + \mathcal{O}\big((\overline{\beta}_t - \overline{\beta}_{t_s})^2\big), \end{aligned} \tag{149}$$

Based on the Assumptions and Eq. (136), we can derive:

$$\begin{aligned} \widehat{I}_{t_i} &= \widehat{I}_{t_{i-1}} - (\overline{\delta}_{t_i} - \overline{\delta}_{t_{i-1}})I_{in} + (\overline{\alpha}_{t_i} - \overline{\alpha}_{t_{i-1}})I^{\theta}_{res}(\widehat{I}_{t_{i-1}}, I_{in}, t_{i-1}) + (\overline{\beta}_{t_i} - \overline{\beta}_{t_{i-1}})\epsilon_\theta(\widehat{I}_{t_{i-1}}, I_{in}, t_{i-1}) \\ &= I_{t_{i-1}} - (\overline{\delta}_{t_i} - \overline{\delta}_{t_{i-1}})I_{in} + (\overline{\alpha}_{t_i} - \overline{\alpha}_{t_{i-1}})(I^{\theta}_{res}(I_{t_{i-1}}, I_{in}, t_{i-1}) + \mathcal{O}(\widehat{I}_{t_{i-1}} - I_{t_{i-1}})) \\ &\quad + (\overline{\beta}_{t_i} - \overline{\beta}_{t_{i-1}})(\epsilon_\theta(I_{t_{i-1}}, I_{in}, t_{i-1}) + \mathcal{O}(\widehat{I}_{t_{i-1}} - I_{t_{i-1}})) \\ &= I_{t_i} + \mathcal{O}(\max(\overline{\alpha}_{t_i} - \overline{\alpha}_{t_{i-1}})^2) + \mathcal{O}(\max(\overline{\beta}_{t_i} - \overline{\beta}_{t_{i-1}})^2) + \mathcal{O}(\widehat{I}_{t_{i-1}} - I_{t_{i-1}}). \end{aligned} \tag{150}$$

By repeating the process recursively M times, we get:

$$\begin{aligned} \widehat{I}_{t_M} &= I_{t_0} + \mathcal{O}(M\max(\overline{\alpha}_{t_i} - \overline{\alpha}_{t_{i-1}})^2) + \mathcal{O}(M\max(\overline{\beta}_{t_i} - \overline{\beta}_{t_{i-1}})^2) \\ &= I_{t_0} + \mathcal{O}(\max(\overline{\alpha}_{t_i} - \overline{\alpha}_{t_{i-1}})) + \mathcal{O}(\max(\overline{\beta}_{t_i} - \overline{\beta}_{t_{i-1}})). \end{aligned} \tag{151}$$

Proof of $k = 2$. We consider the following update for $0 < s < u < r < M$ in Alg. 3:

$$\widehat{I}_{t_u} = I_{t_s} - (\overline{\delta}_{t_u} - \overline{\delta}_{t_s})I_{in} + (\overline{\alpha}_{t_u} - \overline{\alpha}_{t_s})I^{\theta}_{res}(I_{t_s}, I_{in}, t_s) + (\overline{\beta}_{t_u} - \overline{\beta}_{t_s})\epsilon_\theta(I_{t_s}, I_{in}, t_s), \tag{152}$$

$$\begin{aligned}\widehat{I}_{t_r} &= I_{t_s} - (\overline{\delta}_{t_r} - \overline{\delta}_{t_s})I_{in} + (\overline{\alpha}_{t_r} - \overline{\alpha}_{t_s})I^{\theta}_{res}(I_{t_s}, I_{in}, t_s) + (\overline{\beta}_{t_r} - \overline{\beta}_{t_s})\epsilon_\theta(I_{t_s}, I_{in}, t_s) \\ &+ \frac{1}{2r}(\overline{\alpha}_{t_r} - \overline{\alpha}_{t_s})(I^{\theta}_{res}(\widehat{I}_{t_u}, I_{in}, t_u) - I^{\theta}_{res}(I_{t_s}, I_{in}, t_s)) \\ &+ \frac{1}{2r}(\overline{\beta}_{t_r} - \overline{\beta}_{t_s})(\epsilon_\theta(\widehat{I}_{t_u}, I_{in}, t_u) - \epsilon_\theta(I_{t_s}, I_{in}, t_s)).\end{aligned} \tag{153}$$

Taking $n = 1$, we can obtain:

$$\begin{aligned}I_{t_r} &= I_{t_s} - (\overline{\delta}_{t_r} - \overline{\delta}_{t_s})I_{in} + (\overline{\alpha}_{t_r} - \overline{\alpha}_{t_s})I^{\theta}_{res}(I_{t_s}, I_{in}, t_s) + (\overline{\beta}_{t_r} - \overline{\beta}_{t_s})\epsilon_\theta(I_{t_s}, I_{in}, t_s) \\ &+ \frac{1}{2}(\overline{\alpha}_{t_r} - \overline{\alpha}_{t_s})^2 I^{\theta(1)}_{res}(I_{\overline{\alpha}_{t_s}}, I_{in}, \overline{\alpha}_{t_s}) + \mathcal{O}\big((\overline{\alpha}_t - \overline{\alpha}_{t_s})^3\big) \\ &+ \frac{1}{2}(\overline{\beta}_{t_r} - \overline{\beta}_{t_s})^2 \epsilon^{(1)}_\theta(I_{\overline{\beta}_{t_s}}, I_{in}, \overline{\beta}_{t_s}) + \mathcal{O}\big((\overline{\beta}_t - \overline{\beta}_{t_s})^3\big).\end{aligned} \tag{154}$$

From Eq. (153), we have:

$$I^{\theta}_{res}(I_{t_u}, I_{in}, t_u) = I^{\theta}_{res}(I_{t_s}, I_{in}, t_s) + (\overline{\alpha}_{t_u} - \overline{\alpha}_{t_s})\widehat{I}^{\theta(1)}_{res}(I_{\overline{\alpha}_{t_s}}, I_{in}, \overline{\alpha}_{t_s}) + \mathcal{O}((\overline{\alpha}_{t_u} - \overline{\alpha}_{t_s})^2), \tag{155}$$

$$\epsilon_\theta(I_{t_u}, I_{in}, t_u) = \epsilon_\theta(I_{t_s}, I_{in}, t_s) + (\overline{\beta}_{t_u} - \overline{\beta}_{t_s})\widehat{\epsilon}^{(1)}_\theta(I_{\overline{\beta}_{t_s}}, I_{in}, \overline{\beta}_{t_s}) + \mathcal{O}((\overline{\beta}_{t_u} - \overline{\beta}_{t_s})^2), \tag{156}$$

$$\begin{aligned}\widehat{I}_{t_r} &= I_{t_s} - (\overline{\delta}_{t_r} - \overline{\delta}_{t_s})I_{in} + (\overline{\alpha}_{t_r} - \overline{\alpha}_{t_s})I^{\theta}_{res}(I_{t_s}, I_{in}, t_s) + (\overline{\beta}_{t_r} - \overline{\beta}_{t_s})\epsilon_\theta(I_{t_s}, I_{in}, t_s) \\ &+ \frac{1}{2r}(\overline{\alpha}_{t_r} - \overline{\alpha}_{t_s})(I^{\theta}_{res}(\widehat{I}_{t_u}, I_{in}, t_u) - I^{\theta}_{res}(I_{t_u}, I_{in}, t_u) + (\overline{\alpha}_{t_u} - \overline{\alpha}_{t_s})\widehat{I}^{\theta(1)}_{res}(I_{\overline{\alpha}_{t_s}}, I_{in}, \overline{\alpha}_{t_s}) + \mathcal{O}((\overline{\alpha}_{t_u} - \overline{\alpha}_{t_s})^2)) \\ &+ \frac{1}{2r}(\overline{\beta}_{t_r} - \overline{\beta}_{t_s})(\epsilon_\theta(\widehat{I}_{t_u}, I_{in}, t_u) - \epsilon_\theta(I_{t_u}, I_{in}, t_u) + (\overline{\beta}_{t_u} - \overline{\beta}_{t_s})\widehat{\epsilon}^{(1)}_\theta(I_{\overline{\beta}_{t_s}}, I_{in}, \overline{\beta}_{t_s}) + \mathcal{O}((\overline{\beta}_{t_u} - \overline{\beta}_{t_s})^2)),\end{aligned} \tag{157}$$

According to the Lipschitzness of I^{θ}_{res} and ϵ_θ and the conclusion from Eq. (150), we can compute:

$$\|I^{\theta}_{res}(\widehat{I}_{t_u}, I_{in}, t_u) - I^{\theta}_{res}(I_{t_u}, I_{in}, t_u)\| = \mathcal{O}(\|\widehat{I}_{t_u} - I_{t_u}\|) = \mathcal{O}((\overline{\alpha}_{t_u} - \overline{\alpha}_{t_s})^2) + \mathcal{O}((\overline{\beta}_{t_u} - \overline{\beta}_{t_s})^2), \tag{158}$$

$$\|\epsilon_\theta(\widehat{I}_{t_u}, I_{in}, t_u) - \epsilon_\theta(I_{t_u}, I_{in}, t_u)\| = \mathcal{O}(\|\widehat{I}_{t_u} - I_{t_u}\|) = \mathcal{O}((\overline{\alpha}_{t_u} - \overline{\alpha}_{t_s})^2) + \mathcal{O}((\overline{\beta}_{t_u} - \overline{\beta}_{t_s})^2). \tag{159}$$

As $(\overline{\alpha}_{t_u} - \overline{\alpha}_{t_s}) = r(\overline{\alpha}_{t_r} - \overline{\alpha}_{t_s})$ and $(\overline{\beta}_{t_u} - \overline{\beta}_{t_s}) = r(\overline{\beta}_{t_r} - \overline{\beta}_{t_s})$ for linear generation schedule, we subtract $\widehat{I}_{t_r}$ in Eq. (157) from I_{t_r} in Eq. (154) :

$$\begin{aligned}I_{t_r} - \widehat{I}_{t_r} &= (\overline{\alpha}_{t_r} - \overline{\alpha}_{t_s})\big(\frac{(\overline{\alpha}_{t_r} - \overline{\alpha}_{t_s})}{2} - \frac{(\overline{\alpha}_{t_u} - \overline{\alpha}_{t_s})}{2r}\big)\widehat{I}^{\theta(1)}_{res}(I_{\overline{\alpha}_{t_s}}, I_{in}, \overline{\alpha}_{t_s}) + \mathcal{O}((\overline{\alpha}_{t_u} - \overline{\alpha}_{t_s})^3) \\ &+ (\overline{\beta}_{t_r} - \overline{\beta}_{t_s})\big(\frac{(\overline{\beta}_{t_r} - \overline{\beta}_{t_s})}{2} - \frac{(\overline{\beta}_{t_u} - \overline{\beta}_{t_s})}{2r}\big)\widehat{\epsilon}^{(1)}_\theta(I_{\overline{\beta}_{t_s}}, I_{in}, \overline{\beta}_{t_s})\big) + \mathcal{O}((\overline{\beta}_{t_u} - \overline{\beta}_{t_s})^3) \\ &= \mathcal{O}((\overline{\alpha}_{t_r} - \overline{\alpha}_{t_s})^3) + \mathcal{O}((\overline{\beta}_{t_r} - \overline{\beta}_{t_s})^3).\end{aligned} \tag{160}$$

Proof of $k = 3$. We consider the following update for $i - 1 < s < u < v < r < i$ in Alg. 4, and we can obtain:

$$\begin{aligned}\widehat{I}_{t_r} &= I_{t_s} - (\overline{\delta}_{t_r} - \overline{\delta}_{t_s})I_{in} + (\overline{\alpha}_{t_r} - \overline{\alpha}_{t_s})I^{\theta}_{res}(I_{t_s}, I_{in}, t_s) + (\overline{\beta}_{t_r} - \overline{\beta}_{t_s})\epsilon_\theta(I_{t_s}, I_{in}, t_s) \\ &+ \frac{1}{2r_1}(\overline{\alpha}_{t_r} - \overline{\alpha}_{t_s})(I^{\theta}_{res}(I_{\overline{\alpha}_{t_u}}, I_{in}, \overline{\alpha}_{t_u}) - I^{\theta}_{res}(I_{\overline{\alpha}_{t_s}}, I_{in}, \overline{\alpha}_{t_s})) \\ &+ \frac{1}{2r_1}(\overline{\beta}_{t_r} - \overline{\beta}_{t_s})(\epsilon_\theta(I_{\overline{\beta}_{t_u}}, I_{in}, \overline{\beta}_{t_u}) - \epsilon_\theta(I_{\overline{\beta}_{t_s}}, I_{in}, \overline{\beta}_{t_s})) \\ &+ \frac{(\overline{\alpha}_{t_r} - \overline{\alpha}_{t_s})}{3r_1r_2(r_2 - r_1)}(r_1 I^{\theta}_{res}(I_{\overline{\alpha}_{t_v}}, I_{in}, \overline{\alpha}_{t_v}) - r_2 I^{\theta}_{res}(I_{\overline{\alpha}_{t_u}}, I_{in}, \overline{\alpha}_{t_u}) + (r_2 - r_1)I^{\theta}_{res}(I_{\overline{\alpha}_{t_s}}, I_{in}, \overline{\alpha}_{t_s})) \\ &+ \frac{(\overline{\beta}_{t_r} - \overline{\beta}_{t_s})}{3r_1r_2(r_2 - r_1)}(r_1\epsilon_\theta(I_{\overline{\beta}_{t_v}}, I_{in}, \overline{\beta}_{t_v}) - r_2\epsilon_\theta(I_{\overline{\beta}_{t_u}}, I_{in}, \overline{\beta}_{t_u}) + (r_2 - r_1)\epsilon_\theta(I_{\overline{\beta}_{t_s}}, I_{in}, \overline{\beta}_{t_s})) \\ &+ \mathcal{O}\big((\overline{\beta}_{t_r} - \overline{\beta}_{t_s})^4\big) + \mathcal{O}\big((\overline{\alpha}_{t_r} - \overline{\alpha}_{t_s})^4\big).\end{aligned} \tag{161}$$

Similar to aforementioned proof, we have:

$$I_{t_u} = \widehat{I}_{t_u} + \mathcal{O}\big((\overline{\beta}_{t_r} - \overline{\beta}_{t_s})^2\big) + \mathcal{O}\big((\overline{\alpha}_{t_r} - \overline{\alpha}_{t_s})^2\big), \tag{162}$$

$$I_{t_v} = \widehat{I}_{t_v} + \mathcal{O}\big((\overline{\beta}_{t_r} - \overline{\beta}_{t_s})^3\big) + \mathcal{O}\big((\overline{\alpha}_{t_r} - \overline{\alpha}_{t_s})^3\big), \tag{163}$$

$$\begin{aligned}I_{t_r} &= I_{t_s} - (\overline{\delta}_{t_r} - \overline{\delta}_{t_s})I_{in} + (\overline{\alpha}_{t_r} - \overline{\alpha}_{t_s})I^{\theta}_{res}(I_{t_s}, I_{in}, t_s) + (\overline{\beta}_{t_r} - \overline{\beta}_{t_s})\epsilon_\theta(I_{t_s}, I_{in}, t_s) \\ &+ \frac{1}{2}(\overline{\alpha}_{t_r} - \overline{\alpha}_{t_s})^2 I^{\theta(1)}_{res}(I_{\overline{\alpha}_{t_s}}, I_{in}, \overline{\alpha}_{t_s}) + \frac{1}{6}(\overline{\alpha}_{t_r} - \overline{\alpha}_{t_s})^3 I^{\theta(2)}_{res}(I_{\overline{\alpha}_{t_s}}, I_{in}, \overline{\alpha}_{t_s}) + \mathcal{O}\big((\overline{\alpha}_t - \overline{\alpha}_{t_s})^4\big) \\ &+ \frac{1}{2}(\overline{\beta}_{t_r} - \overline{\beta}_{t_s})^2 \epsilon_{\theta(1)}(I_{\overline{\beta}_{t_s}}, I_{in}, \overline{\beta}_{t_s}) + \frac{1}{6}(\overline{\beta}_{t_r} - \overline{\beta}_{t_s})^3 \epsilon_{\theta(2)}(I_{\overline{\beta}_{t_s}}, I_{in}, \overline{\beta}_{t_s}) + \mathcal{O}\big((\overline{\beta}_t - \overline{\beta}_{t_s})^4\big).\end{aligned} \tag{164}$$

By applying Taylor expansion, we can get the conclusion as follows:

$$I_{t_r} - \widehat{I}_{t_r} = \mathcal{O}\big((\overline{\beta}_{t_r} - \overline{\beta}_{t_s})^4\big) + \mathcal{O}\big((\overline{\alpha}_{t_r} - \overline{\alpha}_{t_s})^4\big). \tag{165}$$

C Universal Diffusion Posterior Sampling

Lemma 1 *Tweedie's formula. Let $q(y|\eta)$ be the exponential family distribution:*

$$q(y|\eta) = q_0(y)\exp(\eta^T(y) - \varphi(\eta)), \tag{166}$$

among them, η is called the natural parameter, $\varphi(\eta)$ is called the cumulant generating function for normalizing the density, and $q_0(y)$ is the density up to the scale factor when $\eta = 0$. Then, the posterior mean $\widehat{\eta} := \mathbb{E}[\eta|y]$ should satisfy:

$$(\nabla_y T(y))^T \widehat{\eta} = \nabla_y \log q(y) - \nabla_y \log q_0(y). \tag{167}$$

Proof. Marginal distribution $q(y)$ could be expressed as:

$$q(y) = \int q(y|\eta)q(\eta)d\eta = \int q_0(y)\exp\Big(\eta^T T(y) - \varphi(\eta)\Big)q(\eta)d\eta, \tag{168}$$

Then, the derivative of the marginal distribution $q(y)$ with respect to y becomes:

$$\begin{aligned}\nabla_y q(y) &= \nabla_y q_0(y)\int \exp(\eta^T T(y) - \varphi(\eta))q(\eta)d\eta + \int (\nabla_y T(y))^T \eta q_0(y)\exp(\eta^T T(y) - \varphi(\eta))q(\eta)d\eta \\ &= \frac{\nabla_y q_0(y)}{q_0(y)}\int q(y|\eta)q(\eta)d\eta + (\nabla_y T(y))^T \int \eta q(y|\eta)q(\eta)d\eta \\ &= \frac{\nabla_y q_0(y)}{q_0(y)} q(y) + (\nabla_y T(y))^T \int \eta q(y,\eta)d\eta.\end{aligned} \tag{169}$$

Therefore:

$$\frac{\nabla_y q(y)}{q(y)} = \frac{\nabla_y q_0(y)}{q_0(y)} + (\nabla_y T(y))^T \int \eta q(\eta|y)d\eta, \tag{170}$$

which is equivalent to:

$$\nabla_y \log q(y) = \nabla_y \log q_0(y) + (\nabla_y T(y))^T \mathbb{E}(\eta|y). \tag{171}$$

This concludes the proof.

Proposition 2 *Jensen gap upper bound [12]. Define the absolute centered moment as $m_p := \sqrt[p]{\mathbb{E}[\|X-\mu\|^p]}$, and the mean as $\mu = \mathbb{E}[X]$. Assume that for $\alpha > 0$, there exists a positive number K such that for any $x \in \mathbb{R}$, $|f(c) - f(\mu)| \leq K|x-\mu|^\alpha$. Then:*

$$\begin{aligned}\mathbb{E}[|f(X) - f(\mathbb{E}[X])|] &\leq \int |f(x) - f(\mu)|dq(X) \\ &\leq K\int |x-\mu|^\alpha \, dq(X) \leq M m_\alpha^\alpha,\end{aligned} \tag{172}$$

where M is an upper bound estimator constant that can be taken as K or other constants related to the function f and the distribution $q(X)$.

Lemma 2 *Let $\phi(\cdot)$ be a univariate Gaussian density function with mean μ and variance σ^2, there exists a Lipschitz constant L such that:*

$$|\phi(x) - \phi(y)| \leq L|x-y|, \tag{173}$$

where $L = \frac{1}{\sqrt{2\pi\sigma^2}}\exp\big(-\frac{1}{2\sigma^2}\big)$.

Proof. As ϕ' is continuous and bounded, we use the mean value theorem to get:

$$\forall (x,y) \in \mathbb{R}^2, |\phi(x) - \phi(y)| \leq \|\phi'\|_\infty |x-y|, \tag{174}$$

Since L is the Lipschitz constant, we have that $L \leq \|\phi'\|_\infty$. Taking the limit $y \to x$ gives $\|\phi'\| \leq L$, and thus $\|\phi'\|_\infty \leq L$. Hence:

$$L = \|\phi'\|_\infty = \|-\frac{x-\mu}{\sigma^2}\phi(x)\|_\infty. \tag{175}$$

Since the derivative of ϕ' is given as:

$$\phi'' = \sigma^{-2}(1 - \sigma^{-2}(x-\mu)^2)\phi(x), \tag{176}$$

Setting $\phi'' = 0$, we get $\sigma^{-2}(1 - \sigma^{-2}(x-\mu)^2) = 0$, which gives $x = \mu \pm \sigma$, and we have:

$$L = \|\phi'\|_\infty = \frac{e^{-1/2\sigma^2}}{\sqrt{2\pi\sigma^2}}. \tag{177}$$

Lemma 3 *Let $\phi(\cdot)$ be an isotropic multivariate Gaussian density function with mean μ and variance $\sigma^2\boldsymbol{I}$. There exists a constant L such that $\forall x, y \in \mathbb{R}^d$:*

$$|\phi(x) - \phi(y)| \leq L|x - y|, \tag{178}$$

where $L = \frac{d}{\sqrt{2\pi\sigma^2}} \exp\left(-\frac{1}{2\sigma^2}\right)$

Proof.

$$\|\phi(x) - \phi(y)\| \leq \max_z \|\nabla_z \phi(z)\| \cdot \|x - y\| = \frac{d}{\sqrt{2\pi\sigma^2}} \exp(-\frac{1}{2\sigma^2}) \cdot \|x - y\|, \tag{179}$$

each element of d dimensions $\nabla_z \phi(z)$ are bounded by $\frac{1}{\sqrt{2\pi\sigma^2}} \exp(-\frac{1}{2\sigma^2})$.

Proposition 3 *For the measurement model $I_{in} = \mathcal{A}I_0 + n$ in linear verse problem with $n \sim \mathcal{N}(0, \sigma^2\boldsymbol{I})$, we have:*

$$q(I_{in}|I_t) \simeq q(I_{in}|\widehat{I}_0), \tag{180}$$

where the approximation error can be quantified with the Jensen gap, which is upper bounded by:

$$\mathcal{J} \leq \frac{d}{\sqrt{2\pi\sigma^2}} \exp\left(-\frac{1}{2\sigma^2}\right) \|\nabla_{I_0}\mathcal{A}(I_0)\| m_1, \tag{181}$$

where $\|\nabla_I \mathcal{A}(I)\| := \max_I \|\nabla_{I_0}\mathcal{A}(I_0)\|$ and $m_1 := \int \|I_0 - \widehat{I}_0\| q(I_0|I_t) dI_0$.

Proof. The measurement model $I_{in} = \mathcal{A}I_0 + n$ can be formulated as:

$$\begin{aligned} q(I_{in}|I_0) \sim \mathcal{N}(\mathcal{A}I_0, \sigma^2\boldsymbol{I}) &= \frac{1}{\sqrt{2\pi\sigma^2}} \exp\big(-\frac{(I_{in} - \mathcal{A}I_0)^2}{2\sigma^2}\big) \\ &= \frac{1}{\sqrt{2\pi\sigma^2}} \exp\big(\frac{\mathcal{A}I_0}{\sigma^2} I_{in} - \frac{(\mathcal{A}I_0)^2}{2\sigma^2}\big) \exp\big(-\frac{I_{in}^2}{2\sigma^2}\big) \\ &= \left[\frac{1}{\sqrt{2\pi\sigma^2}} \exp\big(-\frac{I_{in}^2}{2\sigma^2}\big)\right] \exp\big(\frac{\mathcal{A}I_0}{\sigma^2} I_{in} - \frac{(\mathcal{A}I_0)^2}{2\sigma^2}\big). \end{aligned} \tag{182}$$

Hence, as a member of the exponential family distribution $q(y|\eta) = q_0(y)\exp(\eta^T(y) - \varphi(\eta))$, the undetermined functions are:

$$q_0(I_{in}) = \left[\frac{1}{\sqrt{2\pi\sigma^2}} \exp\big(-\frac{I_{in}^2}{2\sigma^2}\big)\right],\ \eta^T(I_{in}) = \frac{\mathcal{A}I_0}{\sigma^2} I_{in},\ \varphi(I_0) = \exp\big(\frac{\mathcal{A}I_0}{\sigma^2} I_{in} - \frac{(\mathcal{A}I_0)^2}{2\sigma^2}\big). \tag{183}$$

In order to exploit the measurement model $q(I_{in}|I_0)$, we factorize $q(I_{in}|I_t)$ as follows:

$$q(I_{in}|I_t) = \int q(I_{in}|I_0) q(I_0|I_t) dI_0 = \mathbb{E}_{I_0 \sim q(I_0|I_t)}[f(I_0)], \tag{184}$$

here, $f(\cdot) := h(\mathcal{A}(\cdot))$, where $\mathcal{A}$ is the measurement operator and $h(\cdot)$ is the multivariate normal distribution with mean $\mathcal{A}(I_0)$ and the covariance $\sigma^2\boldsymbol{I}$. Therefore, we have:

$$\begin{aligned} \mathcal{J}(f, q(I_0|I_t)) &= |\mathbb{E}[f(I_0)] - f(\mathbb{E}[I_0])| = |\mathbb{E}[f(I_0)] - f(\widehat{I}_0)|, && (185) \\ &= |\mathbb{E}[h(\mathcal{A}(I_0))] - h(\mathcal{A}(\widehat{I}_0))|, && (186) \\ &\leq \int |h(\mathcal{A}(I_0)) - h(\mathcal{A}(\widehat{I}_0))| dQ(I_0|I_t), && (187) \\ &\leq \frac{d}{\sqrt{2\pi\sigma^2}} e^{-\frac{1}{2\sigma^2}} \int \|\mathcal{A}(I_0) - \mathcal{A}(\widehat{I}_0)\| dQ(I_0|I_t), && (188) \\ &\leq \frac{d}{\sqrt{2\pi\sigma^2}} e^{-\frac{1}{2\sigma^2}} \|\nabla_{I_0}\mathcal{A}(I_0)\| \int \|I_0 - \widehat{I}_0\| dQ(I_0|I_t), && (189) \\ &\leq \frac{d}{\sqrt{2\pi\sigma^2}} e^{-\frac{1}{2\sigma^2}} \|\nabla_{I_0}\mathcal{A}(I_0)\| m_1, && (190) \end{aligned}$$

where $dQ(I_0|I_t) = q(I_0|I_t)dI_0$.

Proposition 4 *For the measurement model $I_{in} = I_0 + I_{res} + n$ in linear inverse problem with $n \sim \mathcal{N}(0, \sigma^2\boldsymbol{I})$, we have:*

$$q(I_{in}|I_t) \simeq q(I_{in}|\widehat{I}_0, \widehat{I}_{res}), \tag{191}$$

the approximation error can be quantified with the Jensen gap, which is upper bounded by:

$$\mathcal{J} \leq \frac{d}{\sqrt{2\pi\sigma^2}} \exp\left(-\frac{1}{2\sigma^2}\right) m_1^{I_0 + I_{res}}, \tag{192}$$

where $m_1^{I_0+I_{res}} := \int \|(I_0 + I_{res}) - (\widehat{I}_0 + \widehat{I}_{res})\| q(I_0, I_{res}|I_t) dI_0 dI_{res}$.

Proof. The measurement model $I_{in} = I_0 + I_{res} + n$ can be formulated as:

$$\begin{aligned} q(I_{in}|I_0) \sim \mathcal{N}((I_0 + I_{res}), \sigma^2 \boldsymbol{I}) &= \frac{1}{\sqrt{2\pi\sigma^2}} \exp\big(-\frac{(I_{in} - (I_0 + I_{res}))^2}{2\sigma^2}\big) \\ &= \frac{1}{\sqrt{2\pi\sigma^2}} \exp\big(\frac{(I_0 + I_{res})}{\sigma^2} I_{in} - \frac{((I_0 + I_{res}))^2}{2\sigma^2}\big) \exp\big(-\frac{I_{in}^2}{2\sigma^2}\big) \\ &= \Big[\frac{1}{\sqrt{2\pi\sigma^2}} \exp\big(-\frac{I_{in}^2}{2\sigma^2}\big)\Big] \exp\big(\frac{(I_0 + I_{res})}{\sigma^2} I_{in} - \frac{((I_0 + I_{res}))^2}{2\sigma^2}\big). \end{aligned} \tag{193}$$

In order to exploit the measurement model $q(I_{in}|I_0)$, we factorize $q(I_{in}|I_t)$ as follows:

$$q(I_{in}|I_t) = \int\int q(I_{in}|I_0, I_{res}) q(I_0, I_{res}|I_t) dI_0 dI_{res}, \tag{194}$$

here, $f(\cdot) := h(I_0 + I_{res})$, and $h(\cdot)$ is the multivariate normal distribution with mean $I_0 + I_{res}$ and the covariance $\sigma^2 \boldsymbol{I}$. Therefore, we have:

$$\mathcal{J}(f, q(I_0|I_t)) = |\mathbb{E}[f(I_0)] - f(\mathbb{E}[I_0])| = |\mathbb{E}[f(I_0)] - f(\widehat{I}_0)|, \tag{195}$$

$$= |\mathbb{E}[h(I_0 + I_{res})] - h(\widehat{I}_0 + \widehat{I}_{res})|, \tag{196}$$

$$\leq \int |h(I_0 + I_{res}) - h(\widehat{I}_0 + \widehat{I}_{res})| dQ(I_0, I_{res}|I_t), \tag{197}$$

$$\leq \frac{d}{\sqrt{2\pi\sigma^2}} e^{-\frac{1}{2\sigma^2}} \int\int \|(I_0 + I_{res}) - (\widehat{I}_0 + \widehat{I}_{res})\| q(I_0, I_{res}|I_t) dI_0 dI_{res}, \tag{198}$$

$$\leq \frac{d}{\sqrt{2\pi\sigma^2}} e^{-\frac{1}{2\sigma^2}} m_1^{I_0 + I_{res}}, \tag{199}$$

where $q(I_0, I_{res}|I_t)$ is the distribution of the clean image I_0 and the residual components I_{res}. $m_1^{I_0+I_{res}}$ is considered as a generalized absolute distance loss because it measures the mean absolute error between the predicted values and ground-truth values.

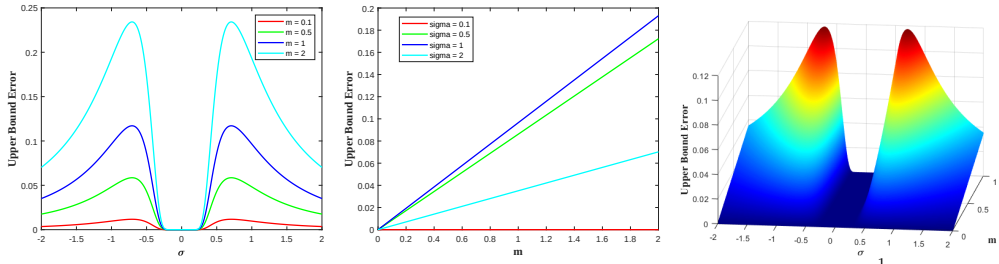

(a) $\mathcal{J} - \sigma$ (b) $\mathcal{J} - m_1^{I_0+I_{res}}$ (c) $\mathcal{J} = \frac{d}{\sqrt{2\pi\sigma^2}} e^{-\frac{1}{2\sigma^2}} m_1^{I_0+I_{res}}$

Figure A1: Relationships among the upper bound error $\mathcal{J}$ and its variables σ and $m = m_1^{I_0+I_{res}}$.

Notably, $m_1^{I_0+I_{res}}$ is finite for most of the distribution in practice once the predicted networks are optimized well. It can be regarded as generalized absolute distance between the observed reference and estimated data. The Jensen gap $\mathcal{J}(f, m_1^{I_0+I_{res}})$ can approach to 0 as $\sigma \to 0$ or ∞, suggesting that the approximation error reduces with extreme measurement noise. Specifically, if the predictions of $\widehat{I}_0$ and $\widehat{I}_{res}$ are accurate, the upper bound $\mathcal{J}(\sigma, m_1^{I_0+I_{res}})|_{\sigma\to 0, m_1^{I_0+I_{res}} \to 0}$ shrinks due to the low variance and distortion. Oppositely, if the predictions lack accuracy, the upper bound of the $\mathcal{J}(\sigma, M)|_{\sigma\to\infty, m_1^{I_0+I_{res}} \to \max(m_1^{I_0+I_{res}})}$ shrinks as well for large variance and limited distortion. We further illustrate the relationships among the upper bound error $\mathcal{J}$ and its variables in Fig. A1. Evidently, the results support the aforementioned analysis. For the universal measurement model $I_{in} = I_0 + I_{res} + n$, we can derive the probability formulation as:

$$q(I_{in}|\widehat{I}_0, \widehat{I}_{res}) \sim \mathcal{N}(I_{in}|I_0 + I_{res}, \sigma^2 \boldsymbol{I}) = \frac{1}{\sqrt{2\pi\sigma^2}} exp[-\frac{(I_{in} - (I_0 + I_{res}))^2}{2\sigma^2}], \tag{200}$$

Consequently, the formulation of universal posterior sampling is:

$$\nabla_{I_t} \log q(I_{in}|I_t) \simeq \nabla_{I_t} \log q(I_{in}|\widehat{I}_0, \widehat{I}_{res}) = -1/\sigma^2 \nabla_{I_t} \|I_{in} - (I_0 + I_{res}^{\theta}(I_t, I_{in}, t))\|, \tag{201}$$

according to the DPS [7], the value of σ^2 varies with time t and can be calculated as $\|I_{in} - (I_0 + I_{res}^{\theta}(I_t, I_{in}, t))\|$.

D Diffusion Generalist Solvers with Universal Posterior Sampling

The inverse process ordinary differential equations of diffusion generalist model are:

$$\frac{dI_t}{dt} = \frac{d\overline{\alpha}_t}{dt} I_{res} - \frac{d\overline{\delta}_t}{dt} I_{in} - \frac{1}{2}\frac{d\overline{\beta}_t^2}{dt}\nabla \log q_t(I_t). \tag{202}$$

According to the Bayes' theorem, we can derive:

$$\nabla_{I_t} \log q(I_t|I_{in}) = \nabla_{I_t} \log \frac{q(I_t)q(I_{in}|I_t)}{q(I_{in})} = \nabla_{I_t} \log q(I_t) + \nabla_{I_t} \log q(I_{in}|I_t), \tag{203}$$

where $\nabla_{I_t} \log P(I_t)$ is the score representing the gradient direction of inverse process and the discarded item $P(I_{in})$ is irrelevant to I_t. By incorporating the universal posterior sampling as conditional guidance, we can get:

$$\begin{aligned}
\frac{dI_t}{dt} &= \frac{d\overline{\alpha}_t}{dt} I_{res} - \frac{d\overline{\delta}_t}{dt} I_{in} - \frac{1}{2}\frac{d\overline{\beta}_t^2}{dt}(\nabla_{I_t} \log q_t(I_t) + \nabla_{I_t} \log q(I_{in}|I_t)) \\
&= \frac{d\overline{\alpha}_t}{dt} I_{res} - \frac{d\overline{\delta}_t}{dt} I_{in} - \frac{1}{2}\frac{d\overline{\beta}_t^2}{dt}(-\frac{\epsilon_\theta(I_t, I_{in}, t)}{\overline{\beta}_t} - 1/\sigma^2 \nabla_{I_t}\|I_{in} - (I_0 + I^\theta_{res}(I_t, I_{in}, t))\|) \\
&= \frac{d\overline{\alpha}_t}{dt} I_{res} - \frac{d\overline{\delta}_t}{dt} I_{in} + \frac{d\overline{\beta}_t}{dt}(\epsilon_\theta(I_t, I_{in}, t) + \overline{\beta}_t/\sigma^2 \nabla_{I_t}\|I_{in} - (I_0 + I^\theta_{res}(I_t, I_{in}, t))\|).
\end{aligned} \tag{204}$$

Eq. (204) is the detailed description of our method. Based on the proposed algorithms in Alg. 2, Alg. 3 and Alg. 4, we can further present varied orders with universal posterior sampling, as depicted in Alg. 5, Alg. 6 and Alg. 7. From the ablation experiment results in the paper, our method has the best balance between restoration performance and efficiency when $k = 2$ and universal posterior sampling is activated. Therefore, we customize an accelerated algorithm for this configuration.

Algorithm 5: First-order Diffusion Generalist Solvers with Universal Posterior Sampling.

Input: I_{in}, I^θ_{res}, ϵ_θ, $\{\overline{\alpha}_{t_i}\}$, $\{\overline{\beta}_{t_i}\}$, $\{\overline{\delta}_{t_i}\}$, $\{t_i\}_{i=0}^M$.

$I_{t_0} = I_T \sim \mathcal{N}(0, \overline{\beta}_{t_0}\boldsymbol{I})$

for $i = 1$ to M **do**

  $\widehat{I}_{res} = I^\theta_{res}(I_{t_{i-1}}, I_{in}, t_{i-1})$

  $\widehat{\epsilon} = (I_{t_{i-1}} - (\overline{\alpha}_{t_{i-1}} - 1)\widehat{I}_{res} - (1 - \overline{\delta}_{t_{i-1}})I_{in})/\overline{\beta}_{t_{i-1}}$

  $\widehat{I}_0 = I_{t_{i-1}} - \overline{\alpha}_{t_{i-1}}\widehat{I}_{res} - \overline{\beta}_{t_{i-1}}\widehat{\epsilon} + \overline{\delta}_{t_{i-1}} I_{in}$

  $\widetilde{\epsilon} = \widehat{\epsilon} + (\overline{\beta}_{t_{i-1}}/\|I_{in} - (\widehat{I}_0 + \widehat{I}_{res})\|)\nabla_{I_{t_{i-1}}}\|I_{in} - (\widehat{I}_0 + \widehat{I}_{res})\|$

  $I_{t_i} = I_{t_{i-1}} - (\overline{\delta}_{t_i} - \overline{\delta}_{t_{i-1}})I_{in} + (\overline{\alpha}_{t_i} - \overline{\alpha}_{t_{i-1}})\widehat{I}_{res} + (\overline{\beta}_{t_i} - \overline{\beta}_{t_{i-1}})\widetilde{\epsilon}$

Output: I_{t_M}.

Algorithm 6: Second-order Diffusion Generalist Solvers with Universal Posterior Sampling.

Input: I_{in}, I^θ_{res}, ϵ_θ, $\{\overline{\alpha}_{t_i}\}$, $\{\overline{\beta}_{t_i}\}$, $\{\overline{\delta}_{t_i}\}$, $\{t_i\}_{i=0}^M$, r.

$I_{t_0} \leftarrow I_T \sim \mathcal{N}(0, \overline{\beta}_{t_0}\boldsymbol{I})$

for $i = 1$ to M **do**

  $t_u = rt_i + (1 - r)t_{i-1}$

  $\widehat{I}^{t_{i-1}}_{res} = I^\theta_{res}(I_{t_{i-1}}, I_{in}, t_{i-1})$

  $\widehat{\epsilon}_{t_{i-1}} = (I_{t_{i-1}} - (\overline{\alpha}_{t_{i-1}} - 1)\widehat{I}^{t_i}_{res} - (1 - \overline{\delta}_{t_{i-1}})I_{in})/\overline{\beta}_{t_{i-1}}$

  $\widehat{I}^{t_{i-1}}_0 = I_{t_{i-1}} - \overline{\alpha}_{t_{i-1}}\widehat{I}^{t_{i-1}}_{res} - \overline{\beta}_{t_{i-1}}\widehat{\epsilon}_{t_{i-1}} + \overline{\delta}_{t_{i-1}} I_{in}$

  $\widetilde{\epsilon}_{t_{i-1}} = \widehat{\epsilon}_{t_{i-1}} + (\overline{\beta}_{t_{i-1}}/\|I_{in} - (\widehat{I}^{t_{i-1}}_0 + \widehat{I}^{t_{i-1}}_{res})\|)\nabla_{I_{t_{i-1}}}\|I_{in} - \widehat{I}^{t_{i-1}}_0 - \widehat{I}^{t_{i-1}}_{res}\|$

  $I_{t_u} = I_{t_i} - (\overline{\delta}_{t_i} - \overline{\delta}_{t_u})I_{in} + (\overline{\alpha}_{t_i} - \overline{\alpha}_{t_u})\widehat{I}^{t_i}_{res} + (\overline{\beta}_{t_i} - \overline{\beta}_{t_u})\widetilde{\epsilon}_{t_i}$

  $\widehat{I}^{t_u}_{res} = I^\theta_{res}(I_{t_u}, t_u, I_{in})$

  $\widehat{\epsilon}_{t_u} = (I_{t_u} - (\overline{\alpha}_{t_u} - 1)\widehat{I}^{t_u}_{res} - (1 - \overline{\delta}_{t_u})I_{in})/\overline{\beta}_{t_u}$

  $\widehat{I}^{t_u}_0 = I_{t_u} - \overline{\alpha}_{t_u}\widehat{I}^{t_u}_{res} - \overline{\beta}_{t_u}\widehat{\epsilon}_{t_u} + \overline{\delta}_{t_u} I_{in}$

  $\widetilde{\epsilon}_{t_u} = \widehat{\epsilon}_{t_u} + (\overline{\beta}_{t_u}/\|I_{in} - (\widehat{I}^{t_u}_0 + \widehat{I}^{t_u}_{res})\|)\nabla_{I_{t_u}}\|I_{in} - \widehat{I}^{t_u}_0 - \widehat{I}^{t_u}_{res}\|$

  $I_{t_i} = I_{t_{i-1}} - (\overline{\delta}_{t_i} - \overline{\delta}_{t_{i-1}})I_{in} + (\overline{\alpha}_{t_i} - \overline{\alpha}_{t_{i-1}})\widehat{I}^{t_{i-1}}_{res} + (\overline{\beta}_{t_i} - \overline{\beta}_{t_{i-1}})\widetilde{\epsilon}_{t_{i-1}} + \frac{1}{2r}(\overline{\alpha}_{t_i} - \overline{\alpha}_{t_{i-1}})(\widehat{I}^{t_u}_{res} - \widehat{I}^{t_{i-1}}_{res}) + \frac{1}{2r}(\overline{\beta}_{t_i} - \overline{\beta}_{t_{i-1}})(\widetilde{\epsilon}_{t_u} - \widetilde{\epsilon}_{t_{i-1}})$

Output: I_{t_M}.

Algorithm 7: Third-order Diffusion Generalist Solver with Universal Posterior Sampling.

Input: I_{in}, I^{θ}_{res}, ϵ_θ, $\{\overline{\alpha}_{t_i}\}$, $\{\overline{\beta}_{t_i}\}$, $\{\overline{\delta}_{t_i}\}$, r_1, r_2.

$I_{t_0} \leftarrow I_T \sim \mathcal{N}(0, \overline{\beta}_{t_0}\boldsymbol{I})$

for $i = 1$ to M **do**

$t_u = r_1 t_i + (1 - r_1)t_{i-1}$, $t_s = r_2 t_i + (1 - r_2)t_{i-1}$

$\widehat{I}^{t_{i-1}}_{res} = I^{\theta}_{res}(I_{t_{i-1}}, I_{in}, t_{i-1})$, $\widehat{\epsilon}_{t_{i-1}} = (I_{t_{i-1}} - (\overline{\alpha}_{t_{i-1}} - 1)\widehat{I}^{t_{i-1}}_{res} - (1 - \overline{\delta}_{t_{i-1}})I_{in})/\overline{\beta}_{t_{i-1}}$,
$\widehat{I}^{t_{i-1}}_0 = I_{t_{i-1}} - \overline{\alpha}_{t_{i-1}}\widehat{I}^{t_{i-1}}_{res} - \overline{\beta}_{t_{i-1}}\widehat{\epsilon}_{t_{i-1}} + \overline{\delta}_{t_{i-1}}I_{in}$

$\widetilde{\epsilon}_{t_{i-1}} = \widehat{\epsilon}_{t_{i-1}} + (\overline{\beta}_{t_{i-1}}/\|I_{in} - (\widehat{I}^{t_{i-1}}_0 + \widehat{I}^{t_{i-1}}_{res})\|)\nabla_{I_{t_{i-1}}}\|I_{in} - \widehat{I}^{t_{i-1}}_0 - \widehat{I}^{t_{i-1}}_{res}\|$

$I_{t_u} = I_{t_i} - (\overline{\delta}_{t_i} - \overline{\delta}_{t_u})I_{in} + (\overline{\alpha}_{t_i} - \overline{\alpha}_{t_u})\widehat{I}^{t_i}_{res} + (\overline{\beta}_{t_i} - \overline{\beta}_{t_u})\widetilde{\epsilon}_{t_i}$

$\widehat{I}^{t_u}_{res} = I^{\theta}_{res}(I_{t_u}, I_{in}, t_u)$, $\widehat{\epsilon}_{t_u} = (I_{t_u} - (\overline{\alpha}_{t_u} - 1)\widehat{I}^{t_u}_{res} - (1 - \overline{\delta}_{t_u})I_{in})/\overline{\beta}_{t_u}$,
$\widehat{I}^{t_u}_0 = I_{t_u} - \overline{\alpha}_{t_u}\widehat{I}^{t_u}_{res} - \overline{\beta}_{t_u}\widehat{\epsilon}_{t_u} + \overline{\delta}_{t_u}I_{in}$

$\widetilde{\epsilon}_{t_u} = \widehat{\epsilon}_{t_u} + (\overline{\beta}_{t_u}/\|I_{in} - (\widehat{I}^{t_u}_0 + \widehat{I}^{t_u}_{res})\|)\nabla_{I_{t_u}}\|I_{in} - \widehat{I}^{t_u}_0 - \widehat{I}^{t_u}_{res}\|$

$I_{t_s} = I_{t_{i-1}} - (\overline{\delta}_{t_s} - \overline{\delta}_{t_{i-1}})I_{in} + (\overline{\alpha}_{t_s} - \overline{\alpha}_{t_{i-1}})\widehat{I}^{t_{i-1}}_{res} + (\overline{\beta}_{t_s} - \overline{\beta}_{t_{i-1}})\widetilde{\epsilon}_{t_{i-1}} + \frac{r_2}{2r_1}(\overline{\alpha}_{t_s} - \overline{\alpha}_{t_{i-1}})(\widehat{I}^{t_u}_{res} - \widehat{I}^{t_{i-1}}_{res}) + \frac{r_2}{2r_1}(\overline{\beta}_{t_s} - \overline{\beta}_{t_{i-1}})(\widetilde{\epsilon}_{t_u} - \widetilde{\epsilon}_{t_{i-1}})$

$\widehat{I}^{t_s}_{res} = I^{\theta}_{res}(I_{t_s}, I_{in}, t_s)$, $\widehat{\epsilon}_{t_s} = (I_{t_s} - (\overline{\alpha}_{t_s} - 1)\widehat{I}^{t_s}_{res} - (1 - \overline{\delta}_{t_s})I_{in})/\overline{\beta}_{t_s}$,
$\widehat{I}^{t_s}_0 = I_{t_s} - \overline{\alpha}_{t_s}\widehat{I}^{t_s}_{res} - \overline{\beta}_{t_s}\widehat{\epsilon}_{t_s} + \overline{\delta}_{t_s}I_{in}$

$\widetilde{\epsilon}_{t_s} = \widehat{\epsilon}_{t_s} + (\overline{\beta}_{t_s}/\|I_{in} - (\widehat{I}^{t_s}_0 + \widehat{I}^{t_s}_{res})\|)\nabla_{I_{t_s}}\|I_{in} - \widehat{I}^{t_s}_0 - \widehat{I}^{t_s}_{res}\|$

$D^{res}_1 = \widehat{I}^{t_u}_{res} - \widehat{I}^{t_{i-1}}_{res}$, $D^{\epsilon}_1 = \widetilde{\epsilon}_{t_u} - \widetilde{\epsilon}_{t_{i-1}}$

$D^{res}_2 = \frac{2}{r_1 r_2(r_2 - r_1)}(r_1\widehat{I}^{t_s}_{res} - r_2\widehat{I}^{t_u}_{res} + (r_2 - r_1)\widehat{I}^{t_{i-1}}_{res})$

$D^{\epsilon}_2 = \frac{2}{r_1 r_2(r_2 - r_1)}(r_1\widetilde{\epsilon}_{t_s} - r_2\widetilde{\epsilon}_{t_u} + (r_2 - r_1)\widetilde{\epsilon}_{t_{i-1}})$

$I_{t_i} = I_{t_{i-1}} - (\overline{\delta}_{t_i} - \overline{\delta}_{t_{i-1}})I_{in} + (\overline{\alpha}_{t_i} - \overline{\alpha}_{t_{i-1}})\widehat{I}^{t_{i-1}}_{res} + (\overline{\beta}_{t_i} - \overline{\beta}_{t_{i-1}})\widetilde{\epsilon}_{t_{i-1}} + \frac{1}{2r_1}(\overline{\alpha}_{t_i} - \overline{\alpha}_{t_{i-1}})D^{res}_1 + \frac{1}{2r_1}(\overline{\beta}_{t_i} - \overline{\beta}_{t_{i-1}})D^{\epsilon}_1 + \frac{1}{6}(\overline{\alpha}_{t_i} - \overline{\alpha}_{t_{i-1}})D^{res}_2 + \frac{1}{6}(\overline{\beta}_{t_i} - \overline{\beta}_{t_{i-1}})D^{\epsilon}_2$

Output: I_{t_M}.

Algorithm 8: Queue-Based Second-order Solvers with Universal Posterior Sampling.

Input: I_{in}, I^{θ}_{res}, ϵ_θ, $\{\overline{\alpha}_{t_i}\}$, $\{\overline{\beta}_{t_i}\}$, $\{\overline{\delta}_{t_i}\}$,$\{t_i\}_{i=0}^{M}$,$r$.

$I_{t_0} \leftarrow I_T \sim \mathcal{N}(0, \overline{\beta}_{t_0}\boldsymbol{I})$,

$R = []$,

$(I_{t_1}, \widehat{I}^{t_1}_{res}, \widetilde{\epsilon}_{t_1}, \widehat{I}^{t_1}_0) = 1^{st}$-order Solver$(t_1)$ in Alg. 5

$R =$ queue_push$(I_{t_1}, \widehat{I}^{t_1}_{res}, \widetilde{\epsilon}_{t_1}, \widehat{I}^{t_1}_0), i = t_1$

while $i < t_M$ **do**

$t_p = t_{i-1}, t_u = t_i, t_q = t_{i+1}, r = (t_u - t_p)/(t_q - t_p)$

$(I_{t_p}, \widehat{I}^{t_p}_{res}, \widetilde{\epsilon}_{t_p}, \widehat{I}^{t_p}_0) =$ queue_pop(R, t_p)

$(I_{t_u}, \widehat{I}^{t_u}_{res}, \widetilde{\epsilon}_{t_u}, \widehat{I}^{t_u}_0) = 1^{st}$-order Solver$(t_u)$ in Alg. 5

$I_{t_q} = I_{t_p} - (\overline{\delta}_{t_q} - \overline{\delta}_{t_p})I_{in} + (\overline{\alpha}_{t_q} - \overline{\alpha}_{t_p})\widehat{I}^{t_p}_{res} + (\overline{\beta}_{t_q} - \overline{\beta}_{t_p})\widehat{\epsilon}_{t_p} + \frac{1}{2r}(\overline{\alpha}_{t_q} - \overline{\alpha}_{t_p})(\widehat{I}^{t_u}_{res} - \widehat{I}^{t_p}_{res}) + \frac{1}{2r}(\overline{\beta}_{t_q} - \overline{\beta}_{t_p})(\widetilde{\epsilon}_{t_u} - \widetilde{\epsilon}_{t_p})$

$R =$ queue_push$(I_{t_u}, \widehat{I}^{t_u}_{res}, \widetilde{\epsilon}_{t_u}, \widehat{I}^{t_u}_0), i = t_q$

Output: I_{t_M}.

Queue-Based Accelerated Strategy. The introduction of variables pertaining to the intermediate time point t_u incurs additional computational overhead, making the process inefficient. To alleviate this problem, we construct a queue-based accelerated strategy by collecting the previous solutions, as illustrated in Fig. 3 in the paper. Specifically, for the initial sampling from t_{i-1} to t_i, we introduce the intermediate step t_u to assist the approximation at time point t_i. Subsequently, t_i is regarded as the intermediate time point of the sampling from t_u to t_{i+1} iteratively. In this context, the sampling steps are controlled by the predefined parameters r without introducing extra calculation. Relevant implementation details are summarized in Alg. 8.

E Experiment Supplementary

E.1 Summary about the Datasets

We evaluate the proposed method on five natural image restoration tasks, including deraining, low-light enhancement, desnowing, dehazing, and deblurring. We select the most widely used datasets for each task, as summarized in Tab. A1.

Table A1: Summary of the natural image restoration datasets utilized in this paper.

Task	Dataset	Synthetic/Real	Train samples	Test samples
Deraining	DID [62]	Synthetic	-	1,200
	DeRaindrop [42]	Real	861	307
	Rain13K [17]	Synthetic	13,711	-
	Rain_100H [60]	Synthetic	-	100
	Rain_100L [60]	Synthetic	-	100
	GT-Rain [3]	Real	26,125	2,100
	RealRain-1k-H [24]	Real	896	224
	RealRain-1k-L [24]	Real	896	224
Low-light Enhancement	LOL [55]	Real	485	15
	MEF [35]	Real	-	17
	VE-LOL-L [29]	Synthetic/Real	900/400	100/100
	NPE [53]	Real	-	8
Desnowing	CSD [4]	Synthetic	8,000	2,000
	Snow100K-Real [30]	Real	-	1,329
Dehazing	SOTS [21]	Synthetic	-	500
	ITS_v2 [21]	Synthetic	13,990	-
	D-HAZY [8]	Synthetic	1,178	294
	NH-HAZE [2]	Real	-	55
	Dense-Haze [1]	Real	-	55
	NHRW [63]	Real	-	150
Deblur	GoPro [38]	Synthetic	2,103	1,111
	RealBlur [45]	Real	3,758	980

Image deraining. We use the merged datasets mentioned in Rain13K [17] and DeRaindrop [42] as training parts, which cover a wide range of different rain streaks and rain densities. We test our model on both deraining and deraindrop scenes using the mixed datasets [60, 62, 42]. Furthermore, we perform zero-shot generalization on real-world datasets such as GT-Rain [3], RealRain-1k-H [24], and RealRain-1k-L [24].

Low-light enhancement. We utilize the LOL [55] and VE-LOL-L [29] datasets with real and synthetic paired images as the benchmark, which consist of a large number of indoor and outdoor scenes with different levels of light and noise. Furthermore, we generalize our method on the MEF [35] dataset with images of multiple exposures to conduct the compound restoration experiments.

Image desnowing. We use the CSD [4] dataset as the desnowing benchmark and employ the Snow100K-Real [30] to perform real-world generalization.

Image dehazing. We use the ITS_v2 [21] and D-HAZY [8] datasets as the dehazing benchmark, which are widely used synthetic fog datasets with different levels of fog and various scenes. Besides, the outdoor fog dataset SOTS [21] is selected for quantitative evaluations. The real-world fog datasets Dense-Haze [1], NHRW [63], and NH-HAZE [2] are utilized for generalization validation on real-world scenes.

Image deblurring. We use the GoPro [38] dataset as the deblurring benchmark, which contains 2,103 training pairs and 1,111 testing pairs. The dataset contains various levels of blur obtained by averaging the clear images captured in very short intervals. To further validate the generalization ability of our model, we perform zero-shot generalization on the RealBlur [45] dataset.

E.2 More Visual Comparisons on Comparable Experiments

We show the visualization results of other degradation categories in Fig. A2 to further demonstrate our superiority. Evidently, Our method generates more stable image samples with high fidelity than other universal image restoration methods. Benefiting from the accuracy of diffusion generalist solvers and stable guidance of universal posterior sampling, we achieve the outstanding reconstruction of the missing details.

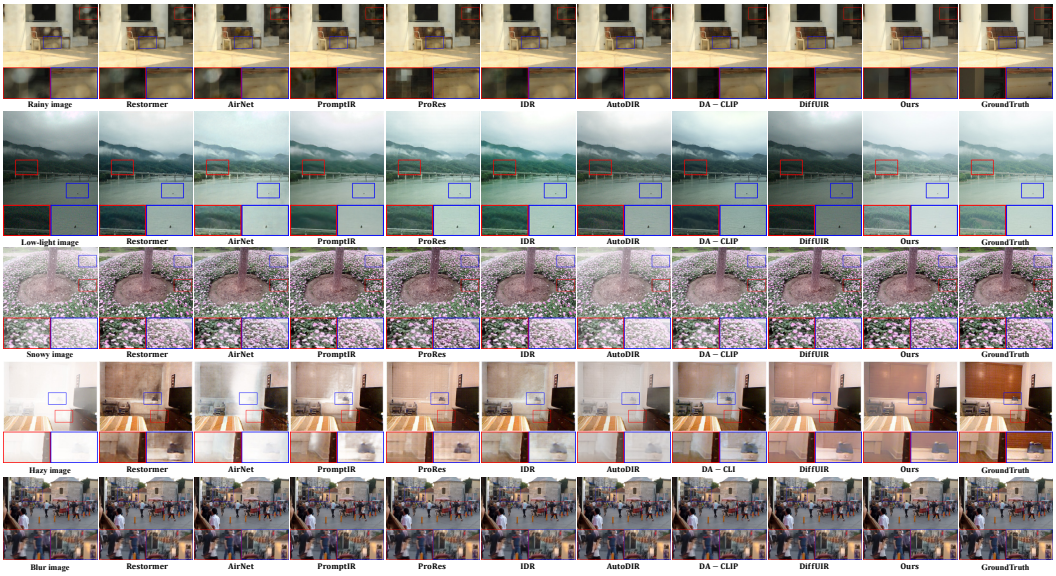

Figure A2: Visualization results of other degradation categories.

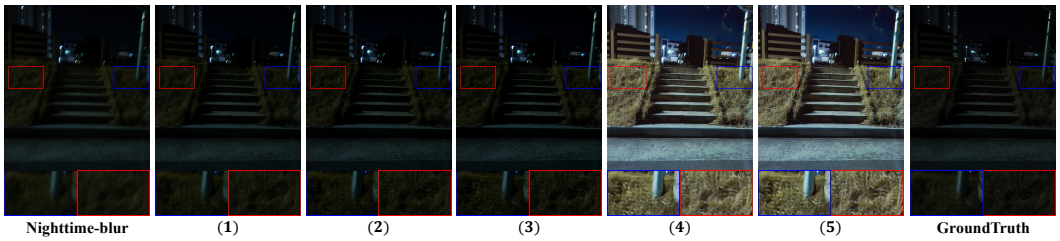

Figure A3: Results of low-light enhancement and deblurring for five iterations on RealBlur [45].

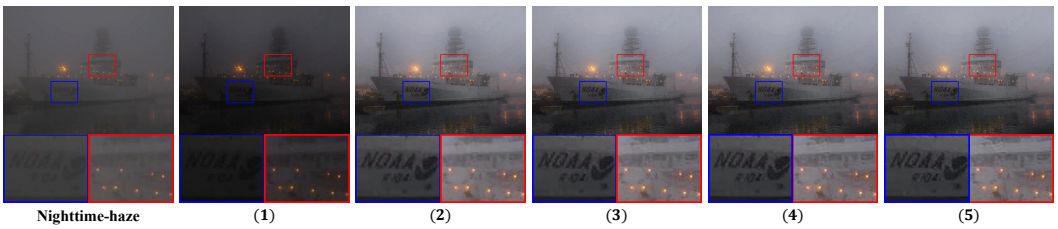

Figure A4: Results of low-light enhancement and dehazing for five iterations on NHRW [63].

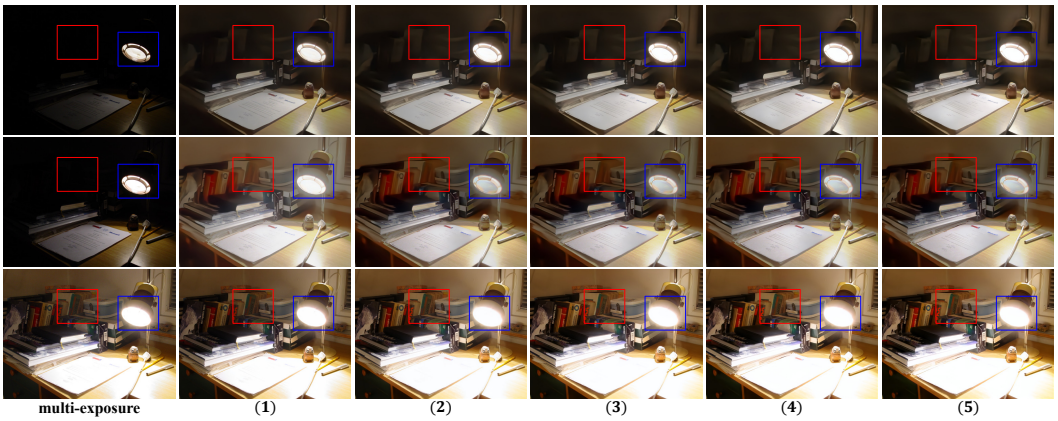

Figure A5: Results of multi-exposure restoration for five iterations on MEF [35].

E.3 Compound Restoration on Real-world Scenes

To demonstrate that our method can handle the more complex restoration tasks that various degradation occurs in one image. We generalize our well-optimized model on RealBlur [45] datasets for low-light enhancement and deblurring, and NHRW [63] datasets for low-light enhancement and dehazing, and MEF [35] datasets for multi-exposure restoration. Specifically, we repeatedly perform our method on the degrade images for five times, and the visual comparisons are displayed in Fig. A3, Fig. A4 and Fig. A5, respectively. As a result, as our method is trained on multiple degraded datasets, it is capable of excellently accomplishing relevant composite tasks. Furthermore, it possesses the ability to eliminate the former degradation and subsequently the latter degradation within its capability range. For well-restored samples, our method incurs no additional information interference, thus ensuring the high fidelity of the restored images.

E.4 Real-world Scene Generalization

Except for the desnowing on the real-world scene, other restoration results of different degradation types are illustrated in Fig. A6. We utilize the RealRain-1k [24] dataset for deraining, NPE [53] dataset for low-light enhancement, Snow100k_real [30] dataset for desnowing, Dense-Haze [1] dataset for dehazing, and RealBlur [45] dataset for deblurring. The results show that our method can generalize to real-world scenes and achieve competitive visual results.

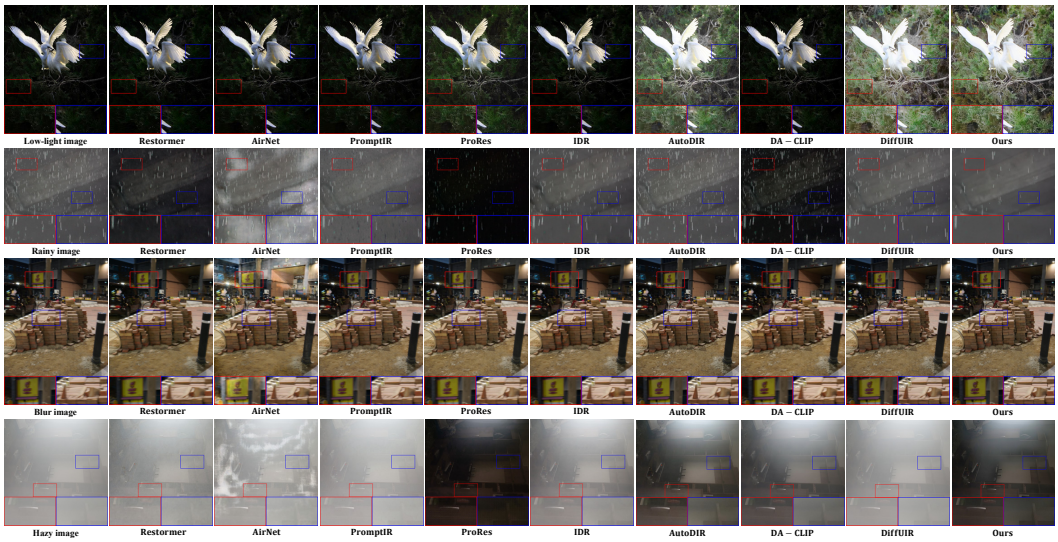

Figure A6: Visual effects of zero-shot generalization on real-world image restoration.

E.5 Generalization on Remote Sensing

Table A7: Summary of the utilized remote sensing image restoration datasets.

Task	Dataset	Synthetic/Real	Train samples	Test samples
Cloud Removal	Sen2_MTC [15]	Real	9,784	467
Denoise	AID [57]	Synthetic	38,173	1,827
Deblur	NWPU-RESISC45 [5]	Synthetic	10,000	1,094
Super-resolve	Second [59]	Synthetic	22,603	1,141
Light Enhancement	PatternNet [68]	Synthetic	28,905	1,495

We further validate the scalability of our method on remote sensing image restoration tasks, including cloud removal, denoising, deblurring, super-resolution, and low-light enhancement. Except for the cloud removal task, there are no existing real-world datasets for other restoration tasks [43], so we adopt a synthetic data generation approach to simulated the datasets, as presented in Tab. A7. Specifically: **i) Cloud Removal:** We use the Sen2_MTC dataset [15] as the benchmark, which contains paired cloudy and cloud-free images. **ii) Denoising:** Due to the lack of real-world noisy remote sensing images, we synthesize a noisy dataset based on the AID dataset [57], considering three mainstream noise types (Gaussian noise, stripe noise, and speckle noise) and their

random combinations. **iii) Deblurring:** We primarily simulate Gaussian blur, motion blur, and defocus blur, and conduct experiments on the NWPU-RESISC45 dataset [5]. **iv) Super-Resolution:** We generate low-resolution images using a four-fold downsampling degradation model with Gaussian blur and construct paired images on the Second dataset [59]. **v) Low-Light Enhancement:** We simulate low-light imaging conditions on the PatternNet dataset [68] through linear transformation, gamma correction, and additive Gaussian noise. The visual comparisons of each method are presented in Fig. A6, and quantitative evaluations are reported in Tab. 5 of this paper. All methods have been re-implemented except for AutoDIR, as no training code has been released for it. Evidently, our visual effect surpasses that of others and achieves the best metric evaluations.

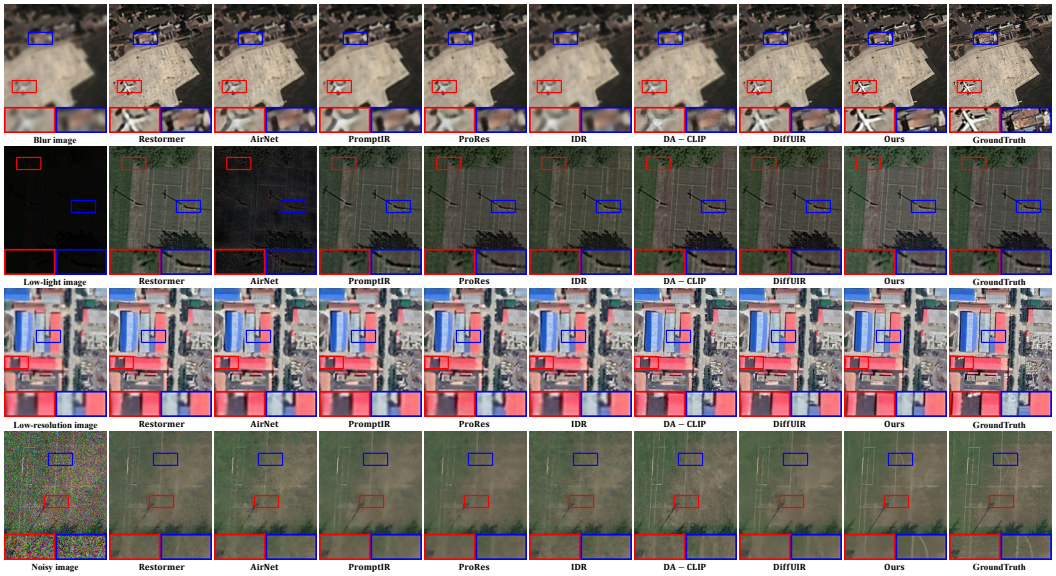

Figure A6: Visual results of remote sensing image restoration.

F Discussions, Limitations, and Future Work

Limitations and broader impact. The main challenge lies in improving the precision and robustness of a unified restoration model when handling highly mixed representations. While we have theoretically proposed a general formulation for a k-order solver, our experiments are limited to first-, second-, and third-order solvers due to GPU memory constraints. This is because unified posterior sampling requires storing the gradient map during inference to compute $\nabla_{I_t} \log q(I_{in}|\widehat{I}_0, \widehat{I}res^{\theta})$ and more time points are needed to compute derivatives. In addition, it is observed that the second order solver with universal posterior sampling reach the performance bottleneck. However, it remains unknown whether it will be saturated in more complex scenes or using larger models. Besides, our solver and strategy are training-free and can potentially be extended to other methods after appropriate modifications. Future work could explore more efficient network architectures to reduce memory usage, enabling larger batch sizes, higher-order solvers, and better task-specific training strategies, such as adaptive learning rate schedules. Despite current limitations, we believe our unified model offers a strong foundation for advancing image restoration.

Future Work. There are several promising directions to enhance our method: (1) With the rise of high-resolution imagery (e.g., 4K, 8K) driven by advances in sensor technology, developing an interpretable multi-dimensional latent diffusion model is crucial to address the computational demands that current architectures struggle with. (2) Apply model distillation to reduce memory overhead and parameter size. (3) Introduce additional single or compound degradation types, expand parameter ranges, and enhance model versatility. (4) Design adaptive learning rate schedules to reduce sampling steps and improve restoration quality.

NeurIPS Paper Checklist

1. **Claims**

   Question: Do the main claims made in the abstract and introduction accurately reflect the paper's contributions and scope?

   Answer: [Yes]

   Justification: Relevant content are all summarized.

   Guidelines:

   - The answer NA means that the abstract and introduction do not include the claims made in the paper.
   - The abstract and/or introduction should clearly state the claims made, including the contributions made in the paper and important assumptions and limitations. A No or NA answer to this question will not be perceived well by the reviewers.
   - The claims made should match theoretical and experimental results, and reflect how much the results can be expected to generalize to other settings.
   - It is fine to include aspirational goals as motivation as long as it is clear that these goals are not attained by the paper.

2. **Limitations**

   Question: Does the paper discuss the limitations of the work performed by the authors?

   Answer: [Yes]

   Justification: See Appendix F.

   Guidelines:

   - The answer NA means that the paper has no limitation while the answer No means that the paper has limitations, but those are not discussed in the paper.
   - The authors are encouraged to create a separate "Limitations" section in their paper.
   - The paper should point out any strong assumptions and how robust the results are to violations of these assumptions (e.g., independence assumptions, noiseless settings, model well-specification, asymptotic approximations only holding locally). The authors should reflect on how these assumptions might be violated in practice and what the implications would be.
   - The authors should reflect on the scope of the claims made, e.g., if the approach was only tested on a few datasets or with a few runs. In general, empirical results often depend on implicit assumptions, which should be articulated.
   - The authors should reflect on the factors that influence the performance of the approach. For example, a facial recognition algorithm may perform poorly when image resolution is low or images are taken in low lighting. Or a speech-to-text system might not be used reliably to provide closed captions for online lectures because it fails to handle technical jargon.
   - The authors should discuss the computational efficiency of the proposed algorithms and how they scale with dataset size.
   - If applicable, the authors should discuss possible limitations of their approach to address problems of privacy and fairness.
   - While the authors might fear that complete honesty about limitations might be used by reviewers as grounds for rejection, a worse outcome might be that reviewers discover limitations that aren't acknowledged in the paper. The authors should use their best judgment and recognize that individual actions in favor of transparency play an important role in developing norms that preserve the integrity of the community. Reviewers will be specifically instructed to not penalize honesty concerning limitations.

3. **Theory assumptions and proofs**

   Question: For each theoretical result, does the paper provide the full set of assumptions and a complete (and correct) proof?

   Answer: [Yes]

   Justification: See Appendix B and Appendix C.

   Guidelines:

   - The answer NA means that the paper does not include theoretical results.
   - All the theorems, formulas, and proofs in the paper should be numbered and cross-referenced.
   - All assumptions should be clearly stated or referenced in the statement of any theorems.

- The proofs can either appear in the main paper or the supplemental material, but if they appear in the supplemental material, the authors are encouraged to provide a short proof sketch to provide intuition.
- Inversely, any informal proof provided in the core of the paper should be complemented by formal proofs provided in appendix or supplemental material.
- Theorems and Lemmas that the proof relies upon should be properly referenced.

4. **Experimental result reproducibility**

   Question: Does the paper fully disclose all the information needed to reproduce the main experimental results of the paper to the extent that it affects the main claims and/or conclusions of the paper (regardless of whether the code and data are provided or not)?

   Answer: [Yes]

   Justification: Code is attached in the supplemental materials.

   Guidelines:

   - The answer NA means that the paper does not include experiments.
   - If the paper includes experiments, a No answer to this question will not be perceived well by the reviewers: Making the paper reproducible is important, regardless of whether the code and data are provided or not.
   - If the contribution is a dataset and/or model, the authors should describe the steps taken to make their results reproducible or verifiable.
   - Depending on the contribution, reproducibility can be accomplished in various ways. For example, if the contribution is a novel architecture, describing the architecture fully might suffice, or if the contribution is a specific model and empirical evaluation, it may be necessary to either make it possible for others to replicate the model with the same dataset, or provide access to the model. In general. releasing code and data is often one good way to accomplish this, but reproducibility can also be provided via detailed instructions for how to replicate the results, access to a hosted model (e.g., in the case of a large language model), releasing of a model checkpoint, or other means that are appropriate to the research performed.
   - While NeurIPS does not require releasing code, the conference does require all submissions to provide some reasonable avenue for reproducibility, which may depend on the nature of the contribution. For example
     (a) If the contribution is primarily a new algorithm, the paper should make it clear how to reproduce that algorithm.
     (b) If the contribution is primarily a new model architecture, the paper should describe the architecture clearly and fully.
     (c) If the contribution is a new model (e.g., a large language model), then there should either be a way to access this model for reproducing the results or a way to reproduce the model (e.g., with an open-source dataset or instructions for how to construct the dataset).
     (d) We recognize that reproducibility may be tricky in some cases, in which case authors are welcome to describe the particular way they provide for reproducibility. In the case of closed-source models, it may be that access to the model is limited in some way (e.g., to registered users), but it should be possible for other researchers to have some path to reproducing or verifying the results.

5. **Open access to data and code**

   Question: Does the paper provide open access to the data and code, with sufficient instructions to faithfully reproduce the main experimental results, as described in supplemental material?

   Answer: [Yes]

   Justification: We use the public datasets.

   Guidelines:

   - The answer NA means that paper does not include experiments requiring code.
   - Please see the NeurIPS code and data submission guidelines (`https://nips.cc/public/guides/CodeSubmissionPolicy`) for more details.
   - While we encourage the release of code and data, we understand that this might not be possible, so "No" is an acceptable answer. Papers cannot be rejected simply for not including code, unless this is central to the contribution (e.g., for a new open-source benchmark).
   - The instructions should contain the exact command and environment needed to run to reproduce the results. See the NeurIPS code and data submission guidelines (`https://nips.cc/public/guides/CodeSubmissionPolicy`) for more details.

- The authors should provide instructions on data access and preparation, including how to access the raw data, preprocessed data, intermediate data, and generated data, etc.
- The authors should provide scripts to reproduce all experimental results for the new proposed method and baselines. If only a subset of experiments are reproducible, they should state which ones are omitted from the script and why.
- At submission time, to preserve anonymity, the authors should release anonymized versions (if applicable).
- Providing as much information as possible in supplemental material (appended to the paper) is recommended, but including URLs to data and code is permitted.

6. **Experimental setting/details**

   Question: Does the paper specify all the training and test details (e.g., data splits, hyperparameters, how they were chosen, type of optimizer, etc.) necessary to understand the results?

   Answer: [Yes]

   Justification: We report our model, hyperparameter settings and related evaluation metrics in the paper. Our solver and strategy are training-free and have no additional hyperparameters.

   Guidelines:

   - The answer NA means that the paper does not include experiments.
   - The experimental setting should be presented in the core of the paper to a level of detail that is necessary to appreciate the results and make sense of them.
   - The full details can be provided either with the code, in appendix, or as supplemental material.

7. **Experiment statistical significance**

   Question: Does the paper report error bars suitably and correctly defined or other appropriate information about the statistical significance of the experiments?

   Answer: [No]

   Justification: Our method has almost no randomness, once the random seed is determined.

   Guidelines:

   - The answer NA means that the paper does not include experiments.
   - The authors should answer "Yes" if the results are accompanied by error bars, confidence intervals, or statistical significance tests, at least for the experiments that support the main claims of the paper.
   - The factors of variability that the error bars are capturing should be clearly stated (for example, train/test split, initialization, random drawing of some parameter, or overall run with given experimental conditions).
   - The method for calculating the error bars should be explained (closed form formula, call to a library function, bootstrap, etc.)
   - The assumptions made should be given (e.g., Normally distributed errors).
   - It should be clear whether the error bar is the standard deviation or the standard error of the mean.
   - It is OK to report 1-sigma error bars, but one should state it. The authors should preferably report a 2-sigma error bar than state that they have a 96% CI, if the hypothesis of Normality of errors is not verified.
   - For asymmetric distributions, the authors should be careful not to show in tables or figures symmetric error bars that would yield results that are out of range (e.g. negative error rates).
   - If error bars are reported in tables or plots, The authors should explain in the text how they were calculated and reference the corresponding figures or tables in the text.

8. **Experiments compute resources**

   Question: For each experiment, does the paper provide sufficient information on the computer resources (type of compute workers, memory, time of execution) needed to reproduce the experiments?

   Answer: [Yes]

   Justification: The GPU type and amount is detailed in Section 4.1

   Guidelines:

   - The answer NA means that the paper does not include experiments.
   - The paper should indicate the type of compute workers CPU or GPU, internal cluster, or cloud provider, including relevant memory and storage.

- The paper should provide the amount of compute required for each of the individual experimental runs as well as estimate the total compute.
- The paper should disclose whether the full research project required more compute than the experiments reported in the paper (e.g., preliminary or failed experiments that didn't make it into the paper).

9. **Code of ethics**

   Question: Does the research conducted in the paper conform, in every respect, with the NeurIPS Code of Ethics `https://neurips.cc/public/EthicsGuidelines`?

   Answer: [Yes]

   Justification: We read and obey the NeurIPS Code of Ethics.

   Guidelines:

   - The answer NA means that the authors have not reviewed the NeurIPS Code of Ethics.
   - If the authors answer No, they should explain the special circumstances that require a deviation from the Code of Ethics.
   - The authors should make sure to preserve anonymity (e.g., if there is a special consideration due to laws or regulations in their jurisdiction).

10. **Broader impacts**

    Question: Does the paper discuss both potential positive societal impacts and negative societal impacts of the work performed?

    Answer: [Yes]

    Justification: High-order solvers increase the computational overhead, but the introduction of queue-based sampling significantly reduces that, making their efficiency competitive compared to existing methods. Universal posterior sampling increases the memory overhead, but it avoids training an additional systems for quality refinement. Consequently, a lightweight model can achieve performance comparable to that of larger models, thereby reducing overall resource consumption. Besides, since our solver and strategy are training-free, we believe that they can potentially be extended to other diffusion-based methods with appropriate modifications.

    Guidelines:

    - The answer NA means that there is no societal impact of the work performed.
    - If the authors answer NA or No, they should explain why their work has no societal impact or why the paper does not address societal impact.
    - Examples of negative societal impacts include potential malicious or unintended uses (e.g., disinformation, generating fake profiles, surveillance), fairness considerations (e.g., deployment of technologies that could make decisions that unfairly impact specific groups), privacy considerations, and security considerations.
    - The conference expects that many papers will be foundational research and not tied to particular applications, let alone deployments. However, if there is a direct path to any negative applications, the authors should point it out. For example, it is legitimate to point out that an improvement in the quality of generative models could be used to generate deepfakes for disinformation. On the other hand, it is not needed to point out that a generic algorithm for optimizing neural networks could enable people to train models that generate Deepfakes faster.
    - The authors should consider possible harms that could arise when the technology is being used as intended and functioning correctly, harms that could arise when the technology is being used as intended but gives incorrect results, and harms following from (intentional or unintentional) misuse of the technology.
    - If there are negative societal impacts, the authors could also discuss possible mitigation strategies (e.g., gated release of models, providing defenses in addition to attacks, mechanisms for monitoring misuse, mechanisms to monitor how a system learns from feedback over time, improving the efficiency and accessibility of ML).

11. **Safeguards**

    Question: Does the paper describe safeguards that have been put in place for responsible release of data or models that have a high risk for misuse (e.g., pretrained language models, image generators, or scraped datasets)?

    Answer: [NA]

    Justification: The paper poses no such risks

    Guidelines:

- The answer NA means that the paper poses no such risks.
- Released models that have a high risk for misuse or dual-use should be released with necessary safeguards to allow for controlled use of the model, for example by requiring that users adhere to usage guidelines or restrictions to access the model or implementing safety filters.
- Datasets that have been scraped from the Internet could pose safety risks. The authors should describe how they avoided releasing unsafe images.
- We recognize that providing effective safeguards is challenging, and many papers do not require this, but we encourage authors to take this into account and make a best faith effort.

12. **Licenses for existing assets**

    Question: Are the creators or original owners of assets (e.g., code, data, models), used in the paper, properly credited and are the license and terms of use explicitly mentioned and properly respected?

    Answer: [Yes]

    Justification: we cite the related assets and follow their license and terms.

    Guidelines:

    - The answer NA means that the paper does not use existing assets.
    - The authors should cite the original paper that produced the code package or dataset.
    - The authors should state which version of the asset is used and, if possible, include a URL.
    - The name of the license (e.g., CC-BY 4.0) should be included for each asset.
    - For scraped data from a particular source (e.g., website), the copyright and terms of service of that source should be provided.
    - If assets are released, the license, copyright information, and terms of use in the package should be provided. For popular datasets, `paperswithcode.com/datasets` has curated licenses for some datasets. Their licensing guide can help determine the license of a dataset.
    - For existing datasets that are re-packaged, both the original license and the license of the derived asset (if it has changed) should be provided.
    - If this information is not available online, the authors are encouraged to reach out to the asset's creators.

13. **New assets**

    Question: Are new assets introduced in the paper well documented and is the documentation provided alongside the assets?

    Answer: [Yes]

    Justification: We include our code in the supplemental materials.

    Guidelines:

    - The answer NA means that the paper does not release new assets.
    - Researchers should communicate the details of the dataset/code/model as part of their submissions via structured templates. This includes details about training, license, limitations, etc.
    - The paper should discuss whether and how consent was obtained from people whose asset is used.
    - At submission time, remember to anonymize your assets (if applicable). You can either create an anonymized URL or include an anonymized zip file.

14. **Crowdsourcing and research with human subjects**

    Question: For crowdsourcing experiments and research with human subjects, does the paper include the full text of instructions given to participants and screenshots, if applicable, as well as details about compensation (if any)?

    Answer: [NA]

    Justification: The paper does not involve crowdsourcing nor research with human subjects.

    Guidelines:

    - The answer NA means that the paper does not involve crowdsourcing nor research with human subjects.
    - Including this information in the supplemental material is fine, but if the main contribution of the paper involves human subjects, then as much detail as possible should be included in the main paper.
    - According to the NeurIPS Code of Ethics, workers involved in data collection, curation, or other labor should be paid at least the minimum wage in the country of the data collector.

15. **Institutional review board (IRB) approvals or equivalent for research with human subjects**

    Question: Does the paper describe potential risks incurred by study participants, whether such risks were disclosed to the subjects, and whether Institutional Review Board (IRB) approvals (or an equivalent approval/review based on the requirements of your country or institution) were obtained?

    Answer: [NA]

    Justification: The paper does not involve crowdsourcing nor research with human subjects.

    Guidelines:

    - The answer NA means that the paper does not involve crowdsourcing nor research with human subjects.
    - Depending on the country in which research is conducted, IRB approval (or equivalent) may be required for any human subjects research. If you obtained IRB approval, you should clearly state this in the paper.
    - We recognize that the procedures for this may vary significantly between institutions and locations, and we expect authors to adhere to the NeurIPS Code of Ethics and the guidelines for their institution.
    - For initial submissions, do not include any information that would break anonymity (if applicable), such as the institution conducting the review.

16. **Declaration of LLM usage**

    Question: Does the paper describe the usage of LLMs if it is an important, original, or non-standard component of the core methods in this research? Note that if the LLM is used only for writing, editing, or formatting purposes and does not impact the core methodology, scientific rigorousness, or originality of the research, declaration is not required.

    Answer: [NA]

    Justification: Our method does not involve LLMs.

    Guidelines:

    - The answer NA means that the core method development in this research does not involve LLMs as any important, original, or non-standard components.
    - Please refer to our LLM policy (`https://neurips.cc/Conferences/2025/LLM`) for what should or should not be described.